



Evidence of pair production of longitudinally polarised vector bosons and study of CP properties in $ZZ \rightarrow 4\ell$ events with the ATLAS detector at $\sqrt{s} = 13$ TeV

The ATLAS Collaboration

A study of the polarisation and CP properties in ZZ production is presented. The used data set corresponds to an integrated luminosity of 140 fb^{-1} of proton–proton collisions at a centre-of-mass energy of 13 TeV recorded by the ATLAS detector at the Large Hadron Collider. The ZZ candidate events are reconstructed using two same-flavour opposite-charge electron or muon pairs. The production of two longitudinally polarised Z bosons is measured with a significance of 4.3 standard deviations, and its cross-section is measured in a fiducial phase space to be $2.45 \pm 0.60 \text{ fb}$, consistent with the next-to-leading-order Standard Model prediction. The inclusive differential cross-section as a function of a CP-sensitive angular observable is also measured. The results are used to constrain anomalous CP-odd neutral triple gauge couplings.

Contents

1	Introduction	2
2	ATLAS detector	4
3	Data and simulation	4
4	Fiducial region, object and event selections	7
4.1	Fiducial region definition	7
4.2	Object selection	7
4.3	Event selection	8
5	Background estimation	8
6	Measurement methods	10
6.1	Polarisation measurements	10
6.2	Study of CP property	12
7	Systematic uncertainties	14
8	Results	16
8.1	Polarisation measurements	16
8.2	Unfolded differential measurement	17
8.3	BSM interpretation	19
9	Conclusion	20

1 Introduction

Measurements of Z boson pair (ZZ) production in proton–proton (pp) collisions at the Large Hadron Collider (LHC) provide an important test of the Standard Model (SM) gauge structure in the electroweak (EW) sector. Representative leading-order Feynman diagrams of ZZ production at the LHC are shown in Figure 1. With increased luminosity, experimental data enables studies beyond precision measurements of integrated and differential cross-sections, such as the weak boson polarisation and charge conjugation (C) and parity (P) properties. The polarisation measurement of massive weak bosons is a direct probe of the Electroweak Symmetry Breaking mechanism, through which the W and Z bosons obtain their longitudinally polarised states. Diboson polarisation measurements, especially those probing longitudinally polarised vector bosons, provide unique sensitivity to physics beyond the SM (BSM) [1].

Polarisation measurements performed with LHC data have mainly focused on single bosons such as in W -boson production [2, 3], Z -boson production [4, 5], and W bosons from top-quark decays [6–8]. Single-boson polarisation states have also been measured in WZ production by the ATLAS [9] and CMS [10] Collaborations. Recently first measurements on joint-polarisation states of weak bosons have also been reported. The production of two transversely polarised W bosons has been measured by the CMS Collaboration in EW production of the same-sign $W^\pm W^\pm$ boson pairs [11], while the the ATLAS Collaboration has measured the joint-polarisation states of longitudinally or transversely polarised bosons in

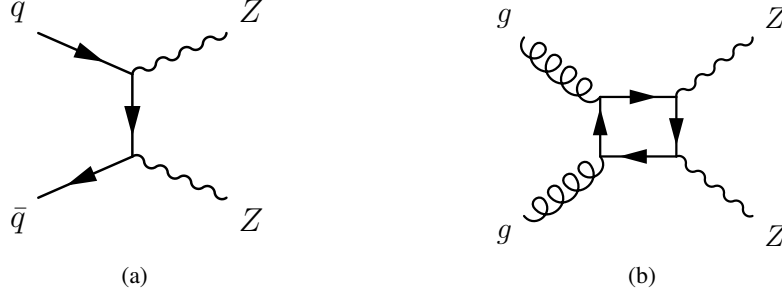


Figure 1: Examples of main leading-order Feynman diagrams for ZZ production in pp collisions: (a) $q\bar{q}$ -initiated, and (b) gg -initiated. The internal fermion lines are quarks.

inclusive WZ production [12]. In the latter, the fraction of diboson events with a simultaneous longitudinal polarisation (LL) was observed with a significance of 7.1 standard deviations.

This paper presents a measurement of the production of two longitudinally polarised Z bosons ($Z_L Z_L$) in the decay channel $ZZ \rightarrow \ell^+ \ell^- \ell'^+ \ell'^-$, where ℓ and ℓ' can be an electron or a muon. The Z -boson candidates are reconstructed with same-flavour, opposite-charge (SFOC) electron or muon pairs, and they are required to be on-shell with $|m_{\ell\ell} - m_Z| < 10$ GeV, where $m_{\ell\ell}$ is the invariant mass of the lepton pair and m_Z is the Z -boson pole mass [13].

The violation of CP symmetries is required to explain the matter-antimatter asymmetry in the universe, and it is well known that there is insufficient CP violation in the SM [14–16]. The measurement of CP-sensitive observables in diboson production can be utilised to explore new sources of CP violation in the gauge-boson sector. CP-violating effects in weak-boson self-interactions were studied in various measurements of diboson production at the LHC by constraining the CP-odd anomalous neutral triple gauge couplings (aNTGC), including those entering the ZZZ and $ZZ\gamma$ vertexes, using ZZ production in ATLAS and CMS [17–23]. Such experimental searches primarily derive constraints on anomalous triple gauge boson couplings (aTGC) using event rates or cross-section measurements without employing dedicated CP-sensitive observables.

This paper presents the differential cross-section for a dedicated CP-odd angular observable, referred to as the *Optimal Observable* (OO). The OO is defined in Section 6 using the decay products of weak bosons in ZZ production, in such a way as to be sensitive to BSM amplitudes through the interference to the SM [24, 25]. The results are then reinterpreted to constrain aNTGC using an effective vertex function approach [26]. The ATLAS Collaboration has previously used such type of dedicated CP-sensitive observables in the EW Zjj production to test CP violation in the weak-boson self-interactions [27].

The CP property is studied using an aNTGC vertex that can be parameterised with two coupling parameters f_Z^4 and f_γ^4 that violate the CP symmetry. By using such parameters, the cross-section in any given bin of the CP-sensitive observable can be parameterised as

$$\sigma^i = \sigma_{\text{SM}}^i + c \cdot \sigma_{\text{interference}}^i + c^2 \cdot \sigma_{\text{quadratic}}^i, \quad (1)$$

where the superscript i is the bin index of the CP-sensitive observable, c is the CP-odd aNTGC, σ_{SM}^i is the prediction from the SM, $\sigma_{\text{interference}}^i$ is the linear interference between the SM and the aNTGC, and $\sigma_{\text{quadratic}}^i$ is the quadratic contribution of the aNTGC. As pointed out in Ref. [28], for the aNTGC, the quadratic term dominates over the linear interference term. Existing constraints on a CP-odd aNTGC stem

primarily from their effect on the cross-section in the high- p_T regime, derived using kinematic observables such as the leading p_T^Z . Such high- p_T sensitive kinematic observables cannot distinguish CP-even and CP-odd effects. This paper presents a search for CP violation using the unfolded OO which is sensitive to the interference terms.

2 ATLAS detector

The ATLAS experiment [29] at the LHC is a multipurpose particle detector with a forward–backward symmetric cylindrical geometry and a near 4π coverage in solid angle.¹ It consists of an inner tracking detector (ID) surrounded by a thin superconducting solenoid providing a 2 T axial magnetic field, electromagnetic and hadron calorimeters, and a muon spectrometer (MS). The inner tracking detector covers the pseudorapidity range $|\eta| < 2.5$. It consists of silicon pixel, silicon microstrip, and transition radiation tracking detectors. Lead/liquid-argon (LAr) sampling calorimeters provide electromagnetic (EM) energy measurements with high granularity. A steel/scintillator-tile hadron calorimeter covers the central pseudorapidity range ($|\eta| < 1.7$). The endcap and forward regions are instrumented with LAr calorimeters for both the EM and hadronic energy measurements up to $|\eta| = 4.9$. The muon spectrometer surrounds the calorimeters and is based on three large superconducting air-core toroidal magnets with eight coils each. The field integral of the toroids ranges between 2.0 and 6.0 T m across most of the detector. The muon spectrometer includes a system of precision tracking chambers and fast detectors for triggering. A two-level trigger system is used to select events. The first-level trigger is implemented in hardware and uses a subset of the detector information to accept events at a rate below 100 kHz. This is followed by a software-based trigger that reduces the accepted event rate to 1 kHz on average depending on the data-taking conditions. An extensive software suite [30] is used in data simulation, in the reconstruction and analysis of real and simulated data, in detector operations, and in the trigger and data acquisition systems of the experiment.

3 Data and simulation

The data collected by the ATLAS experiment during the 2015-2018 data-taking period of the LHC at a centre-of-mass energy of $\sqrt{s} = 13$ TeV is analysed, and corresponds to an integrated luminosity of 140 fb^{-1} . The data events are triggered using single-lepton and dilepton triggers with the minimum trigger threshold, depending on data-taking periods, varying between 20 – 26 GeV for single-lepton triggers and 8 – 24 GeV for dilepton triggers [31, 32]. The trigger efficiency is nearly 100% for signal events after offline event selections.

Simulations of the signal SM processes of the on-shell production of two Z bosons and background processes resulting in two SFOC lepton pairs are derived using Monte Carlo (MC) generators. The $q\bar{q} \rightarrow ZZ$ (Figure 1(a)) process was modelled using the SHERPA 2.2.2 generator [33]. The matrix elements (ME) were calculated at next-to-leading-order (NLO) accuracy in QCD for up to one additional parton emission and leading-order (LO) accuracy for up to three additional parton emissions. The

¹ ATLAS uses a right-handed coordinate system with its origin at the nominal interaction point (IP) in the centre of the detector and the z-axis along the beam pipe. The x-axis points from the IP to the centre of the LHC ring, and the y-axis points upwards. Cylindrical coordinates (r, ϕ) are used in the transverse plane, ϕ being the azimuthal angle around the z-axis. The pseudorapidity is defined in terms of the polar angle θ as $\eta = -\ln \tan(\theta/2)$. Angular distance is measured in units of $\Delta R \equiv \sqrt{(\Delta\eta)^2 + (\Delta\phi)^2}$.

matrix element calculations were matched and merged with the SHERPA parton shower based on the Catani–Seymour dipole factorisation [34, 35], using the MEPS@NLO prescription [36–38]. The virtual QCD corrections were provided by the OpenLoops library [39–41]. The NNPDF3.0_{NNLO} set of parton distribution functions (PDF) [42] and the dedicated set of tuned parton-shower parameters developed by the SHERPA authors were used for generating this sample. The higher-order corrections from NLO electroweak effects were taken into account for the $q\bar{q} \rightarrow ZZ$ sample by applying reweighting corrections as a function of the four-lepton invariant mass $m_{4\ell}$ [43, 44].

An alternative prediction of the $q\bar{q} \rightarrow ZZ$ process with POWHEG Box v2 [45–47] is used for estimating the theory modeling uncertainty. This sample was generated at NLO accuracy in QCD and interfaced with PYTHIA 8.186 [48] for modelling the parton shower, hadronisation, and effect of underlying events using the AZNLO set of tuned parameters (‘tune’) [49]. For the hard-scattering and parton showering, CT10 PDF [50] and CTEQ6L1 PDF [51] sets were used, respectively. A higher-order correction as a function of $m_{4\ell}$ was obtained using a MATRIX NNLO QCD prediction [52–55] and applied to these events. The correction was defined as the ratio of the cross-section at NNLO QCD accuracy to the one at NLO QCD accuracy.

The loop-induced $gg \rightarrow ZZ$ process (Figure 1(b)) was also modelled with the SHERPA 2.2.2 generator using ME calculated with LO accuracy for up to one additional parton emission. As detailed in Ref. [56], the higher-order QCD effects are accounted for by normalising the LO prediction to NNLO using NLO [57, 58] and NNLO [59, 60] predictions. The same parton showering, matching, and merging schemes as for the SHERPA $q\bar{q} \rightarrow ZZ$ simulations were used. The EW production of ZZ in association with two jets, $qq \rightarrow ZZjj$, was modelled by MADGRAPH5_AMC@NLO 2.6.7 [61]. The matrix element was calculated at LO in QCD, and the NNPDF3.0_{NNLO} PDF set was used. PYTHIA 8.244 [62] was used to simulate parton showering, hadronisation, and underlying-event activity using the NNPDF2.3_{LO} [63] PDF set and the A14 tune [64]. The three processes, $q\bar{q} \rightarrow ZZ$, $gg \rightarrow ZZ$, and $qq \rightarrow ZZjj$, collectively simulate the total signal events for this measurement.

In addition to the simulations for the inclusive ZZ production, samples for different polarisation states were also produced. The polarised $q\bar{q} \rightarrow ZZ$ signal samples were simulated using MADGRAPH5_AMC@NLO 2.7.3 [61, 65], with the ME calculated at LO in perturbative QCD and with the NNPDF3.0_{NLO} [42] PDF set. The events were interfaced to PYTHIA 8.240 to model the parton shower, hadronisation, and underlying event, with parameters set according to the A14 tune and using the NNPDF2.3_{LO} set of PDFs. Polarised samples were simulated corresponding to the three helicity states, $Z_T Z_T$ for two transversely polarised Z bosons, $Z_T Z_L$ for one transversely polarised Z boson and one longitudinally polarised Z boson, and $Z_L Z_L$ for two longitudinally polarised Z bosons, respectively, with each Z boson decaying independently into an electron or a muon pair. The Z -boson polarisation is defined in the centre-of-mass (CM) frame of the two Z bosons, which is a natural choice for diboson production [66]. To account for the real part of the NLO corrections, the QCD-induced events were simulated with up to two jets in the matrix element at LO and merged with PYTHIA 8 parton showers using the CKKW-L scheme [67, 68]. The EW production of the polarised ZZ samples was similarly generated with MADGRAPH5_AMC@NLO 2.7.3, and they are used together with the QCD-induced $q\bar{q} \rightarrow ZZ$ samples in the analysis. Generation of polarised MC events for the loop-induced $gg \rightarrow ZZ$ process is not possible, and a MC event reweighting procedure is applied for the modelling as described in detail in Section 6.1. The off-shell Z/γ^* contribution is included in the inclusive ZZ samples but not in the polarised simulations, and the impact is found to be negligible after the event selection with a requirement of two on-shell Z bosons, as described in Section 4.3.

Background events consist of four-lepton events originating from $t\bar{t}Z$ and VVZ processes, as well as four-lepton events containing at least one non-prompt lepton. The $t\bar{t}Z$ events were modelled by the SHERPA 2.2.0 generator at LO accuracy with up to one additional parton emission using the MEPS@LO setup [37, 38] and the NNPDF3.0_{NNLO} PDF set. The sample was scaled to reproduce the prior $t\bar{t}Z$ cross-section measurement from ATLAS [69]. Events from the VVZ processes were simulated by the Sherpa 2.2.2 generator with NLO accuracy in QCD for the inclusive process and LO accuracy in QCD for up to two additional parton emissions. The NNPDF3.0_{NNLO} PDF set and the default SHERPA parton showering scheme were used. The prediction was scaled to match the prior measurement of the triboson production from ATLAS [70].

The events with either of the four leptons originating from non-prompt sources are estimated by using a semi-data-driven method discussed in Section 5. The method uses information about the origin of the non-prompt leptons from simulations of the relevant processes. The production of WZ with the leptonic decays of vector bosons was modelled with SHERPA 2.2.2. The same setup and parameters as with the $q\bar{q} \rightarrow ZZ$ modelling were used. The events with non-prompt leptons arising from Z + jets processes were modelled using SHERPA 2.2.1 at NLO accuracy in QCD for up to two parton emission and LO accuracy for up to four parton emission. The ME were calculated using the COMIX and OPENLOOPS libraries [34]. Matching and merging were performed with the SHERPA parton shower scheme using the MEPS@NLO prescription. The NNPDF3.0_{NNLO} PDF set was used, and the events are normalised to a prediction accurate to NNLO in QCD [71] for the inclusive production. The non-prompt events originating from the $t\bar{t}$ processes were modelled using the POWHEG Box v2 generator at NLO accuracy and the NNPDF3.0_{NLO} PDF set. The prediction was interfaced with PYTHIA 8.230 for modelling parton showering, hadronisation, and underlying event with parameters set according to the A14 tune.

The MC samples used in the BSM aNTGC interpretation of the CP study were generated at LO in QCD with MADGRAPH5_AMC@NLO 2.7.2 using a UFO model [72] as implemented in Ref. [28], and interfaced with PYTHIA 8.244 for the modelling of parton shower, hadronisation, and underlying event. The aNTGC predictions are reweighted by applying a per-bin k -factor, derived by comparing the SHERPA prediction to the LO MADGRAPH5_AMC@NLO $q\bar{q} \rightarrow ZZ$ prediction in each bin of the OO to account for the missing higher-order effects in the BSM prediction.

The predictions from the MC simulations were passed through a detailed simulation of the ATLAS detector [73] based on GEANT4 [74]. The effect of multiple pp interactions in the same bunch crossing, known as pile-up, was emulated by overlaying inelastic pp collisions, simulated with PYTHIA 8.186 using the NNPDF2.3_{LO} set of PDFs and the A3 tune [75]. The events were then reweighted to match the distribution of the average number of interactions per bunch crossing observed in the data for different data-taking periods. The simulated events were reconstructed using the same algorithms used for the data. Additionally, efficiencies for the trigger, lepton reconstruction, identification, and isolation in MC events were corrected to match those measured in the data.

4 Fiducial region, object and event selections

4.1 Fiducial region definition

The fiducial phase space is defined close to the detector’s kinematic acceptance using particle-level prompt² leptons produced by a MC event generator, without simulating the effects of the detector. The particle-level prompt leptons are *dressed* by adding the four-momenta of nearby prompt photons within a small cone of $\Delta R < 0.1$. The dressed electrons (muons) are required to be within the detector’s acceptance such that they satisfy $p_T > 7$ (5) GeV and $|\eta| < 2.47$ (2.7). The fiducial phase space of the analysis does not include the negligible contribution of prompt leptons from τ -lepton decays. Events must have a minimum of four prompt dressed leptons to be grouped into at least two SFOC lepton pairs, and the leading and sub-leading leptons must have $p_T > 20$ GeV. The angular separation between any two leptons is required to satisfy $\Delta R > 0.05$ to reduce the double counting of detector signatures while keeping leptons from possible boosted production scenarios. The invariant mass of any SFOC lepton pair is required to satisfy $m_{\ell\ell} > 5$ GeV.

An event quadruplet is formed from the two SFOC lepton pairs whose invariant masses are closest and next closest to m_Z . In the on-shell ZZ region, the resolution on m_Z is comparable to the mass difference between the two Z bosons, resulting in some events with inconsistent definitions of the leading and sub-leading pairs at particle and detector levels. This increases the resolution-induced bin migrations that need to be corrected for by the unfolding procedure. Therefore, once the quadruplet is formed, the leading (sub-leading)-lepton pair Z_1 (Z_2) is identified as the one with the larger (smaller) value of absolute rapidity, i.e., $y_{\ell\ell}$. Based on these requirements, the events are divided into three categories, $4e$ events with two e^+e^- pairs, 4μ events with two $\mu^+\mu^-$ pairs and $2e2\mu$ events where one of the pairs is e^+e^- and the other is $\mu^+\mu^-$. The invariant mass of each SFOC lepton pair is required to be within $|m_{\ell\ell} - m_Z| < 10$ GeV, and the invariant mass of the four leptons is required to be $m_{4\ell} > 180$ GeV, motivated to select only on-shell ZZ events.

4.2 Object selection

Events are required to contain at least one reconstructed pp collision vertex candidate with at least two associated ID tracks with $p_T > 0.5$ GeV. The vertex with the largest sum of p_T^2 of tracks is considered to be the primary interaction vertex.

Electrons are reconstructed by matching the topological energy clusters deposited in the electromagnetic calorimeters to the tracks in the ID [76]. The electron identification is based on a multivariate-likelihood technique that takes information about clusters’ shower shapes in the electromagnetic calorimeters, ID track properties, and the quality of track-cluster matching. *Baseline* electrons, used for the non-prompt background estimate, are required to satisfy $p_T > 7$ GeV, $|\eta| < 2.47$ and the ‘VeryLoose’ identification criteria [76] and loose association with the primary hard-scatter vertex by requiring $|z_0 \sin \theta| < 0.5$ mm, where z_0 is the longitudinal impact parameter and θ is the polar angle of the track. *Signal* electrons that define signal events are required to satisfy all of the baseline electron criteria and the stricter ‘LooseBLayer’ identification criteria and transverse impact parameter significance of $|d_0|/\sigma_{d_0} < 5$, where d_0 is the transverse impact parameter relative to the beamline, and σ_{d_0} is its uncertainty. Prompt leptons originating from hard scattering are characterised by low activity around them in the $\eta - \phi$ plane. Therefore, a signal

² *Prompt objects* are leptons and photons that do not originate from hadrons.

electron must be isolated from other particles by applying criteria for the p_T -dependent isolation variable, which is defined using the electron's track and calorimeter energy deposits [76].

Muons are identified using information from various parts of the detector, the ID, the MS, and the calorimeters. A 'Loose' identification working point [77] is used. ID tracks identified as muons based on their calorimetric energy deposits or the presence of individual muon segments are included in the region $|\eta| < 0.1$, and the stand-alone MS tracks are added in the region $2.5 < |\eta| < 2.7$. *Baseline* muons used in the non-prompt background estimate are required to satisfy the 'Loose' identification criteria, $p_T > 5$ GeV, $|\eta| < 2.7$ and loose track-to-vertex association of $|z_0 \sin \theta| < 0.5$ mm. *Signal* muons are required to satisfy all criteria for baseline muons and transverse impact parameter significance of $|d_0|/\sigma_{d_0} < 3$. Similarly to the signal electrons, signal muons are required to satisfy additional isolation criteria on the p_T -dependent isolation variable, defined using the tracks and particle-flow objects used in muon reconstruction [77].

Jets are reconstructed from particle-flow objects [78] using the anti- k_T algorithm with a radius parameter of $R = 0.4$ [79, 80]. The jet-energy scale is calibrated using simulation and further corrected with in situ methods [81]. Candidate jets are required to satisfy $p_T > 15$ GeV and $|\eta| < 4.5$, and are used in the non-prompt background estimation studies. A jet-vertex tagger [82] is applied to jets with $p_T < 60$ GeV and $|\eta| < 2.4$ to suppress jets that originate from pile-up. In addition, b -jets are identified using a multivariate b -tagging algorithm [83]. The chosen b -tagging algorithm has an efficiency of 85% for b -jets and a rejection factor of 33 against light-flavour jets, measured in $t\bar{t}$ events [84].

An overlap removal is applied to avoid double counting of the detector signal, favouring leptons with higher p_T and preferring non-calorimeter tagged muons over electrons if they share an ID track. The overlap removal rejects any jets within $\Delta R < 0.2$ of an electron or jets associated with less than three ID tracks if they overlap with a muon.

4.3 Event selection

The reconstructed events must have at least four baseline leptons, and the leading and sub-leading leptons must satisfy $p_T > 20$ GeV. In each event, all possible SFOC lepton pairs are formed by requiring $m_{\ell\ell} > 5$ GeV and $\Delta R_{\ell\ell} > 0.05$ to suppress contributions from the leptonic decays of resonance hadrons. Like the fiducial region, a quadruplet is formed from two SFOC pairs with the lowest values of $|m_{\ell\ell} - m_Z|$. The SFOC lepton pair with the largest value of $y_{\ell\ell}$ is defined as the leading Z boson candidate. To ensure the selection of on-shell ZZ events, the invariant mass of the SFOC lepton pair is required to be $|m_{\ell\ell} - m_Z| < 10$ GeV and the invariant mass of the quadruplet is required to satisfy $m_{4\ell} > 180$ GeV. Each lepton of the quadruplet is required to satisfy the signal lepton definition for the signal region selection. Events with either one or more lepton in a quadruplet failing to meet the signal lepton requirement are used in non-prompt background estimate. Due to the on-shell requirement on both Z bosons, in $4e$ and 4μ final states there are less than 2% of events with mispaired leptons, which has no significant impact for both the CP and polarisation measurements.

5 Background estimation

After the event selection, the background consists of events with one or more of the reconstructed leptons in the quadruplet not originating from a Z boson decay. The background processes with prompt leptons from $t\bar{t}Z$ and fully leptonic decays of triboson processes are estimated using MC simulations. The measurement

also accounts for an additional source of background from non-prompt leptons originating from hadron decays or misidentification of jets. A data-driven *fake-factor* method is used to estimate the non-prompt background.

A *fake-factor* quantity, defined as the ratio of signal leptons to the number of baseline leptons failing to meet the signal lepton criteria, is measured from data in dedicated control regions (CR) enriched with non-prompt leptons. The CR where the fake factors are evaluated consists of events with two prompt leptons from a physics process such as $Z + \text{jets}$ or $t\bar{t}$ and additional leptons from other sources such as jets. The same triggers and object-level kinematic selections as in the signal region are also applied to select the CR events. The $Z + \text{jets}$ CR is selected by requiring an SFOC signal lepton pair from a Z -boson decay with an invariant mass of $76 < m_{\ell\ell} < 106$ GeV and additional baseline leptons. Similar to the signal region, SFOC lepton pairs are formed with leptons having $\Delta R > 0.05$ and $m_{\ell\ell} > 5$ GeV. Additionally, events are required to have a missing transverse energy less than 50 GeV to suppress the contamination from the WZ process. The $t\bar{t}$ CR is defined by requiring an SFOC signal lepton pair, at least one b -tagged jet and at least one additional baseline lepton.

The additional leptons in the $Z + \text{jets}$ and $t\bar{t}$ CRs originate predominantly from non-prompt sources such as heavy- or light-flavour jets and are used to derive the fake factors. The additional non-prompt leptons in $Z + \text{jets}$ events arise dominantly from light-flavour jets, whereas they arise dominantly from heavy-flavour jets in $t\bar{t}$ events. To match the heavy-flavour composition in the signal region, the two types of events are first weighted and combined. The combination weight is evaluated by comparing the fraction of the non-prompt leptons from heavy-flavour decays in the $Z + \text{jets}$ and $t\bar{t}$ CRs to that of the signal region using the simulated samples discussed in Section 3. Since the compositions for the non-prompt electrons and muons are different in the signal region, the weights are evaluated separately to combine the control region events that have additional baseline electrons and muons. When evaluating the fake factors, an estimate of the genuine baseline prompt leptons that fail the signal requirements from the WZ MC simulation is subtracted for both the $Z + \text{jets}$ and $t\bar{t}$ events. The fake factor is measured as a function of p_T and η of the non-prompt leptons and the number of jets in an event.

A fake-lepton enriched region is selected with a minimum of four baseline leptons passing the same kinematic selection as in the signal region, but with at least one baseline-not-signal lepton, which is defined as leptons passing the baseline selection but failing the signal-lepton requirement. The non-prompt event yield in the signal region is then estimated by applying a fake-factor weight to each baseline-not-signal lepton. Four-lepton events containing prompt baseline-not-signal leptons are removed from the estimate using simulations.

The background estimate is validated by comparing the prediction of the fake-factor method to the data in two dedicated validation regions where the non-prompt background events are expected to be dominant. The first one is the different-flavour validation region which has the same event selection requirements as the signal region but requires the leptons forming one of the pairs to have different flavours. The second one is the same-charge validation region, which requires the leptons in one of the pairs to have the same charge. In both of the validation regions, the data agree closely with the sum of the estimated non-prompt background yield and the MC prediction within the statistical uncertainties of the data.

Three sources of uncertainties in the background yield are considered. The first uncertainty is related to the statistical uncertainty of the non-prompt leptons in the control region used to calculate the fake factors and ranges from 10 – 80%. The second set of uncertainty, ranging from 2 – 40%, is related to the theory uncertainties of the subtracted prompt-lepton component in the control region, which are dominated by the QCD scale variations. The third and dominant uncertainty, ranging from 20 – 100%, is the statistical

precision on the number of events with at least four baseline leptons and at least one failing to satisfy the signal-lepton requirement.

6 Measurement methods

6.1 Polarisation measurements

The Z boson can be either transversely polarised or longitudinally polarised, and the polarisation fractions depend on the transverse momentum of the Z boson [85]. These effects lead to different kinematic properties of the production and the final decay states of the Z -boson pair. To extract the fraction of $Z_L Z_L$ events from the reconstructed ZZ candidate events, a multivariate technique based on a boosted decision tree (BDT) [86] is used to enhance the separation between $Z_L Z_L$ and $Z_T Z_X$ ($Z_T Z_T$ or $Z_T Z_L$) events. After a dedicated optimisation study to maximise the $Z_L Z_L$ signal sensitivity, the input variables used in the BDT are the following: $\cos \theta_1$ ($\cos \theta_3$), where θ_1 (θ_3) is the angle between the negatively charged final-state lepton in the Z_1 (Z_2) rest frame and the direction of flight of the Z_1 (Z_2) boson in the four-lepton rest frame; $\cos \theta_{Z_1}^*$, where $\theta_{Z_1}^*$ is the production angle of the Z_1 defined in the four-lepton rest frame; and $\Delta\phi_{\ell_1 \ell_2}$ ($\Delta\phi_{\ell_3 \ell_4}$), the azimuthal separation of the two leptons from Z_1 (Z_2) defined in the four-lepton rest frame. The angles are illustrated in Figure 2. Other kinematic variables, such as the p_T and rapidity of Z_1 and Z_2 also have substantial separation power, but they are not included in the BDT training to reduce theoretical modelling uncertainties.

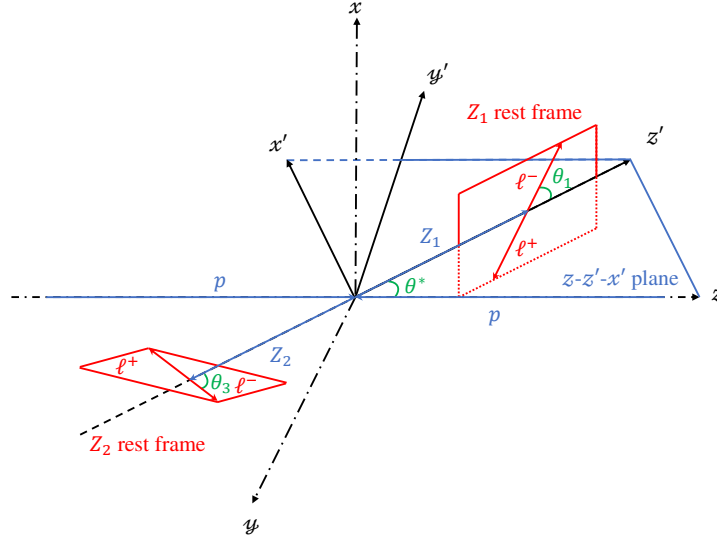


Figure 2: Definition of the angles used for the polarisation measurement and the reference frame used to define the CP-sensitive angles. The xyz -frame (dot-dashed) is the laboratory frame with the z -axis along the beam direction. The $x'y'z'$ -frame (solid) is a new frame used to define the CP-sensitive angles. The z' -axis is defined as the direction of motion of the Z_1 boson in the four-lepton rest frame. The x' -axis defines the reaction plane containing the laboratory z -axis and the z' -axis. The right-hand rule gives the y' -axis.

The MC templates for different ZZ polarisation states were generated at LO in QCD. Higher-order corrections, in both the QCD and EW, on MC templates of the different ZZ polarisation states have to be taken into account when extracting the $Z_L Z_L$ fraction from data. Recently the combined NLO QCD

and EW corrections and the loop-induced $gg \rightarrow ZZ$ corrections to the polarisation structure of ZZ production were calculated at fixed-order with the MoCANLO program [66]. Differential cross-sections for different polarisation states of the $q\bar{q} \rightarrow ZZ$ and $gg \rightarrow ZZ$ processes were provided for several kinematic observables. As in the simulated MC samples, the polarisation definition in the MoCANLO program is also based on the CM frame of the two Z bosons. In order to incorporate the fixed-order, higher-order corrections into the polarisation measurement, a three-step reweighting method is established, using either a one-dimensional (1D) observable or two-dimensional (2D) observables.

- **Step 1: 1D reweighting for each individual polarisation state.** In this step, the reweighting is done separately for the $q\bar{q} \rightarrow ZZ$ and $gg \rightarrow ZZ$ processes. For $q\bar{q} \rightarrow ZZ$, the combined NLO QCD and EW corrections, in a multiplicative approach, as a function of the $\cos \theta_1$ variable are applied by taking the ratio of the differential cross-sections calculated from MoCANLO at NLO and the ones from the MADGRAPH5_AMC@NLO MC samples at the particle level in the fiducial phase space of the measurement, for $Z_T Z_T$, $Z_T Z_L$ and $Z_L Z_L$ events, respectively. An additional reweighting as a function of $\cos \theta_1$ is applied to account for the missing higher-order QCD and parton shower effects by taking the ratio of inclusive SHERPA $q\bar{q} \rightarrow ZZ$ predictions at the particle level to the inclusive MoCANLO calculations. The impact of these two 1D reweighting corrections on the BDT discriminant is mostly of about 20% on the normalisation, and the shape variation is only of 2 – 4%. For the $gg \rightarrow ZZ$ process, which contributes to about 15% of the total signal yield, only the inclusive SHERPA MC sample is available, and the MoCANLO program provides polarised differential cross-sections at LO. Thus the inclusive SHERPA MC sample is reweighted to obtain polarised templates of $Z_T Z_T$, $Z_T Z_L$ and $Z_L Z_L$, by taking the fraction of polarised and inclusive cross-sections calculated by MoCANLO as a function of $\cos \theta_1$. No reweighting is applied to the EW $qq \rightarrow ZZjj$ process and the original MC simulation of polarised samples is used.
- **Step 2: 1D reweighting for the interference effect.** The simulated polarised samples do not consider the interference effects among different polarisation states, while such interference effects are found to be non-negligible in some kinematic regions where the contribution could reach up to 5% [66]. A dedicated template for the interference term is therefore constructed by reweighting the inclusive SHERPA $q\bar{q} \rightarrow ZZ$ events with MoCANLO calculations that include interference contributions, by taking the difference between the inclusive cross-sections and the sum of the three polarised cross-sections as a function of $\cos \theta_1$. For $gg \rightarrow ZZ$ events, the interference effect is found to be negligible and thus ignored. For the subleading EW $qq \rightarrow ZZjj$ process, the interference effect is not included either.
- **Step 3: 2D reweighting for the residual higher-order corrections.** Four templates, including three polarisation states and the interference term, are obtained after the two reweighting steps described above. A closure test is performed by comparing the sum of the four templates and the prediction given by the inclusive SHERPA MC events. Residual discrepancies are observed, which could be due to the non-closure of the 1D reweighting method, resulting from missing higher-order QCD and parton shower effects. An additional 2D reweighting is applied to each of the three polarisation templates to correct the mismodelling by taking the ratio of the non-closure effect and the sum of the three polarisation templates as a function of $\cos \theta_{Z_1}^*$ and $\Delta\phi_{\ell_1 \ell_2}$. The impact of this 2D reweighting on the BDT discriminant is mostly on the shape with a maximum variation of about 10%.

Figure 3 shows the BDT distribution of the three polarisation templates for the $q\bar{q} \rightarrow ZZ$ process before and after the reweighting procedure. To extract the fraction of $Z_L Z_L$ events, a profile binned maximum-likelihood fit [87–89] to the BDT distribution is performed using the final templates for the three polarisation states and the interference term, and other non- ZZ background contributions. The normalisation factors of

the $Z_L Z_L$ template, μ_{LL} , referred as the signal strength, and the combined $Z_T Z_T + Z_T Z_L$ templates, μ_{TX} , are allowed to float in the fit. The signal strength is the ratio of the measured signal contribution relative to the SM expectation. A validation study is performed to show the robustness of the templates, by applying a similar fit to the inclusive POWHEG Box MC events. The extracted $Z_L Z_L$ fraction is compared with the predicted $Z_L Z_L$ fraction, and they are found to be consistent within uncertainties.

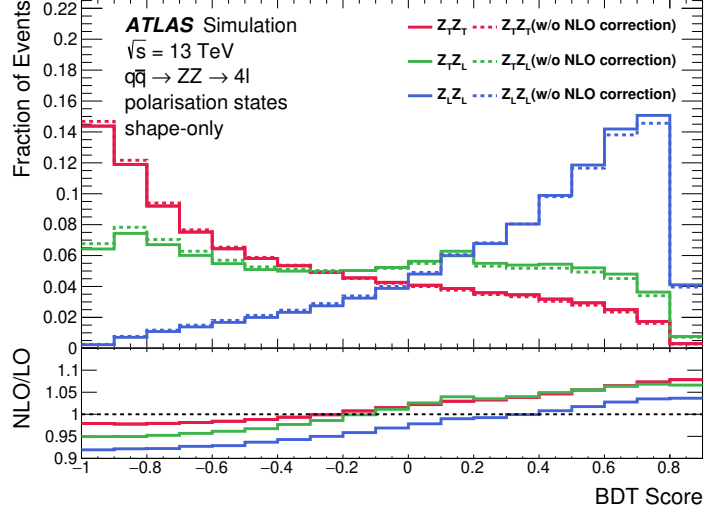


Figure 3: BDT distributions of the three polarisation templates for the $q\bar{q} \rightarrow ZZ$ process, before (dashed lines) and after (solid lines) the reweighting procedure to account for higher-order corrections. All distributions are normalised to the same area. The lower panel shows the ratio of the templates after the corrections to those before the corrections.

6.2 Study of CP property

6.2.1 CP-odd Optimal Observable

The OO defined for the CP study combines the CP-sensitive polar and azimuthal angles of both Z -boson systems, providing additional CP sensitivity from shape differences between the SM and aNTGC predictions. The CP-sensitive polar angles $\theta_1(\theta_3)$ for the $Z_1(Z_2)$ boson are already defined in Section 6.1 and illustrated in Figure 2. The CP-sensitive azimuthal angles ϕ_1 and ϕ_3 are reconstructed in a reference frame illustrated in Figure 2 that allows a direct measure of the Z -boson spin as discussed in Ref. [24, 90]. The CP-sensitive azimuthal angle $\phi_1(\phi_3)$ is the azimuthal angle of the negative lepton in the $Z_1(Z_2)$ rest frame in this new axis system. The differential cross-sections for $\theta_1(\theta_3)$ and $\phi_1(\phi_3)$ are symmetric in the SM but asymmetric in the presence of a CP-odd aNTGC.

To improve the sensitivity, the two CP-sensitive angles $\theta_1(\theta_3)$ and $\phi_1(\phi_3)$ are combined to form an angular observable $T_{yz,1(3)} = \sin \phi_{1(3)} \times \cos \theta_{1(3)}$ that maximises the asymmetry for each Z -boson system. Figures 4(a) and 4(b) show the 2D differential distributions of the CP-sensitive observable T_{yz} of the two Z bosons, the symmetric SM prediction and the asymmetric BSM prediction in the presence of a non-zero f_Z^4 parameter, respectively.

As observed in Figure 4(b), the first (bottom left) and the third (top right) quadrants where both of the Z bosons have negative and positive T_{yz} values, respectively, are the most sensitive regions of the 2D T_{yz} distribution. The OO $\mathcal{O}_{T_{yz,1}T_{yz,3}}$ is defined from the 2D distribution of T_{yz} by grouping together the

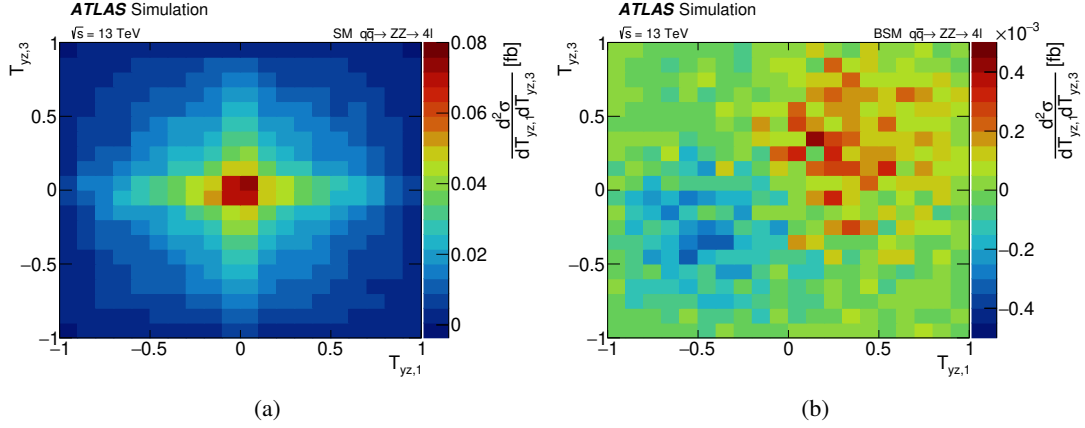


Figure 4: Particle level 2D differential cross-sections of T_{yz} of the two Z bosons for the $q\bar{q} \rightarrow ZZ \rightarrow 4\ell$ process as predicted by (a) the SM and (b) in the presence of the BSM aNTGC vertex. The BSM prediction shows the contribution of the interference effects only, excluding the quadratic term in Equation (1), when $f_Z^4 = 1$.

sensitive and non-sensitive bins to maximise the sensitivity for the four-lepton system. Each bin of the $O_{T_{yz,1}T_{yz,3}}$ observable represents approximately an L-shaped grouping of the bins around the $T_{yz,3} = T_{yz,1}$ line as shown in Figure 5(a). The small fraction of events with miss-paired leptons in the $ZZ \rightarrow 4e$ (4μ) final states was studied and found to have negligible impact on the CP-sensitivity of the OO.

Figure 5(b) shows the measured data compared with the total SM signal and background MC prediction at the detector level of the OO $O_{T_{yz,1}T_{yz,3}}$. The bins 1 to 7 and 24 to 30 in Figure 5(b) represent the first quadrant and the third quadrant, respectively, of the 2D distribution of $T_{yz,1}$ vs $T_{yz,3}$ shown in Figure 4. In these two quadrants, the T_{yz} observables for both Z bosons have the same sign in the SM and are the most CP-sensitive region, along with the two central bins representing the bin number 15 and 16 of the OO. The measured data agree closely with the prediction within the measurement's statistical precision and systematic uncertainties. Figure 5(b) also shows an asymmetric prediction in the presence of a CP odd BSM coupling when $f_Z^4 = 1$.

6.2.2 Detector corrections

Particle-level differential cross-sections for the on-shell ZZ production are obtained by correcting the detector effects such as inefficiency and resolution. The background-subtracted event yields are corrected using an iterative Bayesian unfolding method [91].

The first step of the correction multiplies each bin yield by a fiducial correction factor obtained from the SHERPA SM prediction, which accounts for the events that satisfy the detector level but fail to satisfy the fiducial-level event selections. This correction accounts for the 5 – 20% of the fake fiducial events in various bins caused by the resolution effects. Then, the detector resolution-induced bin migrations are corrected iteratively using the SM particle-level distribution as the initial prior. With an increasing number of iterations, the statistical uncertainty increases, and the residual bias relative to the prior decreases due to the improvement of its knowledge. Two iterations were deemed optimal as a compromise between the increasing statistical uncertainty and decreasing bias. The final step in the unfolding procedure is to correct for the detector inefficiency by dividing the per-bin yield by the ratio of the number of events satisfying

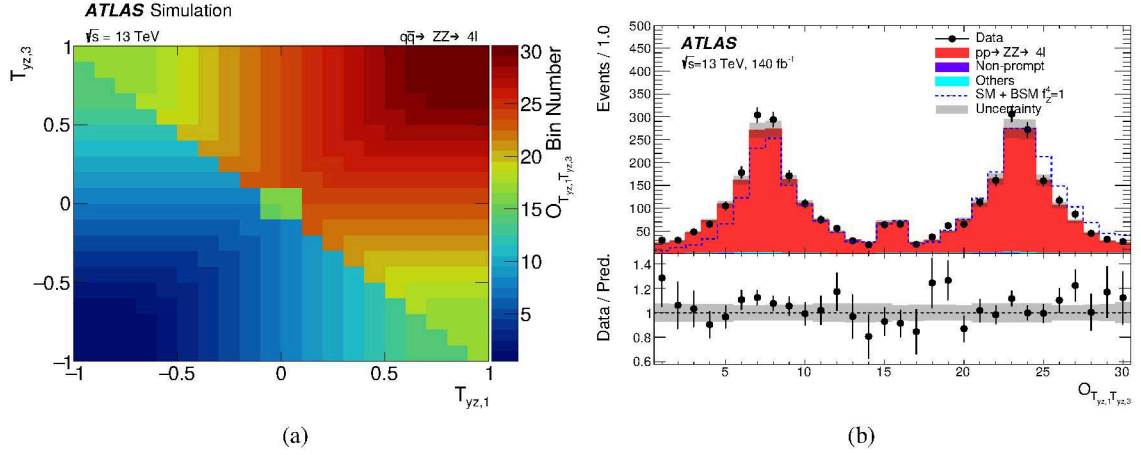


Figure 5: (a) The $2D \rightarrow 1D$ mapping and (b) the detector-level measurement of the OO $O_{T_{yz,1}T_{yz,3}}$. The measured distribution is compared with the SM signal prediction and the total background. The ‘Others’ category includes the contribution from $t\bar{t}Z$ and VVZ processes. The non-prompt background is estimated by using the fake-factor method. The grey band represents the effect of the total theoretical and experimental uncertainties for the detector-level predictions, and the vertical error bars on data represent the statistical uncertainties. The effect of CP-odd BSM coupling is also represented by the dashed histogram.

both the particle- and reconstruction-level selections to the number of events passing the particle-level selections.

A data-driven closure test is performed to evaluate the model dependence of the unfolding method. This test first simulates a pseudo-data sample by reweighting the SM prediction to the shape observed in the data. The pseudo-data sample is then unfolded using the nominal SM prediction. The comparison of the unfolded pseudo-data with the reweighted particle-level prediction gives the intrinsic bias of the unfolding method, which was found to be less than 1% in each bin of the unfolded $O_{T_{yz,1}T_{yz,3}}$ observable in the case of two iterations of unfolding. This resulting bias is taken as a systematic uncertainty of the final result. Moreover, the uncertainty related to the choice of the generator in the unfolding is studied using the alternative POWHEG prediction of the $q\bar{q} \rightarrow ZZ$ process, which is reweighted to match the nominal SHERPA lineshape to avoid double counting of the data-driven bias. The generator bias estimated by comparing the difference between the unfolded results is negligible.

Additionally, an injection test is performed to evaluate the robustness of the unfolding algorithm in the presence of BSM physics in the data. A detector-level distribution for the BSM aNTGC parameter $f_4^Z = 1$ is injected into the SM detector-level prediction. The BSM-injected detector level distribution is then unfolded using the inputs from the nominal SM prediction. When compared, the unfolded distribution agrees closely with the corresponding particle-level distribution within uncertainties.

7 Systematic uncertainties

Both the polarisation and CP property studies presented here are affected by some common sources of theoretical, experimental, and background-related uncertainties.

Theoretical systematic uncertainties affecting the results of this analysis arise from three sources: uncertainties related to the QCD scale dependence, uncertainties related to the choice of the PDF set, and uncertainties related to the higher-order corrections. The impact of each is propagated to the final results. The QCD scale dependency is evaluated individually for three physics processes $q\bar{q} \rightarrow ZZ$, $gg \rightarrow ZZ$, and the EW $qq \rightarrow ZZjj$ by varying the default choice of renormalisation and factorisation scales independently by factors of two and one-half, and then removing combinations where the variations differ by a factor of four. The envelope of the effects from these variations is taken as the final scale uncertainty for each process individually.

The PDF-related uncertainty for each of the signal samples is estimated using the PDF4LHC recommendation [92]. The PDF variations include a set of 100 replica variations on the nominal NNPDF set, two additional variations from the alternative PDF sets of MMHT2014nnlo [93] and CT14nnlo [94], and variations of the strong coupling constant by ± 0.001 around the nominal value of $\alpha_S = 0.118$. The total PDF uncertainty is the absolute envelope of standard deviations of 100 internal variations and of the two alternate PDF variations, added in quadrature with the envelope of the α_S variations.

For the polarisation measurements, dedicated systematic uncertainties are considered in the modelling of the polarisation templates, including theoretical uncertainties from higher-order corrections, PDFs and α_S described above, and the uncertainties associated with the reweighting methods as described in Section 6.1. For both the $q\bar{q} \rightarrow ZZ$ and $gg \rightarrow ZZ$ polarisation templates, the theoretical uncertainties from QCD scales are taken from the MoCANLO calculations by varying the QCD scales as described above, while for the template of the interference term, which is reweighted from the inclusive SHERPA $q\bar{q} \rightarrow ZZ$ samples, these theoretical uncertainties are estimated from the SHERPA sample. The parton showering and hadronisation uncertainty is estimated for the signal by comparing the nominal PYTHIA 8 parton showering with the alternative HERWIG 7 [95, 96] algorithm. Uncertainties from the NLO EW corrections are estimated by taking the difference between the additive and the multiplicative prescription in MoCANLO [66]. For the 1D reweighting method in Section 6.1, the uncertainty is estimated by comparing the reweighted templates using the nominal observable and an alternative observable: the rapidity difference of the two Z bosons. For the additional 2D reweighting, the residual difference between the sum of the four templates and the inclusive prediction from the SHERPA sample is taken as an uncertainty.

For the CP study, additional uncertainties associated with the higher-order corrections applied to the inclusive $q\bar{q} \rightarrow ZZ$ and $gg \rightarrow ZZ$ samples are considered. For the virtual NLO electroweak effects on the $q\bar{q} \rightarrow ZZ$ process, a 100% uncertainty is assigned to the reweighting function to account for non-factorisable effects in events with high QCD activity [97]. The uncertainty in the NLO QCD k -factors for the $gg \rightarrow ZZ$ process is evaluated differentially as a function of the $m_{4\ell}$ as discussed in Ref. [58].

The uncertainties associated with reconstruction, identification, isolation and track-to-vertex matching efficiencies, and momentum resolution and scale of the leptons are the dominant **experimental uncertainties** and originate from imperfect modelling in the simulation and uncertainties in the determination of the correction factors. The uncertainties associated with each scale factor that is applied in the simulation are estimated by modifying the nominal values by their associated uncertainties [77, 98].

An uncertainty of $\pm 0.83\%$ from the measurement of Run 2 data sample luminosity [99] is propagated to the final results. A systematic uncertainty related to the pile-up reweighting is included to cover the uncertainty in the ratio of the predicted and measured pp inelastic cross-sections [100].

The **background-related uncertainties** are from two distinct sources, uncertainties related to the non-prompt background estimate, discussed in Section 5, and the uncertainty related to the background containing four prompt leptons simulated from MC. The simulation of $t\bar{t}Z$ and triboson background

processes are normalised to ATLAS measurements, as outlined in Section 3, and the uncertainty related is estimated by varying the normalisation of the simulated samples by the experimental precision of the ATLAS measurements.

For the CP study, the systematic uncertainties are propagated to the particle level through the unfolding method. The effect of each systematic source is evaluated using simulation. Since the theory variation applied affects both the detector and the particle-level yields, the resulting theory uncertainties on the unfolded cross-sections are minor. Another source of systematic uncertainty related to the intrinsic unfolding bias discussed in Section 6.2.2 is also included in the differential cross-sections and the BSM interpretation.

8 Results

8.1 Polarisation measurements

The profile likelihood fit procedure described in Section 6.1 is performed on the BDT distribution of the data. Systematic uncertainties are modelled as Gaussian-constrained nuisance parameters in the likelihood. Figure 6 shows the post-fit BDT distribution in the signal region. The corresponding pre-fit and post-fit yields in the signal region are detailed in Table 1. The decrease of the yield uncertainty for $Z_T Z_T$ is mainly due to the constraint on the normalisation from the fit and the increase of the yield uncertainty for $Z_L Z_L$ is mainly due to the statistical uncertainty of the signal strength after the fit. The $Z_L Z_L$ signal strength is measured to be $\mu_{LL} = 1.15 \pm 0.27(\text{stat.}) \pm 0.11(\text{syst.}) = 1.15 \pm 0.29$, where the uncertainties are either statistical (stat.) or of systematic (syst.) nature. This corresponds to a significance of 4.3σ . Figure 7 shows the profile likelihood ratio [101] as a function of μ_{LL} . The measured results are consistent with the SM expectation of $\mu_{LL} = 1.00 \pm 0.27$ with an expected significance of 3.8σ . The normalisation factor for the $Z_T Z_X$ template is measured to be $\mu_{TX} = 1.00 \pm 0.05$, also consistent with the SM prediction.

Table 1: Expected and observed numbers of events in the signal region. Numbers are presented before and after the fit to the BDT distribution. The ‘Others’ category represents the contribution from $t\bar{t}Z$ and VVZ . For the $Z_L Z_L$ signal, the pre-fit yield values correspond to the theoretical prediction and corresponding uncertainties. The uncertainties include both of the statistical and systematic contributions. The uncertainty in the total yield can be smaller than the quadrature sum of the contributions because of correlations resulting from the fit.

		Pre-fit	Post-fit
ZZ	$Z_L Z_L$	189.3 \pm 8.7	220 \pm 54
	$Z_T Z_L$	710 \pm 29	711 \pm 29
	$Z_T Z_T$	2170 \pm 120	2147 \pm 60
	Interference	33.7 \pm 2.8	33.4 \pm 2.7
Non-prompt		18.7 \pm 7.1	18.5 \pm 7.0
Others		20.0 \pm 3.7	19.9 \pm 3.7
Total		3140 \pm 150	3149 \pm 57
Data		3149	3149

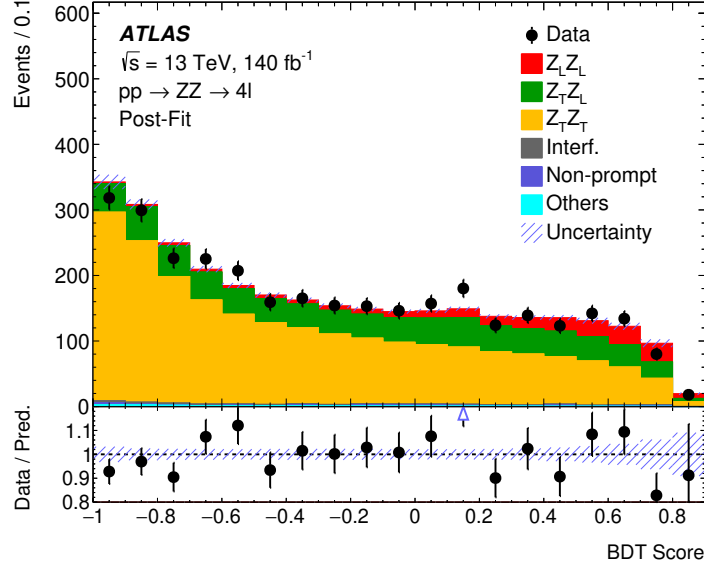


Figure 6: The BDT distribution of the data and the post-fit SM predictions. The ‘Others’ category represents the contribution from $t\bar{t}Z$ and VVZ . The lower panel shows the ratio of the data points to the post-fit total prediction. The arrow indicates that the ratio lies outside the range covered by the vertical axis. The uncertainty bands include both of the statistical and systematic uncertainties as obtained by the fit.

An additional profile likelihood fit is performed to convert the measured μ_{LL} to the measured fiducial cross-section, with the normalisation effects from the theoretical uncertainties of the $Z_L Z_L$ template removed. The fiducial cross-section of the $Z_L Z_L$ production is measured to be $\sigma_{Z_L Z_L}^{\text{obs.}} = 2.45 \pm 0.56(\text{stat.}) \pm 0.21(\text{syst.}) \text{ fb} = 2.45 \pm 0.60 \text{ fb}$, consistent with the SM prediction of $\sigma_{Z_L Z_L}^{\text{pred.}} = 2.10 \pm 0.09 \text{ fb}$. The SM prediction includes NLO QCD and EW corrections for the $q\bar{q} \rightarrow ZZ$ process, the LO prediction for the $gg \rightarrow ZZ$ process, both of which are calculated from MoCANLO, and the LO prediction for the EW $qq \rightarrow ZZjj$ process. The uncertainty on the prediction is dominated by QCD scale and PDF uncertainties. The measurement is limited by data statistical uncertainty and the impact of uncertainties in the measured $Z_L Z_L$ fiducial cross-section is shown in Table 2, with the leading contribution from the theoretical modelling of the polarisation templates.

8.2 Unfolded differential measurement

The differential cross-section for the $ZZ \rightarrow 4\ell$ production as a function of the OO $O_{T_{yz,1}T_{yz,3}}$ is shown in Figure 8 and compared with two different SM predictions, where the $q\bar{q} \rightarrow ZZ$ contribution is predicted either using the SHERPA or POWHEG generators. The band represents the total uncertainties, which are small and flat, related to the theoretical, experimental, and unfolding procedure-related uncertainties on the unfolded differential cross-section. Similarly, for the SM predictions, the uncertainty bands represent the total theoretical uncertainties on the total prediction. For each bin, the measured cross-section from the data agrees closely with both sets of predicted cross-sections.

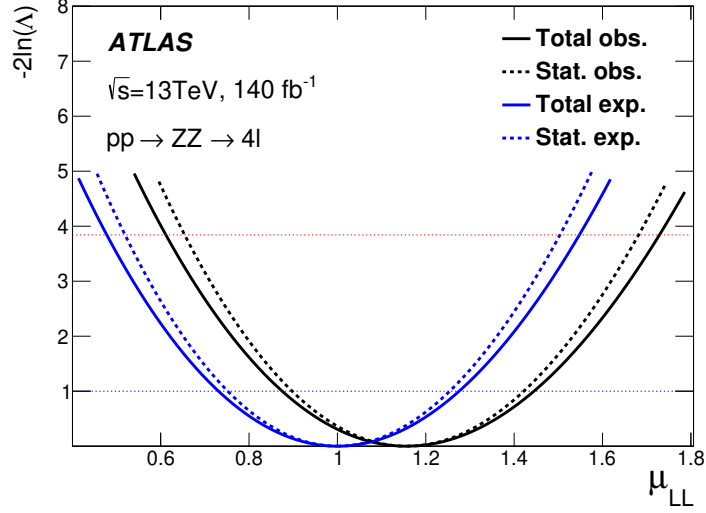


Figure 7: Observed and expected profile likelihood ratio, $-2\ln\Lambda$, as a function of the signal strength μ_{LL} , with (solid curves) and without (dashed curves) systematic uncertainties included.

Table 2: Impact of uncertainties in the measured fiducial cross-section $\sigma_{Z_L Z_L}$ from the fit. The impact from a group of nuisance parameters is defined via quadrature subtraction of the $\sigma_{Z_L Z_L}$ uncertainties: $\sqrt{(\Delta\sigma)^2 - (\Delta\sigma')^2}$, where $\Delta\sigma$ is the uncertainty of the $\sigma_{Z_L Z_L}$ from the nominal fit and the $\Delta\sigma'$ is the uncertainty of the $\sigma_{Z_L Z_L}$ when this group of nuisance parameters are fixed to their best-fit values from the nominal fit.

Contribution	Relative uncertainty [%]
Total	24
Data statistical uncertainty	23
Total systematic uncertainty	8.8
MC statistical uncertainty	1.7
Theoretical systematic uncertainties	
$q\bar{q} \rightarrow ZZ$ interference modelling	6.9
NLO reweighting observable choice for $q\bar{q} \rightarrow ZZ$	3.7
PDF, α_s and parton shower for $q\bar{q} \rightarrow ZZ$	2.2
NLO reweighting non-closure	1.0
QCD scale for $q\bar{q} \rightarrow ZZ$	0.2
NLO EW corrections for $q\bar{q} \rightarrow ZZ$	0.2
$gg \rightarrow ZZ$ modelling	1.4
Experimental systematic uncertainties	
Luminosity	0.8
Muons	0.6
Electrons	0.4
Non-prompt background	0.3
Pile-up reweighting	0.3
Triboson and $t\bar{t}Z$ normalisations	0.1

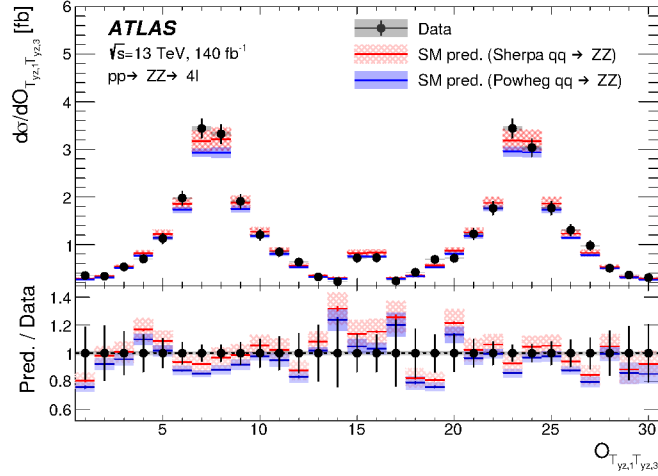


Figure 8: Unfolded differential cross-section as a function of the Optimal Observable $O_{T_{yz,1}T_{yz,3}}$. The grey, red and blue uncertainty bands represent the respective systematic uncertainties in the measured unfolded cross-section and predicted particle-level cross-sections, where the $q\bar{q} \rightarrow ZZ$ contribution is predicted using either the SHERPA or POWHEG generators. The vertical error bars represent the total uncertainties in the measured differential cross-section.

8.3 BSM interpretation

The differential cross-section as a function of $O_{T_{yz,1}T_{yz,3}}$ and the corresponding SM + aNTGC prediction are used to define a likelihood function,

$$\mathcal{L} = \frac{1}{\sqrt{(2\pi)^k |V|}} \exp \left\{ -\frac{1}{2} \left[\vec{\sigma}^{\text{meas.}} - \vec{\sigma}^{\text{pred.}}(\vec{\theta}) \right]^T V^{-1} \left[\vec{\sigma}^{\text{meas.}} - \vec{\sigma}^{\text{pred.}}(\vec{\theta}) \right] \right\} \times \prod_i \mathcal{G}(\theta_i, 0, 1), \quad (2)$$

where $\vec{\sigma}^{\text{meas.}}$ and $\vec{\sigma}^{\text{pred.}}$ are the measured and predicted differential cross-sections as a function of $O_{T_{yz,1}T_{yz,3}}$, respectively, and V is the total covariance matrix defined by the sum of the statistical and systematic covariances in $\vec{\sigma}^{\text{meas.}}$ and $\vec{\sigma}^{\text{pred.}}$. Each systematic uncertainty is treated as fully correlated across bins but uncorrelated with other uncertainty sources. Each source of theoretical uncertainty affecting the SM particle level prediction of the $q\bar{q} \rightarrow ZZ$, $g g \rightarrow ZZ$ and EW $q q \rightarrow ZZ j j$ processes is implemented as nuisance parameters, $\vec{\theta}$, with Gaussian constraints, $\mathcal{G}(\theta_i, 0, 1)$.

Limits are set on CP-odd aNTGC parameters in two scenarios, with linear interference terms only and with quadratic terms included. For each CP-odd aNTGC parameter under test, the other is set to zero, and the test statistics are constructed based on the profile likelihood ratio [101],

$$q = -2 \ln \frac{\mathcal{L}(c, \hat{\hat{\theta}}(c))}{\mathcal{L}(\hat{c}, \hat{\hat{\theta}}(c))}, \quad (3)$$

where c is the aNTGC parameter, \hat{c} and $\hat{\hat{\theta}}$ are the unconditional maximum-likelihood estimators, and $\hat{\hat{\theta}}(c)$ is the conditional maximum-likelihood estimator under the c hypothesis.

Using the test statistic in Equation (3), which is assumed to be distributed according to a χ^2 distribution with one degree of freedom following Wilks' theorem [102], a 95% confidence level for each aNTGC parameter is calculated, as shown in Table 3. Theoretical uncertainties related to the QCD scale, PDF, α_S ,

and parton showering for the $q\bar{q} \rightarrow ZZ$ predictions have the largest impact on the estimated confidence interval.

From Table 3, the constraints on the CP-odd f_Z^4 and f_γ^4 aNTGC parameters using the linear interference term when the quadratic term is set to zero are much worse than those obtained using high- p_T kinematic observables with quadratic terms included [23], as expected. However, these are the first constraints on CP-odd aNTGC parameters using only linear interference terms with a dedicated CP-sensitive OO, based on angular observables. Additional likelihood fits are performed with the quadratic terms included, and the constraints on f_Z^4 and f_γ^4 are improved by one order of magnitude, but since $O_{T_{yz,1}T_{yz,3}}$ is not sensitive to the high- p_T regime, such constraints are still not tighter than those obtained with high- p_T kinematic observables.

Table 3: Expected and observed 95% confidence interval for the two aNTGC operators using the measured particle-level differential cross-section as a function of $O_{T_{yz,1}T_{yz,3}}$. For the ‘Full’ case, both the interference and the quadratic terms are included in the aNTGC prediction.

aNTGC parameter	Interference only		Full	
	Expected	Observed	Expected	Observed
f_Z^4	$[-0.16, 0.16]$	$[-0.12, 0.20]$	$[-0.013, 0.012]$	$[-0.012, 0.012]$
f_γ^4	$[-0.30, 0.30]$	$[-0.34, 0.28]$	$[-0.015, 0.015]$	$[-0.015, 0.015]$

9 Conclusion

Studies of the polarisation and CP properties in $ZZ \rightarrow 4\ell$ production are presented for the first time, using proton–proton collisions at the LHC collected with the ATLAS detector at $\sqrt{s} = 13$ TeV with an integrated luminosity of 140 fb^{-1} . The Z-boson candidates are reconstructed with same-flavour, opposite-charge electron or muon pairs, and they are required to be on-shell with $|m_{\ell\ell} - m_Z| < 10 \text{ GeV}$. The production of two simultaneously longitudinally polarised Z bosons is measured with observed and expected significances of 4.3 and 3.8 standard deviations, respectively. The production cross-section of $Z_L Z_L$ events is measured in a fiducial phase space as $2.45 \pm 0.60 \text{ fb}$, consistent with the Standard Model prediction of $2.10 \pm 0.09 \text{ fb}$ with NLO QCD and EW corrections considered. The differential cross-section of the inclusive ZZ boson production as a function of a CP-sensitive angular observable, $O_{T_{yz,1}T_{yz,3}}$, is also measured. Furthermore, the measured differential cross-section is used to constrain the CP-odd neutral triple gauge couplings f_Z^4 and f_γ^4 . No significant deviations from the SM are observed.

Acknowledgements

We thank CERN for the very successful operation of the LHC, as well as the support staff from our institutions without whom ATLAS could not be operated efficiently.

We acknowledge the support of ANPCyT, Argentina; YerPhI, Armenia; ARC, Australia; BMWFW and FWF, Austria; ANAS, Azerbaijan; CNPq and FAPESP, Brazil; NSERC, NRC and CFI, Canada; CERN; ANID, Chile; CAS, MOST and NSFC, China; Minciencias, Colombia; MEYS CR, Czech Republic; DNRF

and DNSRC, Denmark; IN2P3-CNRS and CEA-DRF/IRFU, France; SRNSFG, Georgia; BMBF, HGF and MPG, Germany; GSRI, Greece; RGC and Hong Kong SAR, China; ISF and Benoziyo Center, Israel; INFN, Italy; MEXT and JSPS, Japan; CNRST, Morocco; NWO, Netherlands; RCN, Norway; MEiN, Poland; FCT, Portugal; MNE/IFA, Romania; MESTD, Serbia; MSSR, Slovakia; ARRS and MIZŠ, Slovenia; DSI/NRF, South Africa; MICINN, Spain; SRC and Wallenberg Foundation, Sweden; SERI, SNSF and Cantons of Bern and Geneva, Switzerland; MOST, Taiwan; TENMAK, Türkiye; STFC, United Kingdom; DOE and NSF, United States of America. In addition, individual groups and members have received support from BCKDF, CANARIE, Compute Canada and CRC, Canada; PRIMUS 21/SCI/017 and UNCE SCI/013, Czech Republic; COST, ERC, ERDF, Horizon 2020 and Marie Skłodowska-Curie Actions, European Union; Investissements d’Avenir Labex, Investissements d’Avenir Idex and ANR, France; DFG and AvH Foundation, Germany; Herakleitos, Thales and Aristeia programmes co-financed by EU-ESF and the Greek NSRF, Greece; BSF-NSF and MINERVA, Israel; Norwegian Financial Mechanism 2014-2021, Norway; NCN and NAWA, Poland; La Caixa Banking Foundation, CERCA Programme Generalitat de Catalunya and PROMETEO and GenT Programmes Generalitat Valenciana, Spain; Göran Gustafssons Stiftelse, Sweden; The Royal Society and Leverhulme Trust, United Kingdom.

The crucial computing support from all WLCG partners is acknowledged gratefully, in particular from CERN, the ATLAS Tier-1 facilities at TRIUMF (Canada), NDGF (Denmark, Norway, Sweden), CC-IN2P3 (France), KIT/GridKA (Germany), INFN-CNAF (Italy), NL-T1 (Netherlands), PIC (Spain), ASGC (Taiwan), RAL (UK) and BNL (USA), the Tier-2 facilities worldwide and large non-WLCG resource providers. Major contributors of computing resources are listed in Ref. [103].

References

- [1] D. Liu and L.-T. Wang, *Prospects for precision measurement of diboson processes in the semileptonic decay channel in future LHC runs*, *Phys. Rev. D* **99** (2019) 055001, arXiv: [1804.08688 \[hep-ph\]](#).
- [2] CMS Collaboration, *Measurement of the Polarization of W Bosons with Large Transverse Momenta in W+Jets Events at the LHC*, *Phys. Rev. Lett.* **107** (2011) 021802, arXiv: [1104.3829 \[hep-ex\]](#).
- [3] ATLAS Collaboration, *Measurement of the polarisation of W bosons produced with large transverse momentum in pp collisions at $\sqrt{s} = 7$ TeV with the ATLAS experiment*, *Eur. Phys. J. C* **72** (2012) 2001, arXiv: [1203.2165 \[hep-ex\]](#).
- [4] ATLAS Collaboration, *Measurement of the angular coefficients in Z-boson events using electron and muon pairs from data taken at $\sqrt{s} = 8$ TeV with the ATLAS detector*, *JHEP* **08** (2016) 159, arXiv: [1606.00689 \[hep-ex\]](#).
- [5] CMS Collaboration, *Angular coefficients of Z bosons produced in pp collisions at $\sqrt{s} = 8$ TeV and decaying to $\mu^+\mu^-$ as a function of transverse momentum and rapidity*, *Phys. Lett. B* **750** (2015) 154, arXiv: [1504.03512 \[hep-ex\]](#).
- [6] ATLAS Collaboration, *Measurement of the W boson polarisation in $t\bar{t}$ events from pp collisions at $\sqrt{s} = 8$ TeV in the lepton+jets channel with ATLAS*, *Eur. Phys. J. C* **77** (2017) 264, arXiv: [1612.02577 \[hep-ex\]](#), Erratum: *Eur. Phys. J. C* **79** (2019) 19.
- [7] CMS Collaboration, *Measurement of the W boson helicity fractions in the decays of top quark pairs to lepton+jets final states produced in pp collisions at $\sqrt{s} = 8$ TeV*, *Phys. Lett. B* **762** (2016) 512, arXiv: [1605.09047 \[hep-ex\]](#).
- [8] ATLAS and CMS Collaborations, *Combination of the W boson polarization measurements in top quark decays using ATLAS and CMS data at $\sqrt{s} = 8$ TeV*, *JHEP* **08** (2020) 051, arXiv: [2005.03799 \[hep-ex\]](#).
- [9] ATLAS Collaboration, *Measurement of $W^\pm Z$ production cross sections and gauge boson polarisation in pp collisions at $\sqrt{s} = 13$ TeV with the ATLAS detector*, *Eur. Phys. J. C* **79** (2019) 535, arXiv: [1902.05759 \[hep-ex\]](#).
- [10] CMS Collaboration, *Measurement of the inclusive and differential WZ production cross sections, polarization angles, and triple gauge couplings in pp collisions at $\sqrt{s} = 13$ TeV*, *JHEP* **07** (2021) 032, arXiv: [2110.11231 \[hep-ex\]](#).
- [11] CMS Collaboration, *Measurements of production cross sections of polarized same-sign W boson pairs in association with two jets in proton–proton collisions at $\sqrt{s} = 13$ TeV*, *Phys. Lett. B* **812** (2021) 136018, arXiv: [2009.09429 \[hep-ex\]](#).
- [12] ATLAS Collaboration, *Observation of gauge boson joint-polarisation states in $W^\pm Z$ production from pp collisions at $\sqrt{s} = 13$ TeV with the ATLAS detector*, *Phys. Lett. B* **843** (2022) 137895, arXiv: [2211.09435 \[hep-ex\]](#).
- [13] R. L. Workman et al., *Review of Particle Physics*, *PTEP* **2022** (2022) 083C01.
- [14] M. B. Gavela, P. Hernández, J. Orloff and O. Pène, *Standard model CP violation and baryon asymmetry*, *Mod. Phys. Lett. A* **9** (1994) 795, arXiv: [hep-ph/9312215](#).

- [15] A. G. Cohen, D. B. Kaplan and A. E. Nelson, *Progress in Electroweak Baryogenesis*, *Ann. Rev. Nucl. Part. Sci.* **43** (1993) 27, arXiv: [hep-ph/9302210](#).
- [16] P. Huet and E. Sather, *Electroweak baryogenesis and standard model CP violation*, *Phys. Rev. D* **51** (1995) 379, arXiv: [hep-ph/9404302](#).
- [17] ATLAS Collaboration, *Measurement of ZZ production in pp collisions at $\sqrt{s} = 7$ TeV and limits on anomalous ZZZ and ZZ γ couplings with the ATLAS detector*, *JHEP* **03** (2013) 128, arXiv: [1211.6096 \[hep-ex\]](#).
- [18] ATLAS Collaboration, *Measurement of the ZZ production cross section in proton–proton collisions at $\sqrt{s} = 8$ TeV using the ZZ $\rightarrow \ell^- \ell^+ \ell'^- \ell'^+$ and ZZ $\rightarrow \ell^- \ell^+ \nu \bar{\nu}$ decay channels with the ATLAS detector*, *JHEP* **01** (2017) 099, arXiv: [1610.07585 \[hep-ex\]](#).
- [19] ATLAS Collaboration, *Measurement of ZZ production in the $\ell\ell\nu\nu$ final state with the ATLAS detector in pp collisions at $\sqrt{s} = 13$ TeV*, *JHEP* **10** (2019) 127, arXiv: [1905.07163 \[hep-ex\]](#).
- [20] ATLAS Collaboration, *ZZ $\rightarrow \ell^+ \ell^- \ell'^+ \ell'^-$ cross-section measurements and search for anomalous triple gauge couplings in 13 TeV pp collisions with the ATLAS detector*, *Phys. Rev. D* **97** (2018) 032005, arXiv: [1709.07703 \[hep-ex\]](#).
- [21] CMS Collaboration, *Measurement of the pp \rightarrow ZZ production cross section and constraints on anomalous triple gauge couplings in four-lepton final states at $\sqrt{s} = 8$ TeV*, *Phys. Lett. B* **740** (2015) 250, arXiv: [1406.0113 \[hep-ex\]](#),
Erratum: *Phys. Lett. B* **757**, 569–569 (2016).
- [22] CMS Collaboration, *Measurements of the ZZ production cross sections in the $2\ell 2\nu$ channel in proton–proton collisions at $\sqrt{s} = 7$ and 8 TeV and combined constraints on triple gauge couplings*, *Eur. Phys. J. C* **75** (2015) 511, arXiv: [1503.05467 \[hep-ex\]](#).
- [23] CMS Collaboration, *Measurements of pp \rightarrow ZZ production cross sections and constraints on anomalous triple gauge couplings at $\sqrt{s} = 13$ TeV*, *Eur. Phys. J. C* **81** (2021) 200, arXiv: [2009.01186 \[hep-ex\]](#).
- [24] R. Rahaman and R. K. Singh, *On polarization parameters of spin-1 particles and anomalous couplings in $e^+e^- \rightarrow ZZ/Z\gamma$* , *Eur. Phys. J. C* **76** (2016) 539, arXiv: [1604.06677 \[hep-ph\]](#).
- [25] R. Rahaman and R. K. Singh, *Anomalous triple gauge boson couplings in ZZ production at the LHC and the role of Z boson polarizations*, *Nucl. Phys. B* **948** (2019) 114754, arXiv: [1810.11657 \[hep-ph\]](#).
- [26] G. J. Gounaris, J. Layssac and F. M. Renard, *Signatures of the anomalous Z γ and ZZ production at lepton and hadron colliders*, *Phys. Rev. D* **61** (2000) 073013, arXiv: [hep-ph/9910395](#).
- [27] ATLAS Collaboration, *Differential cross-section measurements for the electroweak production of dijets in association with a Z boson in proton–proton collisions at ATLAS*, *Eur. Phys. J. C* **81** (2021) 163, arXiv: [2006.15458 \[hep-ex\]](#).
- [28] A. Biekötter, P. Gregg, F. Krauss and M. Schönherr, *Constraining CP violating operators in charged and neutral triple gauge couplings*, *Phys. Lett. B* **817** (2021) 136311, arXiv: [2102.01115 \[hep-ph\]](#).
- [29] ATLAS Collaboration, *The ATLAS Experiment at the CERN Large Hadron Collider*, *JINST* **3** (2008) S08003.

- [30] ATLAS Collaboration, *The ATLAS Collaboration Software and Firmware*, ATL-SOFT-PUB-2021-001, 2021, URL: <https://cds.cern.ch/record/2767187>.
- [31] ATLAS Collaboration, *Performance of electron and photon triggers in ATLAS during LHC Run 2*, *Eur. Phys. J. C* **80** (2020) 47, arXiv: [1909.00761 \[hep-ex\]](#).
- [32] ATLAS Collaboration, *Performance of the ATLAS muon triggers in Run 2*, *JINST* **15** (2020) P09015, arXiv: [2004.13447 \[hep-ex\]](#).
- [33] E. Bothmann et al., *Event Generation with Sherpa 2.2*, *SciPost Phys.* **7** (2019) 034, arXiv: [1905.09127 \[hep-ph\]](#).
- [34] T. Gleisberg and S. Höche, *Comix, a new matrix element generator*, *JHEP* **12** (2008) 039, arXiv: [0808.3674 \[hep-ph\]](#).
- [35] S. Schumann and F. Krauss, *A parton shower algorithm based on Catani–Seymour dipole factorisation*, *JHEP* **03** (2008) 038, arXiv: [0709.1027 \[hep-ph\]](#).
- [36] S. Höche, F. Krauss, M. Schönherr and F. Siegert, *A critical appraisal of NLO+PS matching methods*, *JHEP* **09** (2012) 049, arXiv: [1111.1220 \[hep-ph\]](#).
- [37] S. Catani, F. Krauss, B. R. Webber and R. Kuhn, *QCD Matrix Elements + Parton Showers*, *JHEP* **11** (2001) 063, arXiv: [hep-ph/0109231](#).
- [38] S. Höche, F. Krauss, M. Schönherr and F. Siegert, *QCD matrix elements + parton showers: The NLO case*, *JHEP* **04** (2013) 027, arXiv: [1207.5030 \[hep-ph\]](#).
- [39] F. Cascioli, P. Maierhöfer and S. Pozzorini, *Scattering Amplitudes with Open Loops*, *Phys. Rev. Lett.* **108** (2012) 111601, arXiv: [1111.5206 \[hep-ph\]](#).
- [40] F. Buccioni et al., *OpenLoops 2*, *Eur. Phys. J. C* **79** (2019) 866, arXiv: [1907.13071 \[hep-ph\]](#).
- [41] A. Denner, S. Dittmaier and L. Hofer, *COLLIER: A fortran-based complex one-loop library in extended regularizations*, *Comput. Phys. Commun.* **212** (2017) 220, arXiv: [1604.06792 \[hep-ph\]](#).
- [42] The NNPDF Collaboration, R. D. Ball et al., *Parton distributions for the LHC run II*, *JHEP* **04** (2015) 040, arXiv: [1410.8849 \[hep-ph\]](#).
- [43] B. Biedermann, A. Denner, S. Dittmaier, L. Hofer and B. Jäger, *Electroweak corrections to $pp \rightarrow \mu^+ \mu^- e^+ e^- + X$ at the LHC: a Higgs background study*, *Phys. Rev. Lett.* **116** (2016) 161803, arXiv: [1601.07787 \[hep-ph\]](#).
- [44] B. Biedermann, A. Denner, S. Dittmaier, L. Hofer and B. Jäger, *Next-to-leading-order electroweak corrections to the production of four charged leptons at the LHC*, *JHEP* **01** (2017) 033, arXiv: [1611.05338 \[hep-ph\]](#).
- [45] S. Alioli, P. Nason, C. Oleari and E. Re, *A general framework for implementing NLO calculations in shower Monte Carlo programs: the POWHEG BOX*, *JHEP* **06** (2010) 043, arXiv: [1002.2581 \[hep-ph\]](#).
- [46] T. Melia, P. Nason, R. Rontsch and G. Zanderighi, *W^+W^- , WZ and ZZ production in the POWHEG BOX*, *JHEP* **11** (2011) 078, arXiv: [1107.5051 \[hep-ph\]](#).

- [47] P. Nason and G. Zanderighi, W^+W^- , WZ and ZZ production in the POWHEG-BOX-V2, *Eur. Phys. J. C* **74** (2014) 2702, arXiv: 1311.1365 [hep-ph].
- [48] T. Sjöstrand, S. Mrenna and P. Skands, A brief introduction to PYTHIA 8.1, *Comput. Phys. Commun.* **178** (2008) 852, arXiv: 0710.3820 [hep-ph].
- [49] ATLAS Collaboration, Measurement of the Z/γ^* boson transverse momentum distribution in pp collisions at $\sqrt{s} = 7$ TeV with the ATLAS detector, *JHEP* **09** (2014) 145, arXiv: 1406.3660 [hep-ex].
- [50] H.-L. Lai et al., New parton distributions for collider physics, *Phys. Rev. D* **82** (2010) 074024, arXiv: 1007.2241 [hep-ph].
- [51] J. Pumplin et al., New Generation of Parton Distributions with Uncertainties from Global QCD Analysis, *JHEP* **07** (2002) 012, arXiv: hep-ph/0201195.
- [52] F. Cascioli et al., ZZ production at hadron colliders in NNLO QCD, *Phys. Lett. B* **735** (2014) 311, arXiv: 1405.2219 [hep-ph].
- [53] M. Grazzini, S. Kallweit and D. Rathlev, ZZ production at the LHC: fiducial cross sections and distributions in NNLO QCD, *Phys. Lett. B* **750** (2015) 407, arXiv: 1507.06257 [hep-ph].
- [54] M. Grazzini, S. Kallweit and M. Wiesemann, Fully differential NNLO computations with MATRIX, *Eur. Phys. J. C* **78** (2018) 537, arXiv: 1711.06631 [hep-ph].
- [55] S. Kallweit and M. Wiesemann, ZZ production at the LHC: NNLO predictions for $2\ell 2\nu$ and 4ℓ signatures, *Phys. Lett. B* **786** (2018) 382, arXiv: 1806.05941 [hep-ph].
- [56] ATLAS Collaboration, Measurements of differential cross-sections in four-lepton events in 13 TeV proton–proton collisions with the ATLAS detector, *JHEP* **07** (2021) 005, arXiv: 2103.01918 [hep-ex].
- [57] F. Caola, K. Melnikov, R. Röntsch and L. Tancredi, QCD corrections to ZZ production in gluon fusion at the LHC, *Phys. Rev. D* **92** (2015) 094028, arXiv: 1509.06734 [hep-ph].
- [58] F. Caola, M. Dowling, K. Melnikov, R. Röntsch and L. Tancredi, QCD corrections to vector boson pair production in gluon fusion including interference effects with off-shell Higgs at the LHC, *JHEP* **07** (2016) 087, arXiv: 1605.04610 [hep-ph].
- [59] G. Passarino, Higgs CAT, *Eur. Phys. J. C* **74** (2014) 2866, arXiv: 1312.2397 [hep-ph].
- [60] D. de Florian et al., Handbook of LHC Higgs Cross Sections: 4. Deciphering the Nature of the Higgs Sector, (2016), arXiv: 1610.07922 [hep-ph].
- [61] J. Alwall et al., The automated computation of tree-level and next-to-leading order differential cross sections, and their matching to parton shower simulations, *JHEP* **07** (2014) 079, arXiv: 1405.0301 [hep-ph].
- [62] T. Sjöstrand et al., An introduction to PYTHIA 8.2, *Comput. Phys. Commun.* **191** (2015) 159, arXiv: 1410.3012 [hep-ph].
- [63] NNPDF Collaboration, R. D. Ball et al., Parton distributions with LHC data, *Nucl. Phys. B* **867** (2013) 244, arXiv: 1207.1303 [hep-ph].

- [64] ATLAS Collaboration, *ATLAS Pythia 8 tunes to 7 TeV data*, ATL-PHYS-PUB-2014-021, 2014, URL: <https://cds.cern.ch/record/1966419>.
- [65] D. Buarque Franzosi, O. Mattelaer, R. Ruiz and S. Shil, *Automated predictions from polarized matrix elements*, *JHEP* **04** (2020) 082, arXiv: [1912.01725 \[hep-ph\]](#).
- [66] A. Denner and G. Pelliccioli, *NLO EW and QCD corrections to polarized ZZ production in the four-charged-lepton channel at the LHC*, *JHEP* **10** (2021) 097, arXiv: [2107.06579 \[hep-ph\]](#).
- [67] L. Lönnblad, *Correcting the Colour-Dipole Cascade Model with Fixed Order Matrix Elements*, *JHEP* **05** (2002) 046, arXiv: [hep-ph/0112284](#).
- [68] L. Lönnblad and S. Prestel, *Matching tree-level matrix elements with interleaved showers*, *JHEP* **03** (2012) 019, arXiv: [1109.4829 \[hep-ph\]](#).
- [69] ATLAS Collaboration, *Measurement of the $t\bar{t}Z$ and $t\bar{t}W$ cross sections in proton–proton collisions at $\sqrt{s} = 13$ TeV with the ATLAS detector*, *Phys. Rev. D* **99** (2019) 072009, arXiv: [1901.03584 \[hep-ex\]](#).
- [70] ATLAS Collaboration, *Evidence for the production of three massive vector bosons with the ATLAS detector*, *Phys. Lett. B* **798** (2019) 134913, arXiv: [1903.10415 \[hep-ex\]](#).
- [71] C. Anastasiou, L. Dixon, K. Melnikov and F. Petriello, *High-precision QCD at hadron colliders: Electroweak gauge boson rapidity distributions at next-to-next-to leading order*, *Phys. Rev. D* **69** (2004) 094008, arXiv: [hep-ph/0312266](#).
- [72] C. Degrande et al., *UFO - The Universal FeynRules Output*, *Comput. Phys. Commun.* **183** (2012) 1201, arXiv: [1108.2040 \[hep-ph\]](#).
- [73] ATLAS Collaboration, *The ATLAS Simulation Infrastructure*, *Eur. Phys. J. C* **70** (2010) 823, arXiv: [1005.4568 \[physics.ins-det\]](#).
- [74] S. Agostinelli et al., *GEANT4 – a simulation toolkit*, *Nucl. Instrum. Meth. A* **506** (2003) 250.
- [75] ATLAS Collaboration, *The Pythia 8 A3 tune description of ATLAS minimum bias and inelastic measurements incorporating the Donnachie–Landshoff diffractive model*, ATL-PHYS-PUB-2016-017, 2016, URL: <https://cds.cern.ch/record/2206965>.
- [76] ATLAS Collaboration, *Electron and photon performance measurements with the ATLAS detector using the 2015–2017 LHC proton–proton collision data*, *JINST* **14** (2019) P12006, arXiv: [1908.00005 \[hep-ex\]](#).
- [77] ATLAS Collaboration, *Muon reconstruction and identification efficiency in ATLAS using the full Run 2 pp collision data set at $\sqrt{s} = 13$ TeV*, *Eur. Phys. J. C* **81** (2021) 578, arXiv: [2012.00578 \[hep-ex\]](#).
- [78] ATLAS Collaboration, *Jet reconstruction and performance using particle flow with the ATLAS Detector*, *Eur. Phys. J. C* **77** (2017) 466, arXiv: [1703.10485 \[hep-ex\]](#).
- [79] M. Cacciari, G. P. Salam and G. Soyez, *The anti- k_t jet clustering algorithm*, *JHEP* **04** (2008) 063, arXiv: [0802.1189 \[hep-ph\]](#).
- [80] M. Cacciari, G. P. Salam and G. Soyez, *FastJet user manual*, *Eur. Phys. J. C* **72** (2012) 1896, arXiv: [1111.6097 \[hep-ph\]](#).

- [81] ATLAS Collaboration, *Jet energy scale and resolution measured in proton–proton collisions at $\sqrt{s} = 13$ TeV with the ATLAS detector*, *Eur. Phys. J. C* **81** (2020) 689, arXiv: [2007.02645 \[hep-ex\]](#).
- [82] ATLAS Collaboration, *Performance of pile-up mitigation techniques for jets in pp collisions at $\sqrt{s} = 8$ TeV using the ATLAS detector*, *Eur. Phys. J. C* **76** (2016) 581, arXiv: [1510.03823 \[hep-ex\]](#).
- [83] ATLAS Collaboration, *ATLAS flavour-tagging algorithms for the LHC Run 2 pp collision dataset*, *Eur. Phys. J. C* **83** (2022) 681, arXiv: [2211.16345 \[physics.data-an\]](#).
- [84] ATLAS Collaboration, *ATLAS b-jet identification performance and efficiency measurement with $t\bar{t}$ events in pp collisions at $\sqrt{s} = 13$ TeV*, *Eur. Phys. J. C* **79** (2019) 970, arXiv: [1907.05120 \[hep-ex\]](#).
- [85] W. J. Stirling and E. Vryonidou, *Electroweak gauge boson polarisation at the LHC*, *JHEP* **07** (2012) 124, arXiv: [1204.6427 \[hep-ph\]](#).
- [86] A. Hoecker et al., *TMVA - Toolkit for Multivariate Data Analysis*, 2007, arXiv: [physics/0703039 \[physics.data-an\]](#).
- [87] L. Moneta et al., *The RooStats Project*, *PoS ACAT2010* (2010) 057, arXiv: [1009.1003 \[physics.data-an\]](#).
- [88] W. Verkerke and D. Kirkby, *The RooFit toolkit for data modeling*, 2003, arXiv: [physics/0306116 \[physics.data-an\]](#).
- [89] K. Cranmer, G. Lewis, L. Moneta, A. Shibata and W. Verkerke, *HistFactory: A tool for creating statistical models for use with RooFit and RooStats*, tech. rep., New York U., 2012, URL: <https://cds.cern.ch/record/1456844>.
- [90] F. Boudjema and R. K. Singh, *A Model independent spin analysis of fundamental particles using azimuthal asymmetries*, *JHEP* **07** (2009) 028, arXiv: [0903.4705 \[hep-ph\]](#).
- [91] G. D’Agostini, *A multidimensional unfolding method based on Bayes’ theorem*, *Nucl. Instrum. Meth. A* **362** (1995) 487.
- [92] J. Butterworth et al., *PDF4LHC recommendations for LHC Run II*, *J. Phys. G* **43** (2016) 023001, arXiv: [1510.03865 \[hep-ph\]](#).
- [93] L. A. Harland-Lang, A. D. Martin, P. Motylinski and R. S. Thorne, *Parton distributions in the LHC era: MMHT 2014 PDFs*, *Eur. Phys. J. C* **75** (2015) 204, arXiv: [1412.3989 \[hep-ph\]](#).
- [94] S. Dulat et al., *New parton distribution functions from a global analysis of quantum chromodynamics*, *Phys. Rev. D* **93** (2016) 033006, arXiv: [1506.07443 \[hep-ph\]](#).
- [95] J. Bellm et al., *Herwig 7.0/Herwig++ 3.0 release note*, *Eur. Phys. J. C* **76** (2016) 196, arXiv: [1512.01178 \[hep-ph\]](#).
- [96] M. Bähr et al., *Herwig++ physics and manual*, *Eur. Phys. J. C* **58** (2008) 639, arXiv: [0803.0883 \[hep-ph\]](#).
- [97] S. Gieseke, T. Kasprzik and J. H. Kühn, *Vector-boson pair production and electroweak corrections in HERWIG++*, 2014, arXiv: [1401.3964 \[hep-ph\]](#).

- [98] ATLAS Collaboration, *Electron reconstruction and identification in the ATLAS experiment using the 2015 and 2016 LHC proton–proton collision data at $\sqrt{s} = 13$ TeV*, [Eur. Phys. J. C **79** \(2019\) 639](#), arXiv: [1902.04655 \[hep-ex\]](#).
- [99] ATLAS Collaboration, *Luminosity determination in pp collisions at $\sqrt{s} = 13$ TeV using the ATLAS detector at the LHC*, (2022), arXiv: [2212.09379 \[hep-ex\]](#).
- [100] ATLAS Collaboration, *Measurement of the Inelastic Proton–Proton Cross Section at $\sqrt{s} = 13$ TeV with the ATLAS Detector at the LHC*, [Phys. Rev. Lett. **117** \(2016\) 182002](#), arXiv: [1606.02625 \[hep-ex\]](#).
- [101] G. Cowan, K. Cranmer, E. Gross and O. Vitells, *Asymptotic formulae for likelihood-based tests of new physics*, [Eur. Phys. J. C **71** \(2011\) 1554](#), arXiv: [1007.1727 \[physics.data-an\]](#), Erratum: [Eur. Phys. J. C **73** \(2013\) 2501](#).
- [102] S. S. Wilks, *The Large-Sample Distribution of the Likelihood Ratio for Testing Composite Hypotheses*, [Annals Math. Statist. **9** \(1938\) 60](#).
- [103] ATLAS Collaboration, *ATLAS Computing Acknowledgements*, ATL-SOFT-PUB-2023-001, 2023, URL: <https://cds.cern.ch/record/2869272>.

The ATLAS Collaboration

G. Aad ¹⁰², B. Abbott ¹²⁰, K. Abeling ⁵⁵, N.J. Abicht ⁴⁹, S.H. Abidi ²⁹, A. Aboulhorma ^{35e}, H. Abramowicz ¹⁵¹, H. Abreu ¹⁵⁰, Y. Abulaiti ¹¹⁷, B.S. Acharya ^{69a,69b,q}, C. Adam Bourdarios ⁴, L. Adamczyk ^{86a}, S.V. Addepalli ²⁶, M.J. Addison ¹⁰¹, J. Adelman ¹¹⁵, A. Adiguzel ^{21c}, T. Adye ¹³⁴, A.A. Affolder ¹³⁶, Y. Afik ³⁶, M.N. Agaras ¹³, J. Agarwala ^{73a,73b}, A. Aggarwal ¹⁰⁰, C. Agheorghiesei ^{27c}, A. Ahmad ³⁶, F. Ahmadov ^{38,ak}, W.S. Ahmed ¹⁰⁴, S. Ahuja ⁹⁵, X. Ai ^{62a}, G. Aielli ^{76a,76b}, A. Aikot ¹⁶³, M. Ait Tamlihat ^{35e}, B. Aitbenchikh ^{35a}, I. Aizenberg ¹⁶⁹, M. Akbiyik ¹⁰⁰, T.P.A. Åkesson ⁹⁸, A.V. Akimov ³⁷, D. Akiyama ¹⁶⁸, N.N. Akolkar ²⁴, K. Al Khoury ⁴¹, G.L. Alberghi ^{23b}, J. Albert ¹⁶⁵, P. Albicocco ⁵³, G.L. Albouy ⁶⁰, S. Alderweireldt ⁵², M. Aleksa ³⁶, I.N. Aleksandrov ³⁸, C. Alexa ^{27b}, T. Alexopoulos ¹⁰, F. Alfonsi ^{23b}, M. Algren ⁵⁶, M. Alhroob ¹²⁰, B. Ali ¹³², H.M.J. Ali ⁹¹, S. Ali ¹⁴⁸, S.W. Alibocus ⁹², M. Aliev ¹⁴⁵, G. Alimonti ^{71a}, W. Alkakh ⁵⁵, C. Allaire ⁶⁶, B.M.M. Allbrooke ¹⁴⁶, J.F. Allen ⁵², C.A. Allendes Flores ^{137f}, P.P. Allport ²⁰, A. Aloisio ^{72a,72b}, F. Alonso ⁹⁰, C. Alpigiani ¹³⁸, M. Alvarez Estevez ⁹⁹, A. Alvarez Fernandez ¹⁰⁰, M. Alves Cardoso ⁵⁶, M.G. Alviggi ^{72a,72b}, M. Aly ¹⁰¹, Y. Amaral Coutinho ^{83b}, A. Ambler ¹⁰⁴, C. Amelung ³⁶, M. Amerl ¹⁰¹, C.G. Ames ¹⁰⁹, D. Amidei ¹⁰⁶, S.P. Amor Dos Santos ^{130a}, K.R. Amos ¹⁶³, V. Ananiev ¹²⁵, C. Anastopoulos ¹³⁹, T. Andeen ¹¹, J.K. Anders ³⁶, S.Y. Andrean ^{47a,47b}, A. Andreazza ^{71a,71b}, S. Angelidakis ⁹, A. Angerami ^{41,ao}, A.V. Anisenkov ³⁷, A. Annovi ^{74a}, C. Antel ⁵⁶, M.T. Anthony ¹³⁹, E. Antipov ¹⁴⁵, M. Antonelli ⁵³, F. Anulli ^{75a}, M. Aoki ⁸⁴, T. Aoki ¹⁵³, J.A. Aparisi Pozo ¹⁶³, M.A. Aparo ¹⁴⁶, L. Aperio Bella ⁴⁸, C. Appelt ¹⁸, A. Apyan ²⁶, N. Aranzabal ³⁶, S.J. Arbiol Val ⁸⁷, C. Arcangeletti ⁵³, A.T.H. Arce ⁵¹, E. Arena ⁹², J-F. Arguin ¹⁰⁸, S. Argyropoulos ⁵⁴, J.-H. Arling ⁴⁸, O. Arnaez ⁴, H. Arnold ¹¹⁴, G. Artoni ^{75a,75b}, H. Asada ¹¹¹, K. Asai ¹¹⁸, S. Asai ¹⁵³, N.A. Asbah ⁶¹, J. Assahsah ^{35d}, K. Assamagan ²⁹, R. Astalos ^{28a}, S. Atashi ¹⁶⁰, R.J. Atkin ^{33a}, M. Atkinson ¹⁶², H. Atmani ^{35f}, P.A. Atlasiddha ¹⁰⁶, K. Augsten ¹³², S. Auricchio ^{72a,72b}, A.D. Auriol ²⁰, V.A. Austrup ¹⁰¹, G. Avolio ³⁶, K. Axiotis ⁵⁶, G. Azuelos ^{108,av}, D. Babal ^{28b}, H. Bachacou ¹³⁵, K. Bachas ^{152,w}, A. Bachi ³⁴, F. Backman ^{47a,47b}, A. Badea ⁶¹, T.M. Baer ¹⁰⁶, P. Bagnaia ^{75a,75b}, M. Bahmani ¹⁸, A.J. Bailey ¹⁶³, V.R. Bailey ¹⁶², J.T. Baines ¹³⁴, L. Baines ⁹⁴, O.K. Baker ¹⁷², E. Bakos ¹⁵, D. Bakshi Gupta ⁸, V. Balakrishnan ¹²⁰, R. Balasubramanian ¹¹⁴, E.M. Baldin ³⁷, P. Balek ^{86a}, E. Ballabene ^{23b,23a}, F. Balli ¹³⁵, L.M. Baltes ^{63a}, W.K. Balunas ³², J. Balz ¹⁰⁰, E. Banas ⁸⁷, M. Bandieramonte ¹²⁹, A. Bandyopadhyay ²⁴, S. Bansal ²⁴, L. Barak ¹⁵¹, M. Barakat ⁴⁸, E.L. Barberio ¹⁰⁵, D. Barberis ^{57b,57a}, M. Barbero ¹⁰², M.Z. Barel ¹¹⁴, K.N. Barends ^{33a}, T. Barillari ¹¹⁰, M-S. Barisits ³⁶, T. Barklow ¹⁴³, P. Baron ¹²², D.A. Baron Moreno ¹⁰¹, A. Baroncelli ^{62a}, G. Barone ²⁹, A.J. Barr ¹²⁶, J.D. Barr ⁹⁶, L. Barranco Navarro ^{47a,47b}, F. Barreiro ⁹⁹, J. Barreiro Guimarães da Costa ^{14a}, U. Barron ¹⁵¹, M.G. Barros Teixeira ^{130a}, S. Barsov ³⁷, F. Bartels ^{63a}, R. Bartoldus ¹⁴³, A.E. Barton ⁹¹, P. Bartos ^{28a}, A. Basan ^{100,af}, M. Baselga ⁴⁹, A. Bassalat ^{66,b}, M.J. Basso ^{156a}, C.R. Basson ¹⁰¹, R.L. Bates ⁵⁹, S. Batlamous ^{35e}, J.R. Batley ³², B. Batool ¹⁴¹, M. Battaglia ¹³⁶, D. Battulga ¹⁸, M. Bauce ^{75a,75b}, M. Bauer ³⁶, P. Bauer ²⁴, L.T. Bazzano Hurrell ³⁰, J.B. Beacham ⁵¹, T. Beau ¹²⁷, J.Y. Beauchamp ⁹⁰, P.H. Beauchemin ¹⁵⁸, F. Becherer ⁵⁴, P. Bechtel ²⁴, H.P. Beck ^{19,u}, K. Becker ¹⁶⁷, A.J. Beddall ⁸², V.A. Bednyakov ³⁸, C.P. Bee ¹⁴⁵, L.J. Beemster ¹⁵, T.A. Beermann ³⁶, M. Begalli ^{83d}, M. Begel ²⁹, A. Behera ¹⁴⁵, J.K. Behr ⁴⁸, J.F. Beirer ⁵⁵, F. Beisiegel ²⁴, M. Belfkir ¹⁵⁹, G. Bella ¹⁵¹, L. Bellagamba ^{23b}, A. Bellerive ³⁴, P. Bellos ²⁰, K. Beloborodov ³⁷, D. Benckekroun ^{35a}, F. Bendebba ^{35a}, Y. Benhammou ¹⁵¹, M. Benoit ²⁹, J.R. Bensinger ²⁶,

S. Bentvelsen ¹¹⁴, L. Beresford ⁴⁸, M. Beretta ⁵³, E. Bergeaas Kuutmann ¹⁶¹, N. Berger ⁴,
 B. Bergmann ¹³², J. Beringer ^{17a}, G. Bernardi ⁵, C. Bernius ¹⁴³, F.U. Bernlochner ²⁴,
 F. Bernon ^{36,102}, A. Berrocal Guardia ¹³, T. Berry ⁹⁵, P. Berta ¹³³, A. Berthold ⁵⁰,
 I.A. Bertram ⁹¹, S. Bethke ¹¹⁰, A. Betti ^{75a,75b}, A.J. Bevan ⁹⁴, N.K. Bhalla ⁵⁴, M. Bhamjee ^{33c},
 S. Bhatta ¹⁴⁵, D.S. Bhattacharya ¹⁶⁶, P. Bhattarai ¹⁴³, V.S. Bhopatkar ¹²¹, R. Bi ^{29,ay},
 R.M. Bianchi ¹²⁹, G. Bianco ^{23b,23a}, O. Biebel ¹⁰⁹, R. Bielski ¹²³, M. Biglietti ^{77a}, M. Bindi ⁵⁵,
 A. Bingul ^{21b}, C. Bini ^{75a,75b}, A. Biondini ⁹², C.J. Birch-sykes ¹⁰¹, G.A. Bird ^{20,134},
 M. Birman ¹⁶⁹, M. Biros ¹³³, S. Biryukov ¹⁴⁶, T. Bisanz ⁴⁹, E. Bisceglie ^{43b,43a}, J.P. Biswal ¹³⁴,
 D. Biswas ¹⁴¹, A. Bitadze ¹⁰¹, K. Bjørke ¹²⁵, I. Bloch ⁴⁸, C. Blocker ²⁶, A. Blue ⁵⁹,
 U. Blumenschein ⁹⁴, J. Blumenthal ¹⁰⁰, G.J. Bobbink ¹¹⁴, V.S. Bobrovnikov ³⁷, M. Boehler ⁵⁴,
 B. Boehm ¹⁶⁶, D. Bogavac ³⁶, A.G. Bogdanchikov ³⁷, C. Bohm ^{47a}, V. Boisvert ⁹⁵, P. Bokan ⁴⁸,
 T. Bold ^{86a}, M. Bomben ⁵, M. Bona ⁹⁴, M. Boonekamp ¹³⁵, C.D. Booth ⁹⁵, A.G. Borbély ^{59,as},
 I.S. Bordulev ³⁷, H.M. Borecka-Bielska ¹⁰⁸, G. Borissov ⁹¹, D. Bortoletto ¹²⁶, D. Boscherini ^{23b},
 M. Bosman ¹³, J.D. Bossio Sola ³⁶, K. Bouaouda ^{35a}, N. Bouchhar ¹⁶³, J. Boudreau ¹²⁹,
 E.V. Bouhova-Thacker ⁹¹, D. Boumediene ⁴⁰, R. Bouquet ¹⁶⁵, A. Boveia ¹¹⁹, J. Boyd ³⁶,
 D. Boye ²⁹, I.R. Boyko ³⁸, J. Bracinik ²⁰, N. Brahimi ^{62d}, G. Brandt ¹⁷¹, O. Brandt ³²,
 F. Braren ⁴⁸, B. Brau ¹⁰³, J.E. Brau ¹²³, R. Brenner ¹⁶⁹, L. Brenner ¹¹⁴, R. Brenner ¹⁶¹,
 S. Bressler ¹⁶⁹, D. Britton ⁵⁹, D. Britzger ¹¹⁰, I. Brock ²⁴, G. Brooijmans ⁴¹, W.K. Brooks ^{137f},
 E. Brost ²⁹, L.M. Brown ^{165,n}, L.E. Bruce ⁶¹, T.L. Bruckler ¹²⁶, P.A. Bruckman de Renstrom ⁸⁷,
 B. Brüers ⁴⁸, A. Bruni ^{23b}, G. Bruni ^{23b}, M. Bruschi ^{23b}, N. Bruscino ^{75a,75b}, T. Buanes ¹⁶,
 Q. Buat ¹³⁸, D. Buchin ¹¹⁰, A.G. Buckley ⁵⁹, O. Bulekov ³⁷, B.A. Bullard ¹⁴³, S. Burdin ⁹²,
 C.D. Burgard ⁴⁹, A.M. Burger ⁴⁰, B. Burghgrave ⁸, O. Burlayenko ⁵⁴, J.T.P. Burr ³²,
 C.D. Burton ¹¹, J.C. Burzynski ¹⁴², E.L. Busch ⁴¹, V. Büscher ¹⁰⁰, P.J. Bussey ⁵⁹,
 J.M. Butler ²⁵, C.M. Buttar ⁵⁹, J.M. Butterworth ⁹⁶, W. Buttinger ¹³⁴, C.J. Buxo Vazquez ¹⁰⁷,
 A.R. Buzykaev ³⁷, S. Cabrera Urbán ¹⁶³, L. Cadamuro ⁶⁶, D. Caforio ⁵⁸, H. Cai ¹²⁹,
 Y. Cai ^{14a,14e}, Y. Cai ^{14c}, V.M.M. Cairo ³⁶, O. Cakir ^{3a}, N. Calace ³⁶, P. Calafiura ^{17a},
 G. Calderini ¹²⁷, P. Calfayan ⁶⁸, G. Callea ⁵⁹, L.P. Caloba ^{83b}, D. Calvet ⁴⁰, S. Calvet ⁴⁰,
 T.P. Calvet ¹⁰², M. Calvetti ^{74a,74b}, R. Camacho Toro ¹²⁷, S. Camarda ³⁶, D. Camarero Munoz ²⁶,
 P. Camarri ^{76a,76b}, M.T. Camerlingo ^{72a,72b}, D. Cameron ^{36,h}, C. Camincher ¹⁶⁵,
 M. Campanelli ⁹⁶, A. Camplani ⁴², V. Canale ^{72a,72b}, A. Canesse ¹⁰⁴, J. Cantero ¹⁶³, Y. Cao ¹⁶²,
 F. Capocasa ²⁶, M. Capua ^{43b,43a}, A. Carbone ^{71a,71b}, R. Cardarelli ^{76a}, J.C.J. Cardenas ⁸,
 F. Cardillo ¹⁶³, G. Carducci ^{43b,43a}, T. Carli ³⁶, G. Carlino ^{72a}, J.I. Carlotta ¹³, B.T. Carlson ^{129,x},
 E.M. Carlson ^{165,156a}, L. Carminati ^{71a,71b}, A. Carnelli ¹³⁵, M. Carnesale ^{75a,75b}, S. Caron ¹¹³,
 E. Carquin ^{137f}, S. Carrá ^{71a,71b}, G. Carratta ^{23b,23a}, F. Carrio Argos ^{33g}, J.W.S. Carter ¹⁵⁵,
 T.M. Carter ⁵², M.P. Casado ^{13,k}, M. Caspar ⁴⁸, F.L. Castillo ⁴, L. Castillo Garcia ¹³,
 V. Castillo Gimenez ¹⁶³, N.F. Castro ^{130a,130e}, A. Catinaccio ³⁶, J.R. Catmore ¹²⁵, V. Cavaliere ²⁹,
 N. Cavalli ^{23b,23a}, V. Cavasinni ^{74a,74b}, Y.C. Cekmecelioglu ⁴⁸, E. Celebi ^{21a}, F. Celli ¹²⁶,
 M.S. Centonze ^{70a,70b}, V. Cepaitis ⁵⁶, K. Cerny ¹²², A.S. Cerqueira ^{83a}, A. Cerri ¹⁴⁶,
 L. Cerrito ^{76a,76b}, F. Cerutti ^{17a}, B. Cervato ¹⁴¹, A. Cervelli ^{23b}, G. Cesarini ⁵³, S.A. Cetin ⁸²,
 Z. Chadi ^{35a}, D. Chakraborty ¹¹⁵, J. Chan ¹⁷⁰, W.Y. Chan ¹⁵³, J.D. Chapman ³², E. Chapon ¹³⁵,
 B. Chargeishvili ^{149b}, D.G. Charlton ²⁰, T.P. Charman ⁹⁴, M. Chatterjee ¹⁹, C. Chauhan ¹³³,
 S. Chekanov ⁶, S.V. Chekulaev ^{156a}, G.A. Chelkov ^{38,a}, A. Chen ¹⁰⁶, B. Chen ¹⁵¹, B. Chen ¹⁶⁵,
 H. Chen ^{14c}, H. Chen ²⁹, J. Chen ^{62c}, J. Chen ¹⁴², M. Chen ¹²⁶, S. Chen ¹⁵³, S.J. Chen ^{14c},
 X. Chen ^{62c,135}, X. Chen ^{14b,au}, Y. Chen ^{62a}, C.L. Cheng ¹⁷⁰, H.C. Cheng ^{64a}, S. Cheong ¹⁴³,
 A. Cheplakov ³⁸, E. Cheremushkina ⁴⁸, E. Cherepanova ¹¹⁴, R. Cherkaoui El Moursli ^{35e},
 E. Cheu ⁷, K. Cheung ⁶⁵, L. Chevalier ¹³⁵, V. Chiarella ⁵³, G. Chiarelli ^{74a}, N. Chiedde ¹⁰²,
 G. Chiodini ^{70a}, A.S. Chisholm ²⁰, A. Chitan ^{27b}, M. Chitishvili ¹⁶³, M.V. Chizhov ³⁸,

K. Choi ¹¹, A.R. Chomont ^{75a,75b}, Y. Chou ¹⁰³, E.Y.S. Chow ¹¹³, T. Chowdhury ^{33g}, K.L. Chu ¹⁶⁹, M.C. Chu ^{64a}, X. Chu ^{14a,14e}, J. Chudoba ¹³¹, J.J. Chwastowski ⁸⁷, D. Cieri ¹¹⁰, K.M. Ciesla ^{86a}, V. Cindro ⁹³, A. Ciocio ^{17a}, F. Cirotto ^{72a,72b}, Z.H. Citron ^{169,o}, M. Citterio ^{71a}, D.A. Ciubotaru ^{27b}, B.M. Ciungu ¹⁵⁵, A. Clark ⁵⁶, P.J. Clark ⁵², C. Clarry ¹⁵⁵, J.M. Clavijo Columbie ⁴⁸, S.E. Clawson ⁴⁸, C. Clement ^{47a,47b}, J. Clercx ⁴⁸, L. Clissa ^{23b,23a}, Y. Coadou ¹⁰², M. Cobal ^{69a,69c}, A. Coccaro ^{57b}, R.F. Coelho Barrue ^{130a}, R. Coelho Lopes De Sa ¹⁰³, S. Coelli ^{71a}, H. Cohen ¹⁵¹, A.E.C. Coimbra ^{71a,71b}, B. Cole ⁴¹, J. Collot ⁶⁰, P. Conde Muño ^{130a,130g}, M.P. Connell ^{33c}, S.H. Connell ^{33c}, I.A. Connelly ⁵⁹, E.I. Conroy ¹²⁶, F. Conventi ^{72a,aw}, H.G. Cooke ²⁰, A.M. Cooper-Sarkar ¹²⁶, A. Cordeiro Oudot Choi ¹²⁷, L.D. Corpe ⁴⁰, M. Corradi ^{75a,75b}, F. Corriveau ^{104,ai}, A. Cortes-Gonzalez ¹⁸, M.J. Costa ¹⁶³, F. Costanza ⁴, D. Costanzo ¹³⁹, B.M. Cote ¹¹⁹, G. Cowan ⁹⁵, K. Cranmer ¹⁷⁰, D. Cremonini ^{23b,23a}, S. Crépé-Renaudin ⁶⁰, F. Crescioli ¹²⁷, M. Cristinziani ¹⁴¹, M. Cristoforetti ^{78a,78b}, V. Croft ¹¹⁴, J.E. Crosby ¹²¹, G. Crosetti ^{43b,43a}, A. Cueto ⁹⁹, T. Cuhadar Donszelmann ¹⁶⁰, H. Cui ^{14a,14e}, Z. Cui ⁷, W.R. Cunningham ⁵⁹, F. Curcio ^{43b,43a}, P. Czodrowski ³⁶, M.M. Czurylo ^{63b}, M.J. Da Cunha Sargedas De Sousa ^{57b,57a}, J.V. Da Fonseca Pinto ^{83b}, C. Da Via ¹⁰¹, W. Dabrowski ^{86a}, T. Dado ⁴⁹, S. Dahbi ^{33g}, T. Dai ¹⁰⁶, D. Dal Santo ¹⁹, C. Dallapiccola ¹⁰³, M. Dam ⁴², G. D'amen ²⁹, V. D'Amico ¹⁰⁹, J. Damp ¹⁰⁰, J.R. Dandoy ¹²⁸, M.F. Daneri ³⁰, M. Danninger ¹⁴², V. Dao ³⁶, G. Darbo ^{57b}, S. Darmora ⁶, S.J. Das ^{29,ay}, S. D'Auria ^{71a,71b}, C. David ^{156b}, T. Davidek ¹³³, B. Davis-Purcell ³⁴, I. Dawson ⁹⁴, H.A. Day-hall ¹³², K. De ⁸, R. De Asmundis ^{72a}, N. De Biase ⁴⁸, S. De Castro ^{23b,23a}, N. De Groot ¹¹³, P. de Jong ¹¹⁴, H. De la Torre ¹¹⁵, A. De Maria ^{14c}, A. De Salvo ^{75a}, U. De Sanctis ^{76a,76b}, A. De Santo ¹⁴⁶, J.B. De Vivie De Regie ⁶⁰, D.V. Dedovich ³⁸, J. Degens ¹¹⁴, A.M. Deiana ⁴⁴, F. Del Corso ^{23b,23a}, J. Del Peso ⁹⁹, F. Del Rio ^{63a}, F. Deliot ¹³⁵, C.M. Delitzsch ⁴⁹, M. Della Pietra ^{72a,72b}, D. Della Volpe ⁵⁶, A. Dell'Acqua ³⁶, L. Dell'Asta ^{71a,71b}, M. Delmastro ⁴, P.A. Delsart ⁶⁰, S. Demers ¹⁷², M. Demichev ³⁸, S.P. Denisov ³⁷, L. D'Eramo ⁴⁰, D. Derendarz ⁸⁷, F. Derue ¹²⁷, P. Dervan ⁹², K. Desch ²⁴, C. Deutsch ²⁴, F.A. Di Bello ^{57b,57a}, A. Di Ciaccio ^{76a,76b}, L. Di Ciaccio ⁴, A. Di Domenico ^{75a,75b}, C. Di Donato ^{72a,72b}, A. Di Girolamo ³⁶, G. Di Gregorio ³⁶, A. Di Luca ^{78a,78b}, B. Di Micco ^{77a,77b}, R. Di Nardo ^{77a,77b}, C. Diaconu ¹⁰², M. Diamantopoulou ³⁴, F.A. Dias ¹¹⁴, T. Dias Do Vale ¹⁴², M.A. Diaz ^{137a,137b}, F.G. Diaz Capriles ²⁴, M. Didenko ¹⁶³, E.B. Diehl ¹⁰⁶, L. Diehl ⁵⁴, S. Díez Cornell ⁴⁸, C. Díez Pardos ¹⁴¹, C. Dimitriadi ^{161,24,161}, A. Dimitrievska ^{17a}, J. Dingfelder ²⁴, I-M. Dinu ^{27b}, S.J. Dittmeier ^{63b}, F. Dittus ³⁶, F. Djama ¹⁰², T. Djobava ^{149b}, J.I. Djuvsland ¹⁶, C. Doglioni ^{101,98}, A. Dohnalova ^{28a}, J. Dolejsi ¹³³, Z. Dolezal ¹³³, K.M. Dona ³⁹, M. Donadelli ^{83c}, B. Dong ¹⁰⁷, J. Donini ⁴⁰, A. D'Onofrio ^{77a,77b}, M. D'Onofrio ⁹², J. Dopke ¹³⁴, A. Doria ^{72a}, N. Dos Santos Fernandes ^{130a}, P. Dougan ¹⁰¹, M.T. Dova ⁹⁰, A.T. Doyle ⁵⁹, M.A. Dragnet ¹²⁶, E. Dreyer ¹⁶⁹, I. Drivas-koulouris ¹⁰, M. Drnevich ¹¹⁷, A.S. Drobac ¹⁵⁸, M. Drozdova ⁵⁶, D. Du ^{62a}, T.A. du Pree ¹¹⁴, F. Dubinin ³⁷, M. Dubovsky ^{28a}, E. Duchovni ¹⁶⁹, G. Duckeck ¹⁰⁹, O.A. Ducu ^{27b}, D. Duda ⁵², A. Dudarev ³⁶, E.R. Duden ²⁶, M. D'uffizi ¹⁰¹, L. Duflot ⁶⁶, M. Dührssen ³⁶, C. Dülse ¹⁷¹, A.E. Dumitriu ^{27b}, M. Dunford ^{63a}, S. Dungs ⁴⁹, K. Dunne ^{47a,47b}, A. Duperrin ¹⁰², H. Duran Yildiz ^{3a}, M. Düren ⁵⁸, A. Durglishvili ^{149b}, B.L. Dwyer ¹¹⁵, G.I. Dyckes ^{17a}, M. Dyndal ^{86a}, B.S. Dziedzic ⁸⁷, Z.O. Earnshaw ¹⁴⁶, G.H. Eberwein ¹²⁶, B. Eckerova ^{28a}, S. Eggebrecht ⁵⁵, E. Egidio Purcino De Souza ¹²⁷, L.F. Ehrke ⁵⁶, G. Eigen ¹⁶, K. Einsweiler ^{17a}, T. Ekelof ¹⁶¹, P.A. Ekman ⁹⁸, S. El Farkh ^{35b}, Y. El Ghazali ^{35b}, H. El Jarrari ^{35e,148}, A. El Moussaouy ^{108,ab}, V. Ellajosyula ¹⁶¹, M. Ellert ¹⁶¹, F. Ellinghaus ¹⁷¹, N. Ellis ³⁶, J. Elmsheuser ²⁹, M. Elsing ³⁶, D. Emelianov ¹³⁴, Y. Enari ¹⁵³, I. Ene ^{17a}, S. Epari ¹³, J. Erdmann ⁴⁹, P.A. Erland ⁸⁷,

M. Errenst ¹⁷¹, M. Escalier ⁶⁶, C. Escobar ¹⁶³, E. Etzion ¹⁵¹, G. Evans ^{130a}, H. Evans ⁶⁸,
L.S. Evans ⁹⁵, M.O. Evans ¹⁴⁶, A. Ezhilov ³⁷, S. Ezzarqtouni ^{35a}, F. Fabbri ⁵⁹, L. Fabbri ^{23b,23a},
G. Facini ⁹⁶, V. Fadeyev ¹³⁶, R.M. Fakhrutdinov ³⁷, S. Falciano ^{75a}, L.F. Falda Ulhoa Coelho ³⁶,
P.J. Falke ²⁴, J. Faltova ¹³³, C. Fan ¹⁶², Y. Fan ^{14a}, Y. Fang ^{14a,14e}, M. Fanti ^{71a,71b},
M. Faraj ^{69a,69b}, Z. Farazpay ⁹⁷, A. Farbin ⁸, A. Farilla ^{77a}, T. Farooque ¹⁰⁷, S.M. Farrington ⁵²,
F. Fassi ^{35e}, D. Fassouliotis ⁹, M. Faucci Giannelli ^{76a,76b}, W.J. Fawcett ³², L. Fayard ⁶⁶,
P. Federic ¹³³, P. Federicova ¹³¹, O.L. Fedin ^{37,a}, G. Fedotov ³⁷, M. Feickert ¹⁷⁰,
L. Feligioni ¹⁰², D.E. Fellers ¹²³, C. Feng ^{62b}, M. Feng ^{14b}, Z. Feng ¹¹⁴, M.J. Fenton ¹⁶⁰,
A.B. Fenyuk ³⁷, L. Ferencz ⁴⁸, R.A.M. Ferguson ⁹¹, S.I. Fernandez Luengo ^{137f},
P. Fernandez Martinez ¹³, M.J.V. Fernoux ¹⁰², J. Ferrando ⁴⁸, A. Ferrari ¹⁶¹, P. Ferrari ^{114,113},
R. Ferrari ^{73a}, D. Ferrere ⁵⁶, C. Ferretti ¹⁰⁶, F. Fiedler ¹⁰⁰, P. Fiedler ¹³², A. Filipčič ⁹³,
E.K. Filmer ¹, F. Filthaut ¹¹³, M.C.N. Fiolhais ^{130a,130c,d}, L. Fiorini ¹⁶³, W.C. Fisher ¹⁰⁷,
T. Fitschen ¹⁰¹, P.M. Fitzhugh ¹³⁵, I. Fleck ¹⁴¹, P. Fleischmann ¹⁰⁶, T. Flick ¹⁷¹, M. Flores ^{33d,ap},
L.R. Flores Castillo ^{64a}, L. Flores Sanz De Acedo ³⁶, F.M. Follega ^{78a,78b}, N. Fomin ¹⁶,
J.H. Foo ¹⁵⁵, B.C. Forland ⁶⁸, A. Formica ¹³⁵, A.C. Forti ¹⁰¹, E. Fortin ³⁶, A.W. Fortman ⁶¹,
M.G. Foti ^{17a}, L. Fountas ^{9,1}, D. Fournier ⁶⁶, H. Fox ⁹¹, P. Francavilla ^{74a,74b}, S. Francescato ⁶¹,
S. Franchellucci ⁵⁶, M. Franchini ^{23b,23a}, S. Franchino ^{63a}, D. Francis ³⁶, L. Franco ¹¹³,
V. Franco Lima ³⁶, L. Franconi ⁴⁸, M. Franklin ⁶¹, G. Frattari ²⁶, A.C. Freegard ⁹⁴,
W.S. Freund ^{83b}, Y.Y. Frid ¹⁵¹, J. Friend ⁵⁹, N. Fritzsche ⁵⁰, A. Froch ⁵⁴, D. Froidevaux ³⁶,
J.A. Frost ¹²⁶, Y. Fu ^{62a}, S. Fuenzalida Garrido ^{137f}, M. Fujimoto ¹⁰², E. Fullana Torregrosa ^{163,*},
K.Y. Fung ^{64a}, E. Furtado De Simas Filho ^{83b}, M. Furukawa ¹⁵³, J. Fuster ¹⁶³, A. Gabrielli ^{23b,23a},
A. Gabrielli ¹⁵⁵, P. Gadow ³⁶, G. Gagliardi ^{57b,57a}, L.G. Gagnon ^{17a}, E.J. Gallas ¹²⁶,
B.J. Gallop ¹³⁴, K.K. Gan ¹¹⁹, S. Ganguly ¹⁵³, Y. Gao ⁵², F.M. Garay Walls ^{137a,137b},
B. Garcia ^{29,ay}, C. García ¹⁶³, A. Garcia Alonso ¹¹⁴, A.G. Garcia Caffaro ¹⁷²,
J.E. García Navarro ¹⁶³, M. Garcia-Sciveres ^{17a}, G.L. Gardner ¹²⁸, R.W. Gardner ³⁹,
N. Garelli ¹⁵⁸, D. Garg ⁸⁰, R.B. Garg ^{143,t}, J.M. Gargan ⁵², C.A. Garner ¹⁵⁵, C.M. Garvey ^{33a},
P. Gaspar ^{83b}, V.K. Gassmann ¹⁵⁸, G. Gaudio ^{73a}, V. Gautam ¹³, P. Gauzzi ^{75a,75b}, I.L. Gavrilenko ³⁷,
A. Gavriluk ³⁷, C. Gay ¹⁶⁴, G. Gaycken ⁴⁸, E.N. Gazis ¹⁰, A.A. Geanta ^{27b}, C.M. Gee ¹³⁶,
C. Gemme ^{57b}, M.H. Genest ⁶⁰, S. Gentile ^{75a,75b}, A.D. Gentry ¹¹², S. George ⁹⁵,
W.F. George ²⁰, T. Geralis ⁴⁶, P. Gessinger-Befurt ³⁶, M.E. Geyik ¹⁷¹, M. Ghani ¹⁶⁷,
M. Ghneimat ¹⁴¹, K. Ghorbanian ⁹⁴, A. Ghosal ¹⁴¹, A. Ghosh ¹⁶⁰, A. Ghosh ⁷, B. Giacobbe ^{23b},
S. Giagu ^{75a,75b}, T. Giani ¹¹⁴, P. Giannetti ^{74a}, A. Giannini ^{62a}, S.M. Gibson ⁹⁵, M. Gignac ¹³⁶,
D.T. Gil ^{86b}, A.K. Gilbert ^{86a}, B.J. Gilbert ⁴¹, D. Gillberg ³⁴, G. Gilles ¹¹⁴, N.E.K. Gillwald ⁴⁸,
L. Ginabat ¹²⁷, D.M. Gingrich ^{2,av}, M.P. Giordani ^{69a,69c}, P.F. Giraud ¹³⁵, G. Giugliarelli ^{69a,69c},
D. Giugni ^{71a}, F. Giuli ³⁶, I. Gkialas ^{9,1}, L.K. Gladilin ³⁷, C. Glasman ⁹⁹, G.R. Gledhill ¹²³,
G. Glemža ⁴⁸, M. Glisic ¹²³, I. Gnesi ^{43b,g}, Y. Go ^{29,ay}, M. Goblirsch-Kolb ³⁶, B. Gocke ⁴⁹,
D. Godin ¹⁰⁸, B. Gokturk ^{21a}, S. Goldfarb ¹⁰⁵, T. Golling ⁵⁶, M.G.D. Gololo ^{33g}, D. Golubkov ³⁷,
J.P. Gombas ¹⁰⁷, A. Gomes ^{130a,130b}, G. Gomes Da Silva ¹⁴¹, A.J. Gomez Delegido ¹⁶³,
R. Gonçalves ^{130a,130c}, G. Gonella ¹²³, L. Gonella ²⁰, A. Gongadze ^{149c}, F. Gonnella ²⁰,
J.L. Gonski ⁴¹, R.Y. González Andana ⁵², S. González de la Hoz ¹⁶³, S. Gonzalez Fernandez ¹³,
R. Gonzalez Lopez ⁹², C. Gonzalez Renteria ^{17a}, M.V. Gonzalez Rodrigues ⁴⁸,
R. Gonzalez Suarez ¹⁶¹, S. Gonzalez-Sevilla ⁵⁶, G.R. Gonzalvo Rodriguez ¹⁶³, L. Goossens ³⁶,
B. Gorini ³⁶, E. Gorini ^{70a,70b}, A. Gorišek ⁹³, T.C. Gosart ¹²⁸, A.T. Goshaw ⁵¹, M.I. Gostkin ³⁸,
S. Goswami ¹²¹, C.A. Gottardo ³⁶, S.A. Gotz ¹⁰⁹, M. Gouighri ^{35b}, V. Goumarre ⁴⁸,
A.G. Goussiou ¹³⁸, N. Govender ^{33c}, I. Grabowska-Bold ^{86a}, K. Graham ³⁴, E. Gramstad ¹²⁵,
S. Grancagnolo ^{70a,70b}, M. Grandi ¹⁴⁶, C.M. Grant ^{1,135}, P.M. Gravila ^{27f}, F.G. Gravili ^{70a,70b},
H.M. Gray ^{17a}, M. Greco ^{70a,70b}, C. Greife ²⁴, I.M. Gregor ⁴⁸, P. Grenier ¹⁴³, S.G. Grewe ¹¹⁰,

C. Grieco ¹³, A.A. Grillo ¹³⁶, K. Grimm ³¹, S. Grinstein ^{13,ad}, J.-F. Grivaz ⁶⁶, E. Gross ¹⁶⁹, J. Grosse-Knetter ⁵⁵, C. Grud ¹⁰⁶, J.C. Grundy ¹²⁶, L. Guan ¹⁰⁶, W. Guan ²⁹, C. Gubbels ¹⁶⁴, J.G.R. Guerrero Rojas ¹⁶³, G. Guerrieri ^{69a,69c}, F. Guescini ¹¹⁰, R. Gugel ¹⁰⁰, J.A.M. Guhit ¹⁰⁶, A. Guida ¹⁸, T. Guillemain ⁴, E. Guilloton ^{167,134}, S. Guindon ³⁶, F. Guo ^{14a,14e}, J. Guo ^{62c}, L. Guo ⁴⁸, Y. Guo ¹⁰⁶, R. Gupta ⁴⁸, R. Gupta ¹²⁹, S. Gurbuz ²⁴, S.S. Gurdasani ⁵⁴, G. Gustavino ³⁶, M. Guth ⁵⁶, P. Gutierrez ¹²⁰, L.F. Gutierrez Zagazeta ¹²⁸, M. Gutsche ⁵⁰, C. Gutschow ⁹⁶, C. Gwenlan ¹²⁶, C.B. Gwilliam ⁹², E.S. Haaland ¹²⁵, A. Haas ¹¹⁷, M. Habedank ⁴⁸, C. Haber ^{17a}, H.K. Hadavand ⁸, A. Hadeef ¹⁰⁰, S. Hadzic ¹¹⁰, A.I. Hagan ⁹¹, J.J. Hahn ¹⁴¹, E.H. Haines ⁹⁶, M. Haleem ¹⁶⁶, J. Haley ¹²¹, J.J. Hall ¹³⁹, G.D. Hallowell ¹⁰², L. Halser ¹⁹, K. Hamano ¹⁶⁵, M. Hamer ²⁴, G.N. Hamity ⁵², E.J. Hampshire ⁹⁵, J. Han ^{62b}, K. Han ^{62a}, L. Han ^{14c}, L. Han ^{62a}, S. Han ^{17a}, Y.F. Han ¹⁵⁵, K. Hanagaki ⁸⁴, M. Hance ¹³⁶, D.A. Hangal ^{41,ao}, H. Hanif ¹⁴², M.D. Hank ¹²⁸, R. Hankache ¹⁰¹, J.B. Hansen ⁴², J.D. Hansen ⁴², P.H. Hansen ⁴², K. Hara ¹⁵⁷, D. Harada ⁵⁶, T. Harenberg ¹⁷¹, S. Harkusha ³⁷, M.L. Harris ¹⁰³, Y.T. Harris ¹²⁶, J. Harrison ¹³, N.M. Harrison ¹¹⁹, P.F. Harrison ¹⁶⁷, N.M. Hartman ¹¹⁰, N.M. Hartmann ¹⁰⁹, Y. Hasegawa ¹⁴⁰, R. Hauser ¹⁰⁷, C.M. Hawkes ²⁰, R.J. Hawkings ³⁶, Y. Hayashi ¹⁵³, S. Hayashida ¹¹¹, D. Hayden ¹⁰⁷, C. Hayes ¹⁰⁶, R.L. Hayes ¹¹⁴, C.P. Hays ¹²⁶, J.M. Hays ⁹⁴, H.S. Hayward ⁹², F. He ^{62a}, M. He ^{14a,14e}, Y. He ¹⁵⁴, Y. He ⁴⁸, N.B. Heatley ⁹⁴, V. Hedberg ⁹⁸, A.L. Heggelund ¹²⁵, N.D. Hehir ⁹⁴, C. Heidegger ⁵⁴, K.K. Heidegger ⁵⁴, W.D. Heidorn ⁸¹, J. Heilman ³⁴, S. Heim ⁴⁸, T. Heim ^{17a}, J.G. Heinlein ¹²⁸, J.J. Heinrich ¹²³, L. Heinrich ^{110,at}, J. Hejbal ¹³¹, L. Helary ⁴⁸, A. Held ¹⁷⁰, S. Hellesund ¹⁶, C.M. Helling ¹⁶⁴, S. Hellman ^{47a,47b}, R.C.W. Henderson ⁹¹, L. Henkelmann ³², A.M. Henriques Correia ³⁶, H. Herde ⁹⁸, Y. Hernández Jiménez ¹⁴⁵, L.M. Herrmann ²⁴, T. Herrmann ⁵⁰, G. Herten ⁵⁴, R. Hertenberger ¹⁰⁹, L. Hervas ³⁶, M.E. Hespington ¹⁰⁰, N.P. Hessey ^{156a}, H. Hibi ⁸⁵, E. Hill ¹⁵⁵, S.J. Hillier ²⁰, J.R. Hinds ¹⁰⁷, F. Hinterkeuser ²⁴, M. Hirose ¹²⁴, S. Hirose ¹⁵⁷, D. Hirschbuehl ¹⁷¹, T.G. Hitchings ¹⁰¹, B. Hiti ⁹³, J. Hobbs ¹⁴⁵, R. Hobincu ^{27e}, N. Hod ¹⁶⁹, M.C. Hodgkinson ¹³⁹, B.H. Hodgkinson ³², A. Hoecker ³⁶, D.D. Hofer ¹⁰⁶, J. Hofer ⁴⁸, T. Holm ²⁴, M. Holzbock ¹¹⁰, L.B.A.H. Hommels ³², B.P. Honan ¹⁰¹, J. Hong ^{62c}, T.M. Hong ¹²⁹, B.H. Hooberman ¹⁶², W.H. Hopkins ⁶, Y. Horii ¹¹¹, S. Hou ¹⁴⁸, A.S. Howard ⁹³, J. Howarth ⁵⁹, J. Hoya ⁶, M. Hrabovsky ¹²², A. Hrynevich ⁴⁸, T. Hryn'ova ⁴, P.J. Hsu ⁶⁵, S.-C. Hsu ¹³⁸, Q. Hu ^{62a}, Y.F. Hu ^{14a,14e}, S. Huang ^{64b}, X. Huang ^{14c}, X. Huang ^{14a,14e}, Y. Huang ^{139,m}, Y. Huang ^{14a}, Z. Huang ¹⁰¹, Z. Hubacek ¹³², M. Huebner ²⁴, F. Huegging ²⁴, T.B. Huffman ¹²⁶, C.A. Hugli ⁴⁸, M. Huhtinen ³⁶, S.K. Huiberts ¹⁶, R. Hulsken ¹⁰⁴, N. Huseynov ¹², J. Huston ¹⁰⁷, J. Huth ⁶¹, R. Hyneman ¹⁴³, G. Iacobucci ⁵⁶, G. Iakovidis ²⁹, I. Ibragimov ¹⁴¹, L. Iconomidou-Fayard ⁶⁶, P. Iengo ^{72a,72b}, R. Iguchi ¹⁵³, T. Iizawa ^{126,r}, Y. Ikegami ⁸⁴, N. Ilic ¹⁵⁵, H. Imam ^{35a}, M. Ince Lezki ⁵⁶, T. Ingebretsen Carlson ^{47a,47b}, G. Introzzi ^{73a,73b}, M. Iodice ^{77a}, V. Ippolito ^{75a,75b}, R.K. Irwin ⁹², M. Ishino ¹⁵³, W. Islam ¹⁷⁰, C. Issever ^{18,48}, S. Istin ^{21a,ba}, H. Ito ¹⁶⁸, J.M. Iturbe Ponce ^{64a}, R. Iuppa ^{78a,78b}, A. Ivina ¹⁶⁹, J.M. Izen ⁴⁵, V. Izzo ^{72a}, P. Jacka ^{131,132}, P. Jackson ¹, R.M. Jacobs ⁴⁸, B.P. Jaeger ¹⁴², C.S. Jagfeld ¹⁰⁹, G. Jain ^{156a}, P. Jain ⁵⁴, K. Jakobs ⁵⁴, T. Jakoubek ¹⁶⁹, J. Jamieson ⁵⁹, K.W. Janas ^{86a}, M. Javurkova ¹⁰³, F. Jeanneau ¹³⁵, L. Jeanty ¹²³, J. Jejelava ^{149a,al}, P. Jenni ^{54,i}, C.E. Jessiman ³⁴, S. Jézéquel ⁴, C. Jia ^{62b}, J. Jia ¹⁴⁵, X. Jia ⁶¹, X. Jia ^{14a,14e}, Z. Jia ^{14c}, S. Jiggins ⁴⁸, J. Jimenez Pena ¹³, S. Jin ^{14c}, A. Jinaru ^{27b}, O. Jinnouchi ¹⁵⁴, P. Johansson ¹³⁹, K.A. Johns ⁷, J.W. Johnson ¹³⁶, D.M. Jones ³², E. Jones ⁴⁸, P. Jones ³², R.W.L. Jones ⁹¹, T.J. Jones ⁹², H.L. Joos ^{55,36}, R. Joshi ¹¹⁹, J. Jovicevic ¹⁵, X. Ju ^{17a}, J.J. Junggeburth ^{103,v}, T. Junkermann ^{63a}, A. Juste Rozas ^{13,ad}, M.K. Juzek ⁸⁷, S. Kabana ^{137e}, A. Kaczmarzka ⁸⁷, M. Kado ¹¹⁰, H. Kagan ¹¹⁹, M. Kagan ¹⁴³, A. Kahn ⁴¹, A. Kahn ¹²⁸, C. Kahra ¹⁰⁰, T. Kaji ¹⁵³, E. Kajomovitz ¹⁵⁰, N. Kakati ¹⁶⁹, I. Kalaitzidou ⁵⁴,

C.W. Kalderon ²⁹, A. Kamenshchikov ¹⁵⁵, N.J. Kang ¹³⁶, D. Kar ^{33g}, K. Karava ¹²⁶, M.J. Kareem ^{156b}, E. Karentzos ⁵⁴, I. Karkanias ¹⁵², O. Karkout ¹¹⁴, S.N. Karpov ³⁸, Z.M. Karpova ³⁸, V. Kartvelishvili ⁹¹, A.N. Karyukhin ³⁷, E. Kasimi ¹⁵², J. Katzy ⁴⁸, S. Kaur ³⁴, K. Kawade ¹⁴⁰, M.P. Kawale ¹²⁰, C. Kawamoto ⁸⁸, T. Kawamoto ¹³⁵, E.F. Kay ³⁶, F.I. Kaya ¹⁵⁸, S. Kazakos ¹⁰⁷, V.F. Kazanin ³⁷, Y. Ke ¹⁴⁵, J.M. Keaveney ^{33a}, R. Keeler ¹⁶⁵, G.V. Kehris ⁶¹, J.S. Keller ³⁴, A.S. Kelly ⁹⁶, J.J. Kempster ¹⁴⁶, K.E. Kennedy ⁴¹, P.D. Kennedy ¹⁰⁰, O. Kepka ¹³¹, B.P. Kerridge ¹⁶⁷, S. Kersten ¹⁷¹, B.P. Kerševan ⁹³, S. Keshri ⁶⁶, L. Keszeghova ^{28a}, S. Ketabchi Haghighat ¹⁵⁵, R.A. Khan ¹²⁹, M. Khandoga ¹²⁷, A. Khanov ¹²¹, A.G. Kharlamov ³⁷, T. Kharlamova ³⁷, E.E. Khoda ¹³⁸, M. Kholodenko ³⁷, T.J. Khoo ¹⁸, G. Khorauli ¹⁶⁶, J. Khubua ^{149b}, Y.A.R. Khwaira ⁶⁶, A. Kilgallon ¹²³, D.W. Kim ^{47a,47b}, Y.K. Kim ³⁹, N. Kimura ⁹⁶, M.K. Kingston ⁵⁵, A. Kirchhoff ⁵⁵, C. Kirfel ²⁴, F. Kirfel ²⁴, J. Kirk ¹³⁴, A.E. Kiryunin ¹¹⁰, C. Kitsaki ¹⁰, O. Kivernyk ²⁴, M. Klassen ^{63a}, C. Klein ³⁴, L. Klein ¹⁶⁶, M.H. Klein ¹⁰⁶, M. Klein ⁹², S.B. Klein ⁵⁶, U. Klein ⁹², P. Klimek ³⁶, A. Klimentov ²⁹, T. Klioutchnikova ³⁶, P. Kluit ¹¹⁴, S. Kluth ¹¹⁰, E. Kneringer ⁷⁹, T.M. Knight ¹⁵⁵, A. Knue ⁴⁹, R. Kobayashi ⁸⁸, D. Kobylanskii ¹⁶⁹, S.F. Koch ¹²⁶, M. Kocian ¹⁴³, P. Kodyš ¹³³, D.M. Koeck ¹²³, P.T. Koenig ²⁴, T. Koffas ³⁴, O. Kolay ⁵⁰, M. Kolb ¹³⁵, I. Koletsou ⁴, T. Komarek ¹²², K. Köneke ⁵⁴, A.X.Y. Kong ¹, T. Kono ¹¹⁸, N. Konstantinidis ⁹⁶, P. Kontaxakis ⁵⁶, B. Konya ⁹⁸, R. Kopeliansky ⁶⁸, S. Koperny ^{86a}, K. Korcyl ⁸⁷, K. Kordas ^{152,f}, G. Koren ¹⁵¹, A. Korn ⁹⁶, S. Korn ⁵⁵, I. Korolkov ¹³, N. Korotkova ³⁷, B. Kortman ¹¹⁴, O. Kortner ¹¹⁰, S. Kortner ¹¹⁰, W.H. Kostecka ¹¹⁵, V.V. Kostyukhin ¹⁴¹, A. Kotsokechagia ¹³⁵, A. Kotwal ⁵¹, A. Koulouris ³⁶, A. Kourkoumeli-Charalampidi ^{73a,73b}, C. Kourkoumelis ⁹, E. Kourlitis ^{110,at}, O. Kovanda ¹⁴⁶, R. Kowalewski ¹⁶⁵, W. Kozanecki ¹³⁵, A.S. Kozhin ³⁷, V.A. Kramarenko ³⁷, G. Kramberger ⁹³, P. Kramer ¹⁰⁰, M.W. Krasny ¹²⁷, A. Krasznahorkay ³⁶, J.W. Kraus ¹⁷¹, J.A. Kremer ⁴⁸, T. Kresse ⁵⁰, J. Kretschmar ⁹², K. Kreul ¹⁸, P. Krieger ¹⁵⁵, S. Krishnamurthy ¹⁰³, M. Krivos ¹³³, K. Krizka ²⁰, K. Kroeninger ⁴⁹, H. Kroha ¹¹⁰, J. Kroll ¹³¹, J. Kroll ¹²⁸, K.S. Krowpman ¹⁰⁷, U. Kruchonak ³⁸, H. Krüger ²⁴, N. Krumnack ⁸¹, M.C. Kruse ⁵¹, J.A. Krzysiak ⁸⁷, O. Kuchinskaia ³⁷, S. Kuday ^{3a}, S. Kuehn ³⁶, R. Kuesters ⁵⁴, T. Kuhl ⁴⁸, V. Kukhtin ³⁸, Y. Kulchitsky ^{37,a}, S. Kuleshov ^{137d,137b}, M. Kumar ^{33g}, N. Kumari ⁴⁸, A. Kupco ¹³¹, T. Kupfer ⁴⁹, A. Kupich ³⁷, O. Kuprash ⁵⁴, H. Kurashige ⁸⁵, L.L. Kurchaninov ^{156a}, O. Kurdysh ⁶⁶, Y.A. Kurochkin ³⁷, A. Kurova ³⁷, M. Kuze ¹⁵⁴, A.K. Kvam ¹⁰³, J. Kvita ¹²², T. Kwan ¹⁰⁴, N.G. Kyriacou ¹⁰⁶, L.A.O. Laatu ¹⁰², C. Lacasta ¹⁶³, F. Lacava ^{75a,75b}, H. Lacker ¹⁸, D. Lacour ¹²⁷, N.N. Lad ⁹⁶, E. Ladygin ³⁸, B. Laforge ¹²⁷, T. Lagouri ^{137e}, F.Z. Lahbabi ^{35a}, S. Lai ⁵⁵, I.K. Lakomic ^{86a}, N. Lalloue ⁶⁰, J.E. Lambert ^{165,n}, S. Lammers ⁶⁸, W. Lampl ⁷, C. Lampoudis ^{152,f}, A.N. Lancaster ¹¹⁵, E. Lançon ²⁹, U. Landgraf ⁵⁴, M.P.J. Landon ⁹⁴, V.S. Lang ⁵⁴, R.J. Langenberg ¹⁰³, O.K.B. Langrekken ¹²⁵, A.J. Lankford ¹⁶⁰, F. Lanni ³⁶, K. Lantzsch ²⁴, A. Lanza ^{73a}, A. Lapertosa ^{57b,57a}, J.F. Laporte ¹³⁵, T. Lari ^{71a}, F. Lasagni Manghi ^{23b}, M. Lassnig ³⁶, V. Latonova ¹³¹, A. Laudrain ¹⁰⁰, A. Laurier ¹⁵⁰, S.D. Lawlor ¹³⁹, Z. Lawrence ¹⁰¹, M. Lazzaroni ^{71a,71b}, B. Le ¹⁰¹, E.M. Le Boulicaut ⁵¹, B. Leban ⁹³, A. Lebedev ⁸¹, M. LeBlanc ^{101,ar}, F. Ledroit-Guillon ⁶⁰, A.C.A. Lee ⁹⁶, S.C. Lee ¹⁴⁸, S. Lee ^{47a,47b}, T.F. Lee ⁹², L.L. Leeuw ^{33c}, H.P. Lefebvre ⁹⁵, M. Lefebvre ¹⁶⁵, C. Leggett ^{17a}, G. Lehmann Miotto ³⁶, M. Leigh ⁵⁶, W.A. Leight ¹⁰³, W. Leinonen ¹¹³, A. Leisos ^{152,ac}, M.A.L. Leite ^{83c}, C.E. Leitgeb ⁴⁸, R. Leitner ¹³³, K.J.C. Leney ⁴⁴, T. Lenz ²⁴, S. Leone ^{74a}, C. Leonidopoulos ⁵², A. Leopold ¹⁴⁴, C. Leroy ¹⁰⁸, R. Les ¹⁰⁷, C.G. Lester ³², M. Levchenko ³⁷, J. Levêque ⁴, D. Levin ¹⁰⁶, L.J. Levinson ¹⁶⁹, M.P. Lewicki ⁸⁷, D.J. Lewis ⁴, A. Li ⁵, B. Li ^{62b}, C. Li ^{62a}, C-Q. Li ^{62c}, H. Li ^{62a}, H. Li ^{62b}, H. Li ^{14c}, H. Li ^{14b}, H. Li ^{62b}, J. Li ^{62c}, K. Li ¹³⁸, L. Li ^{62c}, M. Li ^{14a,14e}, Q.Y. Li ^{62a}, S. Li ^{14a,14e}, S. Li ^{62d,62c,e}, T. Li ^{5,c}, X. Li ¹⁰⁴, Z. Li ¹²⁶, Z. Li ¹⁰⁴, Z. Li ⁹², Z. Li ^{14a,14e}, S. Liang ^{14a,14e}, Z. Liang ^{14a}, M. Liberatore ^{135,am}, B. Liberti ^{76a},

K. Lie ^{64c}, J. Lieber Marin ^{83b}, H. Lien ⁶⁸, K. Lin ¹⁰⁷, R.E. Lindley ⁷, J.H. Lindon ², E. Lipeles ¹²⁸, A. Lipniacka ¹⁶, A. Lister ¹⁶⁴, J.D. Little ⁴, B. Liu ^{14a}, B.X. Liu ¹⁴², D. Liu ^{62d,62c}, J.B. Liu ^{62a}, J.K.K. Liu ³², K. Liu ^{62d,62c}, M. Liu ^{62a}, M.Y. Liu ^{62a}, P. Liu ^{14a}, Q. Liu ^{62d,138,62c}, X. Liu ^{62a}, Y. Liu ^{14d,14e}, Y.L. Liu ^{62b}, Y.W. Liu ^{62a}, J. Llorente Merino ¹⁴², S.L. Lloyd ⁹⁴, E.M. Lobodzinska ⁴⁸, P. Loch ⁷, T. Lohse ¹⁸, K. Lohwasser ¹³⁹, E. Loiacono ⁴⁸, M. Lokajicek ^{131,*}, J.D. Lomas ²⁰, J.D. Long ¹⁶², I. Longarini ¹⁶⁰, L. Longo ^{70a,70b}, R. Longo ¹⁶², I. Lopez Paz ⁶⁷, A. Lopez Solis ⁴⁸, J. Lorenz ¹⁰⁹, N. Lorenzo Martinez ⁴, A.M. Lory ¹⁰⁹, O. Loseva ³⁷, X. Lou ^{47a,47b}, X. Lou ^{14a,14e}, A. Lounis ⁶⁶, J. Love ⁶, P.A. Love ⁹¹, G. Lu ^{14a,14e}, M. Lu ⁸⁰, S. Lu ¹²⁸, Y.J. Lu ⁶⁵, H.J. Lubatti ¹³⁸, C. Luci ^{75a,75b}, F.L. Lucio Alves ^{14c}, A. Lucotte ⁶⁰, F. Luehring ⁶⁸, I. Luise ¹⁴⁵, O. Lukianchuk ⁶⁶, O. Lundberg ¹⁴⁴, B. Lund-Jensen ¹⁴⁴, N.A. Luongo ¹²³, M.S. Lutz ¹⁵¹, A.B. Lux ²⁵, D. Lynn ²⁹, H. Lyons ⁹², R. Lysak ¹³¹, E. Lytken ⁹⁸, V. Lyubushkin ³⁸, T. Lyubushkina ³⁸, M.M. Lyukova ¹⁴⁵, H. Ma ²⁹, K. Ma ^{62a}, L.L. Ma ^{62b}, W. Ma ^{62a}, Y. Ma ¹²¹, D.M. Mac Donell ¹⁶⁵, G. Maccarrone ⁵³, J.C. MacDonald ¹⁰⁰, P.C. Machado De Abreu Farias ^{83b}, R. Madar ⁴⁰, W.F. Mader ⁵⁰, T. Madula ⁹⁶, J. Maeda ⁸⁵, T. Maeno ²⁹, H. Maguire ¹³⁹, V. Maiboroda ¹³⁵, A. Maio ^{130a,130b,130d}, K. Maj ^{86a}, O. Majersky ⁴⁸, S. Majewski ¹²³, N. Makovec ⁶⁶, V. Maksimovic ¹⁵, B. Malaescu ¹²⁷, Pa. Malecki ⁸⁷, V.P. Maleev ³⁷, F. Malek ⁶⁰, M. Mali ⁹³, D. Malito ^{95,s}, U. Mallik ⁸⁰, S. Maltezos ¹⁰, S. Malyukov ³⁸, J. Mamuzic ¹³, G. Mancini ⁵³, G. Manco ^{73a,73b}, J.P. Mandalia ⁹⁴, I. Mandić ⁹³, L. Manhaes de Andrade Filho ^{83a}, I.M. Maniatis ¹⁶⁹, J. Manjarres Ramos ^{102,an}, D.C. Mankad ¹⁶⁹, A. Mann ¹⁰⁹, B. Mansoulie ¹³⁵, S. Manzoni ³⁶, X. Mapekula ^{33c}, A. Marantis ^{152,ac}, G. Marchiori ⁵, M. Marcisovsky ¹³¹, C. Marcon ^{71a,71b}, M. Marinescu ²⁰, M. Marjanovic ¹²⁰, E.J. Marshall ⁹¹, Z. Marshall ^{17a}, S. Marti-Garcia ¹⁶³, T.A. Martin ¹⁶⁷, V.J. Martin ⁵², B. Martin dit Latour ¹⁶, L. Martinelli ^{75a,75b}, M. Martinez ^{13,ad}, P. Martinez Agullo ¹⁶³, V.I. Martinez Outschoorn ¹⁰³, P. Martinez Suarez ¹³, S. Martin-Haugh ¹³⁴, V.S. Martoiu ^{27b}, A.C. Martyniuk ⁹⁶, A. Marzin ³⁶, D. Mascione ^{78a,78b}, L. Masetti ¹⁰⁰, T. Mashimo ¹⁵³, J. Masik ¹⁰¹, A.L. Maslennikov ³⁷, L. Massa ^{23b}, P. Massarotti ^{72a,72b}, P. Mastrandrea ^{74a,74b}, A. Mastroberardino ^{43b,43a}, T. Masubuchi ¹⁵³, T. Mathisen ¹⁶¹, J. Matousek ¹³³, N. Matsuzawa ¹⁵³, J. Maurer ^{27b}, B. Maček ⁹³, D.A. Maximov ³⁷, R. Mazini ¹⁴⁸, I. Maznas ¹⁵², M. Mazza ¹⁰⁷, S.M. Mazza ¹³⁶, E. Mazzeo ^{71a,71b}, C. Mc Ginn ²⁹, J.P. Mc Gowan ¹⁰⁴, S.P. Mc Kee ¹⁰⁶, E.F. McDonald ¹⁰⁵, A.E. McDougall ¹¹⁴, J.A. Mcfayden ¹⁴⁶, R.P. McGovern ¹²⁸, G. Mchedlidze ^{149b}, R.P. McKenzie ^{33g}, T.C. McLachlan ⁴⁸, D.J. McLaughlin ⁹⁶, S.J. McMahon ¹³⁴, C.M. Mcpartland ⁹², R.A. McPherson ^{165,ai}, S. Mehlhase ¹⁰⁹, A. Mehta ⁹², D. Melini ¹⁵⁰, B.R. Mellado Garcia ^{33g}, A.H. Melo ⁵⁵, F. Meloni ⁴⁸, A.M. Mendes Jacques Da Costa ¹⁰¹, H.Y. Meng ¹⁵⁵, L. Meng ⁹¹, S. Menke ¹¹⁰, M. Mentink ³⁶, E. Meoni ^{43b,43a}, G. Mercado ¹¹⁵, C. Merlassino ¹²⁶, L. Merola ^{72a,72b}, C. Meroni ^{71a,71b}, G. Merz ¹⁰⁶, O. Meshkov ³⁷, J. Metcalfe ⁶, A.S. Mete ⁶, C. Meyer ⁶⁸, J-P. Meyer ¹³⁵, R.P. Middleton ¹³⁴, L. Mijović ⁵², G. Mikenberg ¹⁶⁹, M. Mikestikova ¹³¹, M. Mikuž ⁹³, H. Mildner ¹⁰⁰, A. Milic ³⁶, C.D. Milke ⁴⁴, D.W. Miller ³⁹, L.S. Miller ³⁴, A. Milov ¹⁶⁹, D.A. Milstead ^{47a,47b}, T. Min ^{14c}, A.A. Minaenko ³⁷, I.A. Minashvili ^{149b}, L. Mince ⁵⁹, A.I. Mincer ¹¹⁷, B. Mindur ^{86a}, M. Mineev ³⁸, Y. Mino ⁸⁸, L.M. Mir ¹³, M. Miralles Lopez ¹⁶³, M. Mironova ^{17a}, A. Mishima ¹⁵³, M.C. Missio ¹¹³, A. Mitra ¹⁶⁷, V.A. Mitsou ¹⁶³, Y. Mitsumori ¹¹¹, O. Miu ¹⁵⁵, P.S. Miyagawa ⁹⁴, T. Mkrtchyan ^{63a}, M. Mlinarevic ⁹⁶, T. Mlinarevic ⁹⁶, M. Mlynarikova ³⁶, S. Mobius ¹⁹, P. Moder ⁴⁸, P. Mogg ¹⁰⁹, A.F. Mohammed ^{14a,14e}, S. Mohapatra ⁴¹, G. Mokgatitswane ^{33g}, L. Moleri ¹⁶⁹, B. Mondal ¹⁴¹, S. Mondal ¹³², G. Monig ¹⁴⁶, K. Mönig ⁴⁸, E. Monnier ¹⁰², L. Monsonis Romero ¹⁶³, J. Montejo Berlingen ¹³, M. Montella ¹¹⁹, F. Montekali ^{77a,77b}, F. Monticelli ⁹⁰, S. Monzani ^{69a,69c}, N. Morange ⁶⁶, A.L. Moreira De Carvalho ^{130a},

M. Moreno Llácer ¹⁶³, C. Moreno Martinez ⁵⁶, P. Morettini ^{57b}, S. Morgenstern ³⁶, M. Morii ⁶¹, M. Morinaga ¹⁵³, A.K. Morley ³⁶, F. Morodei ^{75a,75b}, L. Morvaj ³⁶, P. Moschovakos ³⁶, B. Moser ³⁶, M. Mosidze ^{149b}, T. Moskalets ⁵⁴, P. Moskvitina ¹¹³, J. Moss ^{31,p}, E.J.W. Moyse ¹⁰³, O. Mtintsilana ^{33g}, S. Muanza ¹⁰², J. Mueller ¹²⁹, D. Muenstermann ⁹¹, R. Müller ¹⁹, G.A. Mullier ¹⁶¹, A.J. Mullin ³², J.J. Mullin ¹²⁸, D.P. Mungo ¹⁵⁵, D. Munoz Perez ¹⁶³, F.J. Munoz Sanchez ¹⁰¹, M. Murin ¹⁰¹, W.J. Murray ^{167,134}, A. Murrone ^{71a,71b}, M. Muškinja ^{17a}, C. Mwewa ²⁹, A.G. Myagkov ^{37,a}, A.J. Myers ⁸, G. Myers ⁶⁸, M. Myska ¹³², B.P. Nachman ^{17a}, O. Nackenhorst ⁴⁹, A. Nag ⁵⁰, K. Nagai ¹²⁶, K. Nagano ⁸⁴, J.L. Nagle ^{29,ay}, E. Nagy ¹⁰², A.M. Nairz ³⁶, Y. Nakahama ⁸⁴, K. Nakamura ⁸⁴, K. Nakkalil ⁵, H. Nanjo ¹²⁴, R. Narayan ⁴⁴, E.A. Narayanan ¹¹², I. Naryshkin ³⁷, M. Naseri ³⁴, S. Nasri ¹⁵⁹, C. Nass ²⁴, G. Navarro ^{22a}, J. Navarro-Gonzalez ¹⁶³, R. Nayak ¹⁵¹, A. Nayaz ¹⁸, P.Y. Nechaeva ³⁷, F. Nechansky ⁴⁸, L. Nedic ¹²⁶, T.J. Neep ²⁰, A. Negri ^{73a,73b}, M. Negrini ^{23b}, C. Nellist ¹¹⁴, C. Nelson ¹⁰⁴, K. Nelson ¹⁰⁶, S. Nemecek ¹³¹, M. Nessi ^{36,j}, M.S. Neubauer ¹⁶², F. Neuhaus ¹⁰⁰, J. Neundorff ⁴⁸, R. Newhouse ¹⁶⁴, P.R. Newman ²⁰, C.W. Ng ¹²⁹, Y.W.Y. Ng ⁴⁸, B. Ngair ^{35e}, H.D.N. Nguyen ¹⁰⁸, R.B. Nickerson ¹²⁶, R. Nicolaidou ¹³⁵, J. Nielsen ¹³⁶, M. Niemeyer ⁵⁵, J. Niermann ^{55,36}, N. Nikiforou ³⁶, V. Nikolaenko ^{37,a}, I. Nikolic-Audit ¹²⁷, K. Nikolopoulos ²⁰, P. Nilsson ²⁹, I. Ninca ⁴⁸, H.R. Nindhito ⁵⁶, G. Ninio ¹⁵¹, A. Nisati ^{75a}, N. Nishu ², R. Nisius ¹¹⁰, J-E. Nitschke ⁵⁰, E.K. Nkadimeng ^{33g}, T. Nobe ¹⁵³, D.L. Noel ³², T. Nommensen ¹⁴⁷, M.B. Norfolk ¹³⁹, R.R.B. Norisam ⁹⁶, B.J. Norman ³⁴, J. Novak ⁹³, T. Novak ⁴⁸, L. Novotny ¹³², R. Novotny ¹¹², L. Nozka ¹²², K. Ntekas ¹⁶⁰, N.M.J. Nunes De Moura Junior ^{83b}, E. Nurse ⁹⁶, J. Ocariz ¹²⁷, A. Ochi ⁸⁵, I. Ochoa ^{130a}, S. Oerdek ^{48,y}, J.T. Offermann ³⁹, A. Ogrodnik ¹³³, A. Oh ¹⁰¹, C.C. Ohm ¹⁴⁴, H. Oide ⁸⁴, R. Oishi ¹⁵³, M.L. Ojeda ⁴⁸, M.W. O'Keefe ⁹², Y. Okumura ¹⁵³, L.F. Oleiro Seabra ^{130a}, S.A. Olivares Pino ^{137d}, D. Oliveira Damazio ²⁹, D. Oliveira Goncalves ^{83a}, J.L. Oliver ¹⁶⁰, Ö.O. Öncel ⁵⁴, A.P. O'Neill ¹⁹, A. Onofre ^{130a,130e}, P.U.E. Onyisi ¹¹, M.J. Oreglia ³⁹, G.E. Orellana ⁹⁰, D. Orestano ^{77a,77b}, N. Orlando ¹³, R.S. Orr ¹⁵⁵, V. O'Shea ⁵⁹, L.M. Osojnak ¹²⁸, R. Ospanov ^{62a}, G. Otero y Garzon ³⁰, H. Otono ⁸⁹, P.S. Ott ^{63a}, G.J. Ottino ^{17a}, M. Ouchrif ^{35d}, J. Ouellette ²⁹, F. Ould-Saada ¹²⁵, M. Owen ⁵⁹, R.E. Owen ¹³⁴, K.Y. Oyulmaz ^{21a}, V.E. Ozcan ^{21a}, F. Ozturk ⁸⁷, N. Ozturk ⁸, S. Ozturk ⁸², H.A. Pacey ¹²⁶, A. Pacheco Pages ¹³, C. Padilla Aranda ¹³, G. Padovano ^{75a,75b}, S. Pagan Griso ^{17a}, G. Palacino ⁶⁸, A. Palazzo ^{70a,70b}, S. Palestini ³⁶, J. Pan ¹⁷², T. Pan ^{64a}, D.K. Panchal ¹¹, C.E. Pandini ¹¹⁴, J.G. Panduro Vazquez ⁹⁵, H.D. Pandya ¹, H. Pang ^{14b}, P. Pani ⁴⁸, G. Panizzo ^{69a,69c}, L. Paolozzi ⁵⁶, C. Papadatos ¹⁰⁸, S. Parajuli ⁴⁴, A. Paramonov ⁶, C. Paraskevopoulos ¹⁰, D. Paredes Hernandez ^{64b}, K.R. Park ⁴¹, T.H. Park ¹⁵⁵, M.A. Parker ³², F. Parodi ^{57b,57a}, E.W. Parrish ¹¹⁵, V.A. Parrish ⁵², J.A. Parsons ⁴¹, U. Parzefall ⁵⁴, B. Pascual Dias ¹⁰⁸, L. Pascual Dominguez ¹⁵¹, E. Pasqualucci ^{75a}, S. Passaggio ^{57b}, F. Pastore ⁹⁵, P. Pasuwan ^{47a,47b}, P. Patel ⁸⁷, U.M. Patel ⁵¹, J.R. Pater ¹⁰¹, T. Pauly ³⁶, J. Pearkes ¹⁴³, M. Pedersen ¹²⁵, R. Pedro ^{130a}, S.V. Peleganchuk ³⁷, O. Penc ³⁶, E.A. Pender ⁵², K.E. Pensi ¹⁰⁹, M. Penzin ³⁷, B.S. Peralva ^{83d}, A.P. Pereira Peixoto ⁶⁰, L. Pereira Sanchez ^{47a,47b}, D.V. Perepelitsa ^{29,ay}, E. Perez Codina ^{156a}, M. Perganti ¹⁰, L. Perini ^{71a,71b,*}, H. Pernegger ³⁶, O. Perrin ⁴⁰, K. Peters ⁴⁸, R.F.Y. Peters ¹⁰¹, B.A. Petersen ³⁶, T.C. Petersen ⁴², E. Petit ¹⁰², V. Petousis ¹³², C. Petridou ^{152,f}, A. Petrukhin ¹⁴¹, M. Pettee ^{17a}, N.E. Pettersson ³⁶, A. Petukhov ³⁷, K. Petukhova ¹³³, R. Pezoa ^{137f}, L. Pezzotti ³⁶, G. Pezzullo ¹⁷², T.M. Pham ¹⁷⁰, T. Pham ¹⁰⁵, P.W. Phillips ¹³⁴, G. Piacquadio ¹⁴⁵, E. Pianori ^{17a}, F. Piazza ¹²³, R. Piegai ³⁰, D. Pietreanu ^{27b}, A.D. Pilkington ¹⁰¹, M. Pinamonti ^{69a,69c}, J.L. Pinfold ², B.C. Pinheiro Pereira ^{130a}, A.E. Pinto Pinoargote ^{100,135}, L. Pintucci ^{69a,69c}, K.M. Piper ¹⁴⁶, A. Pirttikoski ⁵⁶, D.A. Pizzi ³⁴, L. Pizzimento ^{64b}, A. Pizzini ¹¹⁴, M.-A. Pleier ²⁹, V. Plesanovs ⁵⁴,

V. Pleskot ¹³³, E. Plotnikova³⁸, G. Poddar ⁴, R. Poettgen ⁹⁸, L. Poggioli ¹²⁷, I. Pokharel ⁵⁵, S. Polacek ¹³³, G. Polesello ^{73a}, A. Poley ^{142,156a}, R. Polifka ¹³², A. Polini ^{23b}, C.S. Pollard ¹⁶⁷, Z.B. Pollock ¹¹⁹, V. Polychronakos ²⁹, E. Pompa Pacchi ^{75a,75b}, D. Ponomarenko ¹¹³, L. Pontecorvo ³⁶, S. Popa ^{27a}, G.A. Popeneciu ^{27d}, A. Poreba ³⁶, D.M. Portillo Quintero ^{156a}, S. Pospisil ¹³², M.A. Postill ¹³⁹, P. Postolache ^{27c}, K. Potamianos ¹⁶⁷, P.A. Potepa ^{86a}, I.N. Potrap ³⁸, C.J. Potter ³², H. Potti ¹, T. Poulsen ⁴⁸, J. Poveda ¹⁶³, M.E. Pozo Astigarraga ³⁶, A. Prades Ibanez ¹⁶³, J. Pretel ⁵⁴, D. Price ¹⁰¹, M. Primavera ^{70a}, M.A. Principe Martin ⁹⁹, R. Privara ¹²², T. Procter ⁵⁹, M.L. Proffitt ¹³⁸, N. Proklova ¹²⁸, K. Prokofiev ^{64c}, G. Proto ¹¹⁰, S. Protopopescu ²⁹, J. Proudfoot ⁶, M. Przybycien ^{86a}, W.W. Przygoda ^{86b}, J.E. Puddefoot ¹³⁹, D. Pudzha ³⁷, D. Pyatiizbyantseva ³⁷, J. Qian ¹⁰⁶, D. Qichen ¹⁰¹, Y. Qin ¹⁰¹, T. Qiu ⁵², A. Quadt ⁵⁵, M. Queitsch-Maitland ¹⁰¹, G. Quetant ⁵⁶, R.P. Quinn ¹⁶⁴, G. Rabanal Bolanos ⁶¹, D. Rafanoharana ⁵⁴, F. Ragusa ^{71a,71b}, J.L. Rainbolt ³⁹, J.A. Raine ⁵⁶, S. Rajagopalan ²⁹, E. Ramakoti ³⁷, I.A. Ramirez-Berend ³⁴, K. Ran ^{48,14e}, N.P. Rapheeha ^{33g}, H. Rasheed ^{27b}, V. Raskina ¹²⁷, D.F. Rassloff ^{63a}, S. Rave ¹⁰⁰, B. Ravina ⁵⁵, I. Ravinovich ¹⁶⁹, M. Raymond ³⁶, A.L. Read ¹²⁵, N.P. Readioff ¹³⁹, D.M. Rebuzzi ^{73a,73b}, G. Redlinger ²⁹, A.S. Reed ¹¹⁰, K. Reeves ²⁶, J.A. Reidelsturz ^{171,aa}, D. Reikher ¹⁵¹, A. Rej ^{49,z}, C. Rembser ³⁶, A. Renardi ⁴⁸, M. Renda ^{27b}, M.B. Rendel¹¹⁰, F. Renner ⁴⁸, A.G. Rennie ¹⁶⁰, A.L. Rescia ⁴⁸, S. Resconi ^{71a}, M. Ressegotti ^{57b,57a}, S. Rettie ³⁶, J.G. Reyes Rivera ¹⁰⁷, E. Reynolds ^{17a}, O.L. Rezanova ³⁷, P. Reznicek ¹³³, N. Ribaric ⁹¹, E. Ricci ^{78a,78b}, R. Richter ¹¹⁰, S. Richter ^{47a,47b}, E. Richter-Was ^{86b}, M. Ridel ¹²⁷, S. Ridouani ^{35d}, P. Rieck ¹¹⁷, P. Riedler ³⁶, E.M. Riefel ^{47a,47b}, J.O. Rieger¹¹⁴, M. Rijssenbeek ¹⁴⁵, A. Rimoldi ^{73a,73b}, M. Rimoldi ³⁶, L. Rinaldi ^{23b,23a}, T.T. Rinn ²⁹, M.P. Rinnagel ¹⁰⁹, G. Ripellino ¹⁶¹, I. Riu ¹³, P. Rivadeneira ⁴⁸, J.C. Rivera Vergara ¹⁶⁵, F. Rizatdinova ¹²¹, E. Rizvi ⁹⁴, B.A. Roberts ¹⁶⁷, B.R. Roberts ^{17a}, S.H. Robertson ^{104,ai}, D. Robinson ³², C.M. Robles Gajardo^{137f}, M. Robles Manzano ¹⁰⁰, A. Robson ⁵⁹, A. Rocchi ^{76a,76b}, C. Roda ^{74a,74b}, S. Rodriguez Bosca ^{63a}, Y. Rodriguez Garcia ^{22a}, A. Rodriguez Rodriguez ⁵⁴, A.M. Rodríguez Vera ^{156b}, S. Roe³⁶, J.T. Roemer ¹⁶⁰, A.R. Roepe-Gier ¹³⁶, J. Roggel ¹⁷¹, O. Røhne ¹²⁵, R.A. Rojas ¹⁰³, C.P.A. Roland ¹²⁷, J. Roloff ²⁹, A. Romaniouk ³⁷, E. Romano ^{73a,73b}, M. Romano ^{23b}, A.C. Romero Hernandez ¹⁶², N. Rompotis ⁹², L. Roos ¹²⁷, S. Rosati ^{75a}, B.J. Rosser ³⁹, E. Rossi ¹²⁶, E. Rossi ^{72a,72b}, L.P. Rossi ^{57b}, L. Rossini ⁵⁴, R. Rosten ¹¹⁹, M. Rotaru ^{27b}, B. Rottler ⁵⁴, C. Rougier ^{102,an}, D. Rousseau ⁶⁶, D. Rousso ³², A. Roy ¹⁶², S. Roy-Garand ¹⁵⁵, A. Rozanov ¹⁰², Z.M.A. Rozario ⁵⁹, Y. Rozen ¹⁵⁰, X. Ruan ^{33g}, A. Rubio Jimenez ¹⁶³, A.J. Ruby ⁹², V.H. Ruelas Rivera ¹⁸, T.A. Ruggeri ¹, A. Ruggiero ¹²⁶, A. Ruiz-Martinez ¹⁶³, A. Rummler ³⁶, Z. Rurikova ⁵⁴, N.A. Rusakovich ³⁸, H.L. Russell ¹⁶⁵, G. Russo ^{75a,75b}, J.P. Rutherford ⁷, S. Rutherford Colmenares ³², K. Rybacki⁹¹, M. Rybar ¹³³, E.B. Rye ¹²⁵, A. Ryzhov ⁴⁴, J.A. Sabater Iglesias ⁵⁶, P. Sabatini ¹⁶³, L. Sabetta ^{75a,75b}, H.F-W. Sadrozinski ¹³⁶, F. Safai Tehrani ^{75a}, B. Safarzadeh Samani ¹³⁴, M. Safdari ¹⁴³, S. Saha ¹⁶⁵, M. Sahinsoy ¹¹⁰, M. Saimpert ¹³⁵, M. Saito ¹⁵³, T. Saito ¹⁵³, D. Salamani ³⁶, A. Salnikov ¹⁴³, J. Salt ¹⁶³, A. Salvador Salas ¹⁵¹, D. Salvatore ^{43b,43a}, F. Salvatore ¹⁴⁶, A. Salzburger ³⁶, D. Sammel ⁵⁴, D. Sampsonidis ^{152,f}, D. Sampsonidou ¹²³, J. Sánchez ¹⁶³, A. Sanchez Pineda ⁴, V. Sanchez Sebastian ¹⁶³, H. Sandaker ¹²⁵, C.O. Sander ⁴⁸, J.A. Sandesara ¹⁰³, M. Sandhoff ¹⁷¹, C. Sandoval ^{22b}, D.P.C. Sankey ¹³⁴, T. Sano ⁸⁸, A. Sansoni ⁵³, L. Santi ^{75a,75b}, C. Santoni ⁴⁰, H. Santos ^{130a,130b}, S.N. Santpur ^{17a}, A. Santra ¹⁶⁹, K.A. Saoucha ^{116b}, J.G. Saraiva ^{130a,130d}, J. Sardain ⁷, O. Sasaki ⁸⁴, K. Sato ¹⁵⁷, C. Sauer^{63b}, F. Sauerburger ⁵⁴, E. Sauvan ⁴, P. Savard ^{155,av}, R. Sawada ¹⁵³, C. Sawyer ¹³⁴, L. Sawyer ⁹⁷, I. Sayago Galvan¹⁶³, C. Sbarra ^{23b}, A. Sbrizzi ^{23b,23a}, T. Scanlon ⁹⁶, J. Schaarschmidt ¹³⁸, P. Schacht ¹¹⁰, U. Schäfer ¹⁰⁰, A.C. Schaffer ^{66,44}, D. Schaile ¹⁰⁹, R.D. Schamberger ¹⁴⁵, C. Scharf ¹⁸, M.M. Schefer ¹⁹,

V.A. Schegelsky ³⁷, D. Scheirich ¹³³, F. Schenck ¹⁸, M. Schernau ¹⁶⁰, C. Scheulen ⁵⁵, C. Schiavi ^{57b,57a}, E.J. Schioppa ^{70a,70b}, M. Schioppa ^{43b,43a}, B. Schlag ^{143,t}, K.E. Schleicher ⁵⁴, S. Schlenker ³⁶, J. Schmeing ¹⁷¹, M.A. Schmidt ¹⁷¹, K. Schmieden ¹⁰⁰, C. Schmitt ¹⁰⁰, N. Schmitt ¹⁰⁰, S. Schmitt ⁴⁸, L. Schoeffel ¹³⁵, A. Schoening ^{63b}, P.G. Scholer ⁵⁴, E. Schopf ¹²⁶, M. Schott ¹⁰⁰, J. Schovancova ³⁶, S. Schramm ⁵⁶, F. Schroeder ¹⁷¹, T. Schroer ⁵⁶, H-C. Schultz-Coulon ^{63a}, M. Schumacher ⁵⁴, B.A. Schumm ¹³⁶, Ph. Schune ¹³⁵, A.J. Schuy ¹³⁸, H.R. Schwartz ¹³⁶, A. Schwartzman ¹⁴³, T.A. Schwarz ¹⁰⁶, Ph. Schwemling ¹³⁵, R. Schwienhorst ¹⁰⁷, A. Sciandra ¹³⁶, G. Sciolla ²⁶, F. Scuri ^{74a}, C.D. Sebastiani ⁹², K. Sedlaczek ¹¹⁵, P. Seema ¹⁸, S.C. Seidel ¹¹², A. Seiden ¹³⁶, B.D. Seidlitz ⁴¹, C. Seitz ⁴⁸, J.M. Seixas ^{83b}, G. Sekhniaidze ^{72a}, S.J. Sekula ⁴⁴, L. Selem ⁶⁰, N. Semprini-Cesari ^{23b,23a}, D. Sengupta ⁵⁶, V. Senthikumar ¹⁶³, L. Serin ⁶⁶, L. Serkin ^{69a,69b}, M. Sessa ^{76a,76b}, H. Severini ¹²⁰, F. Sforza ^{57b,57a}, A. Sfyrly ⁵⁶, E. Shabalina ⁵⁵, R. Shaheen ¹⁴⁴, J.D. Shahinian ¹²⁸, D. Shaked Renous ¹⁶⁹, L.Y. Shan ^{14a}, M. Shapiro ^{17a}, A. Sharma ³⁶, A.S. Sharma ¹⁶⁴, P. Sharma ⁸⁰, S. Sharma ⁴⁸, P.B. Shatalov ³⁷, K. Shaw ¹⁴⁶, S.M. Shaw ¹⁰¹, A. Shcherbakova ³⁷, Q. Shen ^{62c,5}, P. Sherwood ⁹⁶, L. Shi ⁹⁶, X. Shi ^{14a}, C.O. Shimmin ¹⁷², J.D. Shinner ⁹⁵, I.P.J. Shipsey ¹²⁶, S. Shirabe ^{56,j}, M. Shiyakova ^{38,ag}, J. Shlomi ¹⁶⁹, M.J. Shochet ³⁹, J. Shojaii ¹⁰⁵, D.R. Shope ¹²⁵, B. Shrestha ¹²⁰, S. Shrestha ^{119,az}, E.M. Shrif ^{33g}, M.J. Shroff ¹⁶⁵, P. Sicho ¹³¹, A.M. Sickles ¹⁶², E. Sideras Haddad ^{33g}, A. Sidoti ^{23b}, F. Siegert ⁵⁰, Dj. Sijacki ¹⁵, R. Sikora ^{86a}, F. Sili ⁹⁰, J.M. Silva ²⁰, M.V. Silva Oliveira ²⁹, S.B. Silverstein ^{47a}, S. Simion ⁶⁶, R. Simoniello ³⁶, E.L. Simpson ⁵⁹, H. Simpson ¹⁴⁶, L.R. Simpson ¹⁰⁶, N.D. Simpson ⁹⁸, S. Simsek ⁸², S. Sindhu ⁵⁵, P. Sinervo ¹⁵⁵, S. Singh ¹⁵⁵, S. Sinha ⁴⁸, S. Sinha ¹⁰¹, M. Sioli ^{23b,23a}, I. Siral ³⁶, E. Sitnikova ⁴⁸, S.Yu. Sivoklov ^{37,*}, J. Sjölin ^{47a,47b}, A. Skaf ⁵⁵, E. Skorda ^{20,aq}, P. Skubic ¹²⁰, M. Slawinska ⁸⁷, V. Smakhtin ¹⁶⁹, B.H. Smart ¹³⁴, J. Smiesko ³⁶, S.Yu. Smirnov ³⁷, Y. Smirnov ³⁷, L.N. Smirnova ^{37,a}, O. Smirnova ⁹⁸, A.C. Smith ⁴¹, E.A. Smith ³⁹, H.A. Smith ¹²⁶, J.L. Smith ⁹², R. Smith ¹⁴³, M. Smizanska ⁹¹, K. Smolek ¹³², A.A. Snesarev ³⁷, S.R. Snider ¹⁵⁵, H.L. Snoek ¹¹⁴, S. Snyder ²⁹, R. Sobie ^{165,ai}, A. Soffer ¹⁵¹, C.A. Solans Sanchez ³⁶, E.Yu. Soldatov ³⁷, U. Soldevila ¹⁶³, A.A. Solodkov ³⁷, S. Solomon ²⁶, A. Soloshenko ³⁸, K. Solovieva ⁵⁴, O.V. Solovyanov ⁴⁰, V. Solovyev ³⁷, P. Sommer ³⁶, A. Sonay ¹³, W.Y. Song ^{156b}, J.M. Sonneveld ¹¹⁴, A. Sopczak ¹³², A.L. Soppio ⁹⁶, F. Sopkova ^{28b}, I.R. Sotarriva Alvarez ¹⁵⁴, V. Sothilingam ^{63a}, O.J. Soto Sandoval ^{137c,137b}, S. Sottocornola ⁶⁸, R. Soualah ^{116b}, Z. Soumami ^{35e}, D. South ⁴⁸, N. Soybelman ¹⁶⁹, S. Spagnolo ^{70a,70b}, M. Spalla ¹¹⁰, D. Sperlich ⁵⁴, G. Spigo ³⁶, S. Spinali ⁹¹, D.P. Spiteri ⁵⁹, M. Spousta ¹³³, E.J. Staats ³⁴, A. Stabile ^{71a,71b}, R. Stamen ^{63a}, A. Stampekis ²⁰, M. Standke ²⁴, E. Stanecka ⁸⁷, M.V. Stange ⁵⁰, B. Stanislaus ^{17a}, M.M. Stanitzki ⁴⁸, B. Stapf ⁴⁸, E.A. Starchenko ³⁷, G.H. Stark ¹³⁶, J. Stark ^{102,an}, D.M. Starko ^{156b}, P. Staroba ¹³¹, P. Starovoitov ^{63a}, S. Stärz ¹⁰⁴, R. Staszewski ⁸⁷, G. Stavropoulos ⁴⁶, J. Steentoft ¹⁶¹, P. Steinberg ²⁹, B. Stelzer ^{142,156a}, H.J. Stelzer ¹²⁹, O. Stelzer-Chilton ^{156a}, H. Stenzel ⁵⁸, T.J. Stevenson ¹⁴⁶, G.A. Stewart ³⁶, J.R. Stewart ¹²¹, M.C. Stockton ³⁶, G. Stoicea ^{27b}, M. Stolarski ^{130a}, S. Stonjek ¹¹⁰, A. Straessner ⁵⁰, J. Strandberg ¹⁴⁴, S. Strandberg ^{47a,47b}, M. Stratmann ¹⁷¹, M. Strauss ¹²⁰, T. Streblor ¹⁰², P. Strizenec ^{28b}, R. Ströhmer ¹⁶⁶, D.M. Strom ¹²³, L.R. Strom ⁴⁸, R. Stroynowski ⁴⁴, A. Strubig ^{47a,47b}, S.A. Stucci ²⁹, B. Stugu ¹⁶, J. Stupak ¹²⁰, N.A. Styles ⁴⁸, D. Su ¹⁴³, S. Su ^{62a}, W. Su ^{62d}, X. Su ^{62a,66}, K. Sugizaki ¹⁵³, V.V. Sulin ³⁷, M.J. Sullivan ⁹², D.M.S. Sultan ^{78a,78b}, L. Sultanaliev ³⁷, S. Sultansoy ^{3b}, T. Sumida ⁸⁸, S. Sun ¹⁰⁶, S. Sun ¹⁷⁰, O. Sunneborn Gudnadottir ¹⁶¹, N. Sur ¹⁰², M.R. Sutton ¹⁴⁶, H. Suzuki ¹⁵⁷, M. Svatos ¹³¹, M. Swiatlowski ^{156a}, T. Swirski ¹⁶⁶, I. Sykora ^{28a}, M. Sykora ¹³³, T. Sykora ¹³³, D. Ta ¹⁰⁰, K. Tackmann ^{48,ae}, A. Taffard ¹⁶⁰, R. Tafirout ^{156a}, J.S. Tafoya Vargas ⁶⁶, E.P. Takeva ⁵²,

Y. Takubo ¹⁰⁸⁴, M. Talby ¹⁰², A.A. Talyshev ³⁷, K.C. Tam ^{64b}, N.M. Tamir ¹⁵¹, A. Tanaka ¹⁵³, J. Tanaka ¹⁵³, R. Tanaka ⁶⁶, M. Tanasini ^{57b,57a}, Z. Tao ¹⁶⁴, S. Tapia Araya ^{137f}, S. Tapprogge ¹⁰⁰, A. Tarek Abouelfadl Mohamed ¹⁰⁷, S. Tarem ¹⁵⁰, K. Tariq ^{14a}, G. Tarna ^{102,27b}, G.F. Tartarelli ^{71a}, P. Tas ¹³³, M. Tasevsky ¹³¹, E. Tassi ^{43b,43a}, A.C. Tate ¹⁶², G. Tateno ¹⁵³, Y. Tayalati ^{35e,ah}, G.N. Taylor ¹⁰⁵, W. Taylor ^{156b}, A.S. Tee ¹⁷⁰, R. Teixeira De Lima ¹⁴³, P. Teixeira-Dias ⁹⁵, J.J. Teoh ¹⁵⁵, K. Terashi ¹⁵³, J. Terron ⁹⁹, S. Terzo ¹³, M. Testa ⁵³, R.J. Teuscher ^{155,ai}, A. Thaler ⁷⁹, O. Theiner ⁵⁶, N. Themistokleous ⁵², T. Theveneaux-Pelzer ¹⁰², O. Thielmann ¹⁷¹, D.W. Thomas ⁹⁵, J.P. Thomas ²⁰, E.A. Thompson ^{17a}, P.D. Thompson ²⁰, E. Thomson ¹²⁸, Y. Tian ⁵⁵, V. Tikhomirov ^{37,a}, Yu.A. Tikhonov ³⁷, S. Timoshenko ³⁷, D. Timoshyn ¹³³, E.X.L. Ting ¹, P. Tipton ¹⁷², S.H. Tlou ^{33g}, A. Tnourji ⁴⁰, K. Todome ¹⁵⁴, S. Todorova-Nova ¹³³, S. Todt ⁵⁰, M. Togawa ⁸⁴, J. Tojo ⁸⁹, S. Tokár ^{28a}, K. Tokushuku ⁸⁴, O. Toldaiev ⁶⁸, R. Tombs ³², M. Tomoto ^{84,111}, L. Tompkins ^{143,t}, K.W. Topolnicki ^{86b}, E. Torrence ¹²³, H. Torres ^{102,an}, E. Torró Pastor ¹⁶³, M. Toscani ³⁰, C. Tosciri ³⁹, M. Tost ¹¹, D.R. Tovey ¹³⁹, A. Traeet ¹⁶, I.S. Trandafir ^{27b}, T. Trefzger ¹⁶⁶, A. Tricoli ²⁹, I.M. Trigger ^{156a}, S. Trincaz-Duvoid ¹²⁷, D.A. Trischuk ²⁶, B. Trocmé ⁶⁰, C. Troncon ^{71a}, L. Truong ^{33c}, M. Trzebinski ⁸⁷, A. Trzupsek ⁸⁷, F. Tsai ¹⁴⁵, M. Tsai ¹⁰⁶, A. Tsiamis ^{152,f}, P.V. Tsiareshka ³⁷, S. Tsigaridas ^{156a}, A. Tsigotis ^{152,ac}, V. Tsiskaridze ¹⁵⁵, E.G. Tskhadadze ^{149a}, M. Tsopoulou ^{152,f}, Y. Tsujikawa ⁸⁸, I.I. Tsukerman ³⁷, V. Tsulaia ^{17a}, S. Tsuno ⁸⁴, O. Tsur ¹⁵⁰, K. Tsur ¹¹⁸, D. Tsybychev ¹⁴⁵, Y. Tu ^{64b}, A. Tudorache ^{27b}, V. Tudorache ^{27b}, A.N. Tuna ³⁶, S. Turchikhin ^{57b,57a}, I. Turk Cakir ^{3a}, R. Turra ^{71a}, T. Turtuvshin ^{38,aj}, P.M. Tuts ⁴¹, S. Tzamarias ^{152,f}, P. Tzanis ¹⁰, E. Tzovara ¹⁰⁰, F. Ukegawa ¹⁵⁷, P.A. Ulloa Poblete ^{137c,137b}, E.N. Umaka ²⁹, G. Unal ³⁶, M. Unal ¹¹, A. Undrus ²⁹, G. Unel ¹⁶⁰, J. Urban ^{28b}, P. Urquijo ¹⁰⁵, P. Urrejola ^{137a}, G. Usai ⁸, R. Ushioda ¹⁵⁴, M. Usman ¹⁰⁸, Z. Uysal ^{21b}, V. Vacek ¹³², B. Vachon ¹⁰⁴, K.O.H. Vadla ¹²⁵, T. Vafeiadis ³⁶, A. Vaitkus ⁹⁶, C. Valderanis ¹⁰⁹, E. Valdes Santurio ^{47a,47b}, M. Valente ^{156a}, S. Valentinetti ^{23b,23a}, A. Valero ¹⁶³, E. Valiente Moreno ¹⁶³, A. Vallier ^{102,an}, J.A. Valls Ferrer ¹⁶³, D.R. Van Arneman ¹¹⁴, T.R. Van Daalen ¹³⁸, A. Van Der Graaf ⁴⁹, P. Van Gemmeren ⁶, M. Van Rijnbach ^{125,36}, S. Van Stroud ⁹⁶, I. Van Vulpen ¹¹⁴, M. Vanadia ^{76a,76b}, W. Vandelli ³⁶, M. Vandenbroucke ¹³⁵, E.R. Vandewall ¹²¹, D. Vannicola ¹⁵¹, L. Vannoli ^{57b,57a}, R. Vari ^{75a}, E.W. Varnes ⁷, C. Varni ^{17b}, T. Varol ¹⁴⁸, D. Varouchas ⁶⁶, L. Varriale ¹⁶³, K.E. Varvell ¹⁴⁷, M.E. Vasile ^{27b}, L. Vaslin ⁸⁴, G.A. Vasquez ¹⁶⁵, A. Vasyukov ³⁸, F. Vazeille ⁴⁰, T. Vazquez Schroeder ³⁶, J. Veatch ³¹, V. Vecchio ¹⁰¹, M.J. Veen ¹⁰³, I. Veliscek ¹²⁶, L.M. Veloce ¹⁵⁵, F. Veloso ^{130a,130c}, S. Veneziano ^{75a}, A. Ventura ^{70a,70b}, S. Ventura Gonzalez ¹³⁵, A. Verbytskyi ¹¹⁰, M. Verducci ^{74a,74b}, C. Vergis ²⁴, M. Verissimo De Araujo ^{83b}, W. Verkerke ¹¹⁴, J.C. Vermeulen ¹¹⁴, C. Vernieri ¹⁴³, M. Vessella ¹⁰³, M.C. Vetterli ^{142,av}, A. Vgenopoulos ^{152,f}, N. Viaux Maira ^{137f}, T. Vickey ¹³⁹, O.E. Vickey Boeriu ¹³⁹, G.H.A. Viehhauser ¹²⁶, L. Vigani ^{63b}, M. Villa ^{23b,23a}, M. Villaplana Perez ¹⁶³, E.M. Villhauer ⁵², E. Vilucchi ⁵³, M.G. Vincter ³⁴, G.S. Virdee ²⁰, A. Vishwakarma ⁵², A. Visibile ¹¹⁴, C. Vittori ³⁶, I. Vivarelli ¹⁴⁶, E. Voevodina ¹¹⁰, F. Vogel ¹⁰⁹, J.C. Voigt ⁵⁰, P. Vokac ¹³², Yu. Volkotrub ^{86a}, J. Von Ahnen ⁴⁸, E. Von Toerne ²⁴, B. Vormwald ³⁶, V. Vorobel ¹³³, K. Vorobev ³⁷, M. Vos ¹⁶³, K. Voss ¹⁴¹, J.H. Vossebeld ⁹², M. Vozak ¹¹⁴, L. Vozdecky ⁹⁴, N. Vranjes ¹⁵, M. Vranjes Milosavljevic ¹⁵, M. Vreeswijk ¹¹⁴, R. Vuillermet ³⁶, O. Vujinovic ¹⁰⁰, I. Vukotic ³⁹, S. Wada ¹⁵⁷, C. Wagner ¹⁰³, J.M. Wagner ^{17a}, W. Wagner ¹⁷¹, S. Wahdan ¹⁷¹, H. Wahlberg ⁹⁰, M. Wakida ¹¹¹, J. Walder ¹³⁴, R. Walker ¹⁰⁹, W. Walkowiak ¹⁴¹, A. Wall ¹²⁸, T. Wamorkar ⁶, A.Z. Wang ¹³⁶, C. Wang ¹⁰⁰, C. Wang ^{62c}, H. Wang ^{17a}, J. Wang ^{64a}, R.-J. Wang ¹⁰⁰, R. Wang ⁶¹, R. Wang ⁶, S.M. Wang ¹⁴⁸, S. Wang ^{62b}, T. Wang ^{62a}, W.T. Wang ⁸⁰, W. Wang ^{14a}, X. Wang ^{14c}, X. Wang ¹⁶², X. Wang ^{62c}, Y. Wang ^{62d}, Y. Wang ^{14c}, Z. Wang ¹⁰⁶, Z. Wang ^{62d,51,62c},

Z. Wang ¹⁰⁶, A. Warburton ¹⁰⁴, R.J. Ward ²⁰, N. Warrack ⁵⁹, A.T. Watson ²⁰, H. Watson ⁵⁹, M.F. Watson ²⁰, E. Watton ^{59,134}, G. Watts ¹³⁸, B.M. Waugh ⁹⁶, C. Weber ²⁹, H.A. Weber ¹⁸, M.S. Weber ¹⁹, S.M. Weber ^{63a}, C. Wei ^{62a}, Y. Wei ¹²⁶, A.R. Weidberg ¹²⁶, E.J. Weik ¹¹⁷, J. Weingarten ⁴⁹, M. Weirich ¹⁰⁰, C. Weiser ⁵⁴, C.J. Wells ⁴⁸, T. Wenaus ²⁹, B. Wendland ⁴⁹, T. Wengler ³⁶, N.S. Wenke ¹¹⁰, N. Wermes ²⁴, M. Wessels ^{63a}, A.M. Wharton ⁹¹, A.S. White ⁶¹, A. White ⁸, M.J. White ¹, D. Whiteson ¹⁶⁰, L. Wickremasinghe ¹²⁴, W. Wiedenmann ¹⁷⁰, C. Wiel ⁵⁰, M. Wielers ¹³⁴, C. Wigglesworth ⁴², D.J. Wilbern ¹²⁰, H.G. Wilkens ³⁶, D.M. Williams ⁴¹, H.H. Williams ¹²⁸, S. Williams ³², S. Willocq ¹⁰³, B.J. Wilson ¹⁰¹, P.J. Windischhofer ³⁹, F.I. Winkel ³⁰, F. Winklmeier ¹²³, B.T. Winter ⁵⁴, J.K. Winter ¹⁰¹, M. Wittgen ¹⁴³, M. Wobisch ⁹⁷, Z. Wolffs ¹¹⁴, J. Wollrath ¹⁶⁰, M.W. Wolter ⁸⁷, H. Wolters ^{130a,130c}, A.F. Wongel ⁴⁸, E.L. Woodward ⁴¹, S.D. Worm ⁴⁸, B.K. Wosiek ⁸⁷, K.W. Woźniak ⁸⁷, S. Wozniowski ⁵⁵, K. Wraight ⁵⁹, C. Wu ²⁰, J. Wu ^{14a,14e}, M. Wu ^{64a}, M. Wu ¹¹³, S.L. Wu ¹⁷⁰, X. Wu ⁵⁶, Y. Wu ^{62a}, Z. Wu ¹³⁵, J. Wuerzinger ^{110,at}, T.R. Wyatt ¹⁰¹, B.M. Wynne ⁵², S. Xella ⁴², L. Xia ^{14c}, M. Xia ^{14b}, J. Xiang ^{64c}, M. Xie ^{62a}, X. Xie ^{62a}, S. Xin ^{14a,14e}, A. Xiong ¹²³, J. Xiong ^{17a}, D. Xu ^{14a}, H. Xu ^{62a}, L. Xu ^{62a}, R. Xu ¹²⁸, T. Xu ¹⁰⁶, Y. Xu ^{14b}, Z. Xu ⁵², Z. Xu ^{14c}, B. Yabsley ¹⁴⁷, S. Yacoub ^{33a}, Y. Yamaguchi ¹⁵⁴, E. Yamashita ¹⁵³, H. Yamauchi ¹⁵⁷, T. Yamazaki ^{17a}, Y. Yamazaki ⁸⁵, J. Yan ^{62c}, S. Yan ¹²⁶, Z. Yan ²⁵, H.J. Yang ^{62c,62d}, H.T. Yang ^{62a}, S. Yang ^{62a}, T. Yang ^{64c}, X. Yang ³⁶, X. Yang ^{14a}, Y. Yang ⁴⁴, Y. Yang ^{62a}, Z. Yang ^{62a}, W.-M. Yao ^{17a}, Y.C. Yap ⁴⁸, H. Ye ^{14c}, H. Ye ⁵⁵, J. Ye ^{14a}, S. Ye ²⁹, X. Ye ^{62a}, Y. Yeh ⁹⁶, I. Yeletsikh ³⁸, B.K. Yeo ^{17b}, M.R. Yexley ⁹⁶, P. Yin ⁴¹, K. Yorita ¹⁶⁸, S. Younas ^{27b}, C.J.S. Young ³⁶, C. Young ¹⁴³, C. Yu ^{14a,14e,ax}, Y. Yu ^{62a}, M. Yuan ¹⁰⁶, R. Yuan ^{62b}, L. Yue ⁹⁶, M. Zaazoua ^{62a}, B. Zabinski ⁸⁷, E. Zaid ⁵², T. Zakareishvili ^{149b}, N. Zakharchuk ³⁴, S. Zambito ⁵⁶, J.A. Zamora Saa ^{137d,137b}, J. Zang ¹⁵³, D. Zanzi ⁵⁴, O. Zaplatilek ¹³², C. Zeitnitz ¹⁷¹, H. Zeng ^{14a}, J.C. Zeng ¹⁶², D.T. Zenger Jr ²⁶, O. Zenin ³⁷, T. Ženiš ^{28a}, S. Zenz ⁹⁴, S. Zerradi ^{35a}, D. Zerwas ⁶⁶, M. Zhai ^{14a,14e}, B. Zhang ^{14c}, D.F. Zhang ¹³⁹, J. Zhang ^{62b}, J. Zhang ⁶, K. Zhang ^{14a,14e}, L. Zhang ^{14c}, P. Zhang ^{14a,14e}, R. Zhang ¹⁷⁰, S. Zhang ¹⁰⁶, S. Zhang ⁴⁴, T. Zhang ¹⁵³, X. Zhang ^{62c}, X. Zhang ^{62b}, Y. Zhang ^{62c,5}, Y. Zhang ⁹⁶, Y. Zhang ^{14c}, Z. Zhang ^{17a}, Z. Zhang ⁶⁶, H. Zhao ¹³⁸, P. Zhao ⁵¹, T. Zhao ^{62b}, Y. Zhao ¹³⁶, Z. Zhao ^{62a}, A. Zhemchugov ³⁸, J. Zheng ^{14c}, K. Zheng ¹⁶², X. Zheng ^{62a}, Z. Zheng ¹⁴³, D. Zhong ¹⁶², B. Zhou ¹⁰⁶, H. Zhou ⁷, N. Zhou ^{62c}, Y. Zhou ⁷, C.G. Zhu ^{62b}, J. Zhu ¹⁰⁶, Y. Zhu ^{62c}, Y. Zhu ^{62a}, X. Zhuang ^{14a}, K. Zhukov ³⁷, V. Zhulanov ³⁷, N.I. Zimine ³⁸, J. Zinsser ^{63b}, M. Ziolkowski ¹⁴¹, L. Živković ¹⁵, A. Zoccoli ^{23b,23a}, K. Zoch ⁶¹, T.G. Zorbas ¹³⁹, O. Zormpa ⁴⁶, W. Zou ⁴¹, L. Zwalinski ³⁶.

¹Department of Physics, University of Adelaide, Adelaide; Australia.

²Department of Physics, University of Alberta, Edmonton AB; Canada.

^{3(a)}Department of Physics, Ankara University, Ankara; ^(b)Division of Physics, TOBB University of Economics and Technology, Ankara; Türkiye.

⁴LAPP, Université Savoie Mont Blanc, CNRS/IN2P3, Annecy; France.

⁵APC, Université Paris Cité, CNRS/IN2P3, Paris; France.

⁶High Energy Physics Division, Argonne National Laboratory, Argonne IL; United States of America.

⁷Department of Physics, University of Arizona, Tucson AZ; United States of America.

⁸Department of Physics, University of Texas at Arlington, Arlington TX; United States of America.

⁹Physics Department, National and Kapodistrian University of Athens, Athens; Greece.

¹⁰Physics Department, National Technical University of Athens, Zografou; Greece.

¹¹Department of Physics, University of Texas at Austin, Austin TX; United States of America.

¹²Institute of Physics, Azerbaijan Academy of Sciences, Baku; Azerbaijan.

- ¹³Institut de Física d'Altes Energies (IFAE), Barcelona Institute of Science and Technology, Barcelona; Spain.
- ¹⁴(^a)Institute of High Energy Physics, Chinese Academy of Sciences, Beijing; (^b)Physics Department, Tsinghua University, Beijing; (^c)Department of Physics, Nanjing University, Nanjing; (^d)School of Science, Shenzhen Campus of Sun Yat-sen University; (^e)University of Chinese Academy of Science (UCAS), Beijing; China.
- ¹⁵Institute of Physics, University of Belgrade, Belgrade; Serbia.
- ¹⁶Department for Physics and Technology, University of Bergen, Bergen; Norway.
- ¹⁷(^a)Physics Division, Lawrence Berkeley National Laboratory, Berkeley CA; (^b)University of California, Berkeley CA; United States of America.
- ¹⁸Institut für Physik, Humboldt Universität zu Berlin, Berlin; Germany.
- ¹⁹Albert Einstein Center for Fundamental Physics and Laboratory for High Energy Physics, University of Bern, Bern; Switzerland.
- ²⁰School of Physics and Astronomy, University of Birmingham, Birmingham; United Kingdom.
- ²¹(^a)Department of Physics, Bogazici University, Istanbul; (^b)Department of Physics Engineering, Gaziantep University, Gaziantep; (^c)Department of Physics, Istanbul University, Istanbul; Türkiye.
- ²²(^a)Facultad de Ciencias y Centro de Investigaciones, Universidad Antonio Nariño, Bogotá; (^b)Departamento de Física, Universidad Nacional de Colombia, Bogotá; (^c)Pontificia Universidad Javeriana, Bogota; Colombia.
- ²³(^a)Dipartimento di Fisica e Astronomia A. Righi, Università di Bologna, Bologna; (^b)INFN Sezione di Bologna; Italy.
- ²⁴Physikalisches Institut, Universität Bonn, Bonn; Germany.
- ²⁵Department of Physics, Boston University, Boston MA; United States of America.
- ²⁶Department of Physics, Brandeis University, Waltham MA; United States of America.
- ²⁷(^a)Transilvania University of Brasov, Brasov; (^b)Horia Hulubei National Institute of Physics and Nuclear Engineering, Bucharest; (^c)Department of Physics, Alexandru Ioan Cuza University of Iasi, Iasi; (^d)National Institute for Research and Development of Isotopic and Molecular Technologies, Physics Department, Cluj-Napoca; (^e)University Politehnica Bucharest, Bucharest; (^f)West University in Timisoara, Timisoara; (^g)Faculty of Physics, University of Bucharest, Bucharest; Romania.
- ²⁸(^a)Faculty of Mathematics, Physics and Informatics, Comenius University, Bratislava; (^b)Department of Subnuclear Physics, Institute of Experimental Physics of the Slovak Academy of Sciences, Kosice; Slovak Republic.
- ²⁹Physics Department, Brookhaven National Laboratory, Upton NY; United States of America.
- ³⁰Universidad de Buenos Aires, Facultad de Ciencias Exactas y Naturales, Departamento de Física, y CONICET, Instituto de Física de Buenos Aires (IFIBA), Buenos Aires; Argentina.
- ³¹California State University, CA; United States of America.
- ³²Cavendish Laboratory, University of Cambridge, Cambridge; United Kingdom.
- ³³(^a)Department of Physics, University of Cape Town, Cape Town; (^b)iThemba Labs, Western Cape; (^c)Department of Mechanical Engineering Science, University of Johannesburg, Johannesburg; (^d)National Institute of Physics, University of the Philippines Diliman (Philippines); (^e)University of South Africa, Department of Physics, Pretoria; (^f)University of Zululand, KwaDlangezwa; (^g)School of Physics, University of the Witwatersrand, Johannesburg; South Africa.
- ³⁴Department of Physics, Carleton University, Ottawa ON; Canada.
- ³⁵(^a)Faculté des Sciences Ain Chock, Réseau Universitaire de Physique des Hautes Energies - Université Hassan II, Casablanca; (^b)Faculté des Sciences, Université Ibn-Tofail, Kénitra; (^c)Faculté des Sciences Semlalia, Université Cadi Ayyad, LPHEA-Marrakech; (^d)LPMR, Faculté des Sciences, Université Mohamed Premier, Oujda; (^e)Faculté des sciences, Université Mohammed V, Rabat; (^f)Institute of Applied

Physics, Mohammed VI Polytechnic University, Ben Guerir; Morocco.

³⁶CERN, Geneva; Switzerland.

³⁷Affiliated with an institute covered by a cooperation agreement with CERN.

³⁸Affiliated with an international laboratory covered by a cooperation agreement with CERN.

³⁹Enrico Fermi Institute, University of Chicago, Chicago IL; United States of America.

⁴⁰LPC, Université Clermont Auvergne, CNRS/IN2P3, Clermont-Ferrand; France.

⁴¹Nevis Laboratory, Columbia University, Irvington NY; United States of America.

⁴²Niels Bohr Institute, University of Copenhagen, Copenhagen; Denmark.

⁴³(^a) Dipartimento di Fisica, Università della Calabria, Rende; (^b) INFN Gruppo Collegato di Cosenza, Laboratori Nazionali di Frascati; Italy.

⁴⁴Physics Department, Southern Methodist University, Dallas TX; United States of America.

⁴⁵Physics Department, University of Texas at Dallas, Richardson TX; United States of America.

⁴⁶National Centre for Scientific Research "Demokritos", Agia Paraskevi; Greece.

⁴⁷(^a) Department of Physics, Stockholm University; (^b) Oskar Klein Centre, Stockholm; Sweden.

⁴⁸Deutsches Elektronen-Synchrotron DESY, Hamburg and Zeuthen; Germany.

⁴⁹Fakultät Physik, Technische Universität Dortmund, Dortmund; Germany.

⁵⁰Institut für Kern- und Teilchenphysik, Technische Universität Dresden, Dresden; Germany.

⁵¹Department of Physics, Duke University, Durham NC; United States of America.

⁵²SUPA - School of Physics and Astronomy, University of Edinburgh, Edinburgh; United Kingdom.

⁵³INFN e Laboratori Nazionali di Frascati, Frascati; Italy.

⁵⁴Physikalisches Institut, Albert-Ludwigs-Universität Freiburg, Freiburg; Germany.

⁵⁵II. Physikalisches Institut, Georg-August-Universität Göttingen, Göttingen; Germany.

⁵⁶Département de Physique Nucléaire et Corpusculaire, Université de Genève, Genève; Switzerland.

⁵⁷(^a) Dipartimento di Fisica, Università di Genova, Genova; (^b) INFN Sezione di Genova; Italy.

⁵⁸II. Physikalisches Institut, Justus-Liebig-Universität Giessen, Giessen; Germany.

⁵⁹SUPA - School of Physics and Astronomy, University of Glasgow, Glasgow; United Kingdom.

⁶⁰LPSC, Université Grenoble Alpes, CNRS/IN2P3, Grenoble INP, Grenoble; France.

⁶¹Laboratory for Particle Physics and Cosmology, Harvard University, Cambridge MA; United States of America.

⁶²(^a) Department of Modern Physics and State Key Laboratory of Particle Detection and Electronics, University of Science and Technology of China, Hefei; (^b) Institute of Frontier and Interdisciplinary Science and Key Laboratory of Particle Physics and Particle Irradiation (MOE), Shandong University, Qingdao; (^c) School of Physics and Astronomy, Shanghai Jiao Tong University, Key Laboratory for Particle Astrophysics and Cosmology (MOE), SKLPPC, Shanghai; (^d) Tsung-Dao Lee Institute, Shanghai; China.

⁶³(^a) Kirchhoff-Institut für Physik, Ruprecht-Karls-Universität Heidelberg, Heidelberg; (^b) Physikalisches Institut, Ruprecht-Karls-Universität Heidelberg, Heidelberg; Germany.

⁶⁴(^a) Department of Physics, Chinese University of Hong Kong, Shatin, N.T., Hong Kong; (^b) Department of Physics, University of Hong Kong, Hong Kong; (^c) Department of Physics and Institute for Advanced Study, Hong Kong University of Science and Technology, Clear Water Bay, Kowloon, Hong Kong; China.

⁶⁵Department of Physics, National Tsing Hua University, Hsinchu; Taiwan.

⁶⁶IJCLab, Université Paris-Saclay, CNRS/IN2P3, 91405, Orsay; France.

⁶⁷Centro Nacional de Microelectrónica (IMB-CNM-CSIC), Barcelona; Spain.

⁶⁸Department of Physics, Indiana University, Bloomington IN; United States of America.

⁶⁹(^a) INFN Gruppo Collegato di Udine, Sezione di Trieste, Udine; (^b) ICTP, Trieste; (^c) Dipartimento Politecnico di Ingegneria e Architettura, Università di Udine, Udine; Italy.

⁷⁰(^a) INFN Sezione di Lecce; (^b) Dipartimento di Matematica e Fisica, Università del Salento, Lecce; Italy.

⁷¹(^a) INFN Sezione di Milano; (^b) Dipartimento di Fisica, Università di Milano, Milano; Italy.

- ^{72(a)} INFN Sezione di Napoli; ^(b) Dipartimento di Fisica, Università di Napoli, Napoli; Italy.
- ^{73(a)} INFN Sezione di Pavia; ^(b) Dipartimento di Fisica, Università di Pavia, Pavia; Italy.
- ^{74(a)} INFN Sezione di Pisa; ^(b) Dipartimento di Fisica E. Fermi, Università di Pisa, Pisa; Italy.
- ^{75(a)} INFN Sezione di Roma; ^(b) Dipartimento di Fisica, Sapienza Università di Roma, Roma; Italy.
- ^{76(a)} INFN Sezione di Roma Tor Vergata; ^(b) Dipartimento di Fisica, Università di Roma Tor Vergata, Roma; Italy.
- ^{77(a)} INFN Sezione di Roma Tre; ^(b) Dipartimento di Matematica e Fisica, Università Roma Tre, Roma; Italy.
- ^{78(a)} INFN-TIFPA; ^(b) Università degli Studi di Trento, Trento; Italy.
- ⁷⁹ Universität Innsbruck, Department of Astro and Particle Physics, Innsbruck; Austria.
- ⁸⁰ University of Iowa, Iowa City IA; United States of America.
- ⁸¹ Department of Physics and Astronomy, Iowa State University, Ames IA; United States of America.
- ⁸² Istinye University, Sariyer, Istanbul; Türkiye.
- ^{83(a)} Departamento de Engenharia Elétrica, Universidade Federal de Juiz de Fora (UFJF), Juiz de Fora; ^(b) Universidade Federal do Rio De Janeiro COPPE/EE/IF, Rio de Janeiro; ^(c) Instituto de Física, Universidade de São Paulo, São Paulo; ^(d) Rio de Janeiro State University, Rio de Janeiro; Brazil.
- ⁸⁴ KEK, High Energy Accelerator Research Organization, Tsukuba; Japan.
- ⁸⁵ Graduate School of Science, Kobe University, Kobe; Japan.
- ^{86(a)} AGH University of Krakow, Faculty of Physics and Applied Computer Science, Krakow; ^(b) Marian Smoluchowski Institute of Physics, Jagiellonian University, Krakow; Poland.
- ⁸⁷ Institute of Nuclear Physics Polish Academy of Sciences, Krakow; Poland.
- ⁸⁸ Faculty of Science, Kyoto University, Kyoto; Japan.
- ⁸⁹ Research Center for Advanced Particle Physics and Department of Physics, Kyushu University, Fukuoka ; Japan.
- ⁹⁰ Instituto de Física La Plata, Universidad Nacional de La Plata and CONICET, La Plata; Argentina.
- ⁹¹ Physics Department, Lancaster University, Lancaster; United Kingdom.
- ⁹² Oliver Lodge Laboratory, University of Liverpool, Liverpool; United Kingdom.
- ⁹³ Department of Experimental Particle Physics, Jožef Stefan Institute and Department of Physics, University of Ljubljana, Ljubljana; Slovenia.
- ⁹⁴ School of Physics and Astronomy, Queen Mary University of London, London; United Kingdom.
- ⁹⁵ Department of Physics, Royal Holloway University of London, Egham; United Kingdom.
- ⁹⁶ Department of Physics and Astronomy, University College London, London; United Kingdom.
- ⁹⁷ Louisiana Tech University, Ruston LA; United States of America.
- ⁹⁸ Fysiska institutionen, Lunds universitet, Lund; Sweden.
- ⁹⁹ Departamento de Física Teórica C-15 and CIAFF, Universidad Autónoma de Madrid, Madrid; Spain.
- ¹⁰⁰ Institut für Physik, Universität Mainz, Mainz; Germany.
- ¹⁰¹ School of Physics and Astronomy, University of Manchester, Manchester; United Kingdom.
- ¹⁰² CPPM, Aix-Marseille Université, CNRS/IN2P3, Marseille; France.
- ¹⁰³ Department of Physics, University of Massachusetts, Amherst MA; United States of America.
- ¹⁰⁴ Department of Physics, McGill University, Montreal QC; Canada.
- ¹⁰⁵ School of Physics, University of Melbourne, Victoria; Australia.
- ¹⁰⁶ Department of Physics, University of Michigan, Ann Arbor MI; United States of America.
- ¹⁰⁷ Department of Physics and Astronomy, Michigan State University, East Lansing MI; United States of America.
- ¹⁰⁸ Group of Particle Physics, University of Montreal, Montreal QC; Canada.
- ¹⁰⁹ Fakultät für Physik, Ludwig-Maximilians-Universität München, München; Germany.
- ¹¹⁰ Max-Planck-Institut für Physik (Werner-Heisenberg-Institut), München; Germany.

- ¹¹¹Graduate School of Science and Kobayashi-Maskawa Institute, Nagoya University, Nagoya; Japan.
- ¹¹²Department of Physics and Astronomy, University of New Mexico, Albuquerque NM; United States of America.
- ¹¹³Institute for Mathematics, Astrophysics and Particle Physics, Radboud University/Nikhef, Nijmegen; Netherlands.
- ¹¹⁴Nikhef National Institute for Subatomic Physics and University of Amsterdam, Amsterdam; Netherlands.
- ¹¹⁵Department of Physics, Northern Illinois University, DeKalb IL; United States of America.
- ¹¹⁶(^a) New York University Abu Dhabi, Abu Dhabi; (^b) University of Sharjah, Sharjah; United Arab Emirates.
- ¹¹⁷Department of Physics, New York University, New York NY; United States of America.
- ¹¹⁸Ochanomizu University, Otsuka, Bunkyo-ku, Tokyo; Japan.
- ¹¹⁹Ohio State University, Columbus OH; United States of America.
- ¹²⁰Homer L. Dodge Department of Physics and Astronomy, University of Oklahoma, Norman OK; United States of America.
- ¹²¹Department of Physics, Oklahoma State University, Stillwater OK; United States of America.
- ¹²²Palacký University, Joint Laboratory of Optics, Olomouc; Czech Republic.
- ¹²³Institute for Fundamental Science, University of Oregon, Eugene, OR; United States of America.
- ¹²⁴Graduate School of Science, Osaka University, Osaka; Japan.
- ¹²⁵Department of Physics, University of Oslo, Oslo; Norway.
- ¹²⁶Department of Physics, Oxford University, Oxford; United Kingdom.
- ¹²⁷LPNHE, Sorbonne Université, Université Paris Cité, CNRS/IN2P3, Paris; France.
- ¹²⁸Department of Physics, University of Pennsylvania, Philadelphia PA; United States of America.
- ¹²⁹Department of Physics and Astronomy, University of Pittsburgh, Pittsburgh PA; United States of America.
- ¹³⁰(^a) Laboratório de Instrumentação e Física Experimental de Partículas - LIP, Lisboa; (^b) Departamento de Física, Faculdade de Ciências, Universidade de Lisboa, Lisboa; (^c) Departamento de Física, Universidade de Coimbra, Coimbra; (^d) Centro de Física Nuclear da Universidade de Lisboa, Lisboa; (^e) Departamento de Física, Universidade do Minho, Braga; (^f) Departamento de Física Teórica y del Cosmos, Universidad de Granada, Granada (Spain); (^g) Departamento de Física, Instituto Superior Técnico, Universidade de Lisboa, Lisboa; Portugal.
- ¹³¹Institute of Physics of the Czech Academy of Sciences, Prague; Czech Republic.
- ¹³²Czech Technical University in Prague, Prague; Czech Republic.
- ¹³³Charles University, Faculty of Mathematics and Physics, Prague; Czech Republic.
- ¹³⁴Particle Physics Department, Rutherford Appleton Laboratory, Didcot; United Kingdom.
- ¹³⁵IRFU, CEA, Université Paris-Saclay, Gif-sur-Yvette; France.
- ¹³⁶Santa Cruz Institute for Particle Physics, University of California Santa Cruz, Santa Cruz CA; United States of America.
- ¹³⁷(^a) Departamento de Física, Pontificia Universidad Católica de Chile, Santiago; (^b) Millennium Institute for Subatomic physics at high energy frontier (SAPHIR), Santiago; (^c) Instituto de Investigación Multidisciplinario en Ciencia y Tecnología, y Departamento de Física, Universidad de La Serena; (^d) Universidad Andres Bello, Department of Physics, Santiago; (^e) Instituto de Alta Investigación, Universidad de Tarapacá, Arica; (^f) Departamento de Física, Universidad Técnica Federico Santa María, Valparaíso; Chile.
- ¹³⁸Department of Physics, University of Washington, Seattle WA; United States of America.
- ¹³⁹Department of Physics and Astronomy, University of Sheffield, Sheffield; United Kingdom.
- ¹⁴⁰Department of Physics, Shinshu University, Nagano; Japan.

- ¹⁴¹Department Physik, Universität Siegen, Siegen; Germany.
- ¹⁴²Department of Physics, Simon Fraser University, Burnaby BC; Canada.
- ¹⁴³SLAC National Accelerator Laboratory, Stanford CA; United States of America.
- ¹⁴⁴Department of Physics, Royal Institute of Technology, Stockholm; Sweden.
- ¹⁴⁵Departments of Physics and Astronomy, Stony Brook University, Stony Brook NY; United States of America.
- ¹⁴⁶Department of Physics and Astronomy, University of Sussex, Brighton; United Kingdom.
- ¹⁴⁷School of Physics, University of Sydney, Sydney; Australia.
- ¹⁴⁸Institute of Physics, Academia Sinica, Taipei; Taiwan.
- ¹⁴⁹(^a) E. Andronikashvili Institute of Physics, Iv. Javakhishvili Tbilisi State University, Tbilisi; (^b) High Energy Physics Institute, Tbilisi State University, Tbilisi; (^c) University of Georgia, Tbilisi; Georgia.
- ¹⁵⁰Department of Physics, Technion, Israel Institute of Technology, Haifa; Israel.
- ¹⁵¹Raymond and Beverly Sackler School of Physics and Astronomy, Tel Aviv University, Tel Aviv; Israel.
- ¹⁵²Department of Physics, Aristotle University of Thessaloniki, Thessaloniki; Greece.
- ¹⁵³International Center for Elementary Particle Physics and Department of Physics, University of Tokyo, Tokyo; Japan.
- ¹⁵⁴Department of Physics, Tokyo Institute of Technology, Tokyo; Japan.
- ¹⁵⁵Department of Physics, University of Toronto, Toronto ON; Canada.
- ¹⁵⁶(^a) TRIUMF, Vancouver BC; (^b) Department of Physics and Astronomy, York University, Toronto ON; Canada.
- ¹⁵⁷Division of Physics and Tomonaga Center for the History of the Universe, Faculty of Pure and Applied Sciences, University of Tsukuba, Tsukuba; Japan.
- ¹⁵⁸Department of Physics and Astronomy, Tufts University, Medford MA; United States of America.
- ¹⁵⁹United Arab Emirates University, Al Ain; United Arab Emirates.
- ¹⁶⁰Department of Physics and Astronomy, University of California Irvine, Irvine CA; United States of America.
- ¹⁶¹Department of Physics and Astronomy, University of Uppsala, Uppsala; Sweden.
- ¹⁶²Department of Physics, University of Illinois, Urbana IL; United States of America.
- ¹⁶³Instituto de Física Corpuscular (IFIC), Centro Mixto Universidad de Valencia - CSIC, Valencia; Spain.
- ¹⁶⁴Department of Physics, University of British Columbia, Vancouver BC; Canada.
- ¹⁶⁵Department of Physics and Astronomy, University of Victoria, Victoria BC; Canada.
- ¹⁶⁶Fakultät für Physik und Astronomie, Julius-Maximilians-Universität Würzburg, Würzburg; Germany.
- ¹⁶⁷Department of Physics, University of Warwick, Coventry; United Kingdom.
- ¹⁶⁸Waseda University, Tokyo; Japan.
- ¹⁶⁹Department of Particle Physics and Astrophysics, Weizmann Institute of Science, Rehovot; Israel.
- ¹⁷⁰Department of Physics, University of Wisconsin, Madison WI; United States of America.
- ¹⁷¹Fakultät für Mathematik und Naturwissenschaften, Fachgruppe Physik, Bergische Universität Wuppertal, Wuppertal; Germany.
- ¹⁷²Department of Physics, Yale University, New Haven CT; United States of America.
- ^a Also Affiliated with an institute covered by a cooperation agreement with CERN.
- ^b Also at An-Najah National University, Nablus; Palestine.
- ^c Also at APC, Université Paris Cité, CNRS/IN2P3, Paris; France.
- ^d Also at Borough of Manhattan Community College, City University of New York, New York NY; United States of America.
- ^e Also at Center for High Energy Physics, Peking University; China.
- ^f Also at Center for Interdisciplinary Research and Innovation (CIRI-AUTH), Thessaloniki; Greece.
- ^g Also at Centro Studi e Ricerche Enrico Fermi; Italy.

- ^h Also at CERN Tier-0; Switzerland.
- ⁱ Also at CERN, Geneva; Switzerland.
- ^j Also at Département de Physique Nucléaire et Corpusculaire, Université de Genève, Genève; Switzerland.
- ^k Also at Departament de Física de la Universitat Autònoma de Barcelona, Barcelona; Spain.
- ^l Also at Department of Financial and Management Engineering, University of the Aegean, Chios; Greece.
- ^m Also at Department of Physics and Astronomy, University of Sheffield, Sheffield; United Kingdom.
- ⁿ Also at Department of Physics and Astronomy, University of Victoria, Victoria BC; Canada.
- ^o Also at Department of Physics, Ben Gurion University of the Negev, Beer Sheva; Israel.
- ^p Also at Department of Physics, California State University, Sacramento; United States of America.
- ^q Also at Department of Physics, King's College London, London; United Kingdom.
- ^r Also at Department of Physics, Oxford University, Oxford; United Kingdom.
- ^s Also at Department of Physics, Royal Holloway University of London, Egham; United Kingdom.
- ^t Also at Department of Physics, Stanford University, Stanford CA; United States of America.
- ^u Also at Department of Physics, University of Fribourg, Fribourg; Switzerland.
- ^v Also at Department of Physics, University of Massachusetts, Amherst MA; United States of America.
- ^w Also at Department of Physics, University of Thessaly; Greece.
- ^x Also at Department of Physics, Westmont College, Santa Barbara; United States of America.
- ^y Also at Deutsches Elektronen-Synchrotron DESY, Hamburg and Zeuthen; Germany.
- ^z Also at Fakultät Physik, Technische Universität Dortmund, Dortmund; Germany.
- ^{aa} Also at Fakultät für Mathematik und Naturwissenschaften, Fachgruppe Physik, Bergische Universität Wuppertal, Wuppertal; Germany.
- ^{ab} Also at Group of Particle Physics, University of Montreal, Montreal QC; Canada.
- ^{ac} Also at Hellenic Open University, Patras; Greece.
- ^{ad} Also at Institutio Catalana de Recerca i Estudis Avancats, ICREA, Barcelona; Spain.
- ^{ae} Also at Institut für Experimentalphysik, Universität Hamburg, Hamburg; Germany.
- ^{af} Also at Institut für Physik, Universität Mainz, Mainz; Germany.
- ^{ag} Also at Institute for Nuclear Research and Nuclear Energy (INRNE) of the Bulgarian Academy of Sciences, Sofia; Bulgaria.
- ^{ah} Also at Institute of Applied Physics, Mohammed VI Polytechnic University, Ben Guerir; Morocco.
- ^{ai} Also at Institute of Particle Physics (IPP); Canada.
- ^{aj} Also at Institute of Physics and Technology, Ulaanbaatar; Mongolia.
- ^{ak} Also at Institute of Physics, Azerbaijan Academy of Sciences, Baku; Azerbaijan.
- ^{al} Also at Institute of Theoretical Physics, Ilia State University, Tbilisi; Georgia.
- ^{am} Also at IRFU, CEA, Université Paris-Saclay, Gif-sur-Yvette; France.
- ^{an} Also at L2IT, Université de Toulouse, CNRS/IN2P3, UPS, Toulouse; France.
- ^{ao} Also at Lawrence Livermore National Laboratory, Livermore; United States of America.
- ^{ap} Also at National Institute of Physics, University of the Philippines Diliman (Philippines); Philippines.
- ^{aq} Also at School of Physics and Astronomy, University of Birmingham, Birmingham; United Kingdom.
- ^{ar} Also at School of Physics and Astronomy, University of Manchester, Manchester; United Kingdom.
- ^{as} Also at SUPA - School of Physics and Astronomy, University of Glasgow, Glasgow; United Kingdom.
- ^{at} Also at Technical University of Munich, Munich; Germany.
- ^{au} Also at The Collaborative Innovation Center of Quantum Matter (CICQM), Beijing; China.
- ^{av} Also at TRIUMF, Vancouver BC; Canada.
- ^{aw} Also at Università di Napoli Parthenope, Napoli; Italy.
- ^{ax} Also at University of Chinese Academy of Sciences (UCAS), Beijing; China.
- ^{ay} Also at University of Colorado Boulder, Department of Physics, Colorado; United States of America.

^{az} Also at Washington College, Chestertown, MD; United States of America.

^{ba} Also at Yeditepe University, Physics Department, Istanbul; Türkiye.

* Deceased